Genetic and biotechnological development of the pennate marine diatom *Phaeodactylum tricornutum* for high-value bioproducts and carbon bio-mitigation.

Volume I of I

Simrat Kaur

A thesis submitted to National University of Ireland, Galway

For the degree of Doctor of Philosophy

College of Science, School of Natural Sciences

Discipline of Botany and Plant Science

Under the supervision of Prof Charles Spillane

Head of Botany and Plant Science

April 2014

Table of Contents

DECLARATION

The thesis entitled ‘Genetic and biotechnological development of the pennate marine diatom *Phaeodactylum tricornutum* for high-value bioproducts and carbon bio-mitigation’ is my own research and has not been submitted for another degree, either at National University of Ireland, Galway or elsewhere.

Signed: _____

Simrat Kaur

ACKNOWLEDGMENTS

I would like to thank my supervisor Prof. Charles Spillane for his directions and guidance throughout my PhD research. He has been a kind and critical boss who provided me relative freedom to enhance my scientific skills and always encouraged my collaborative efforts with other researchers.

The second person whom I am very grateful is Prof. Rhodri Ceredig who has throughout been very helpful in my mutagenesis research project. He always agreed for any scientific discussions related to experiments or results analysis and suggested many useful ideas.

I thank Dr Clifford Eoghan who introduced me to all the useful equipments in his laboratory that I used for my CO_2 experiments. I also thank him for the useful discussions and suggestions.

Now, I want to thank all the technical officers at NUI Galway who helped me in conducting my experiments at the University instrumentation facilities- Dr Shirley Hanley, Senior Technical Officer (STO) for the flow cytometry; Brenden Harhen, STO in liquid chromatography lab; Pierce Lalor, STO, Department of Anatomy for preparation of diamond cut resin sections and making of grids for the transmission electron microscopy; Mary O′Brien from engineering lab and Patrick O'Rafferty, STO botany for always bringing me the seawater and other general laboratory equipments.

Special thanks to past and present members of my lab. Beginning with Kristina who started helping me from my first day in Galway, Peter McKeown who always agreed to evaluate my manuscripts and reports, Mohan K Muniyappa and Channakeshavaiah who offered a great help during my cloning experiments. Special thanks to Sandesh, Antoine, Matheus Gomes, Martin Braud, Duygu Selcucklu, Dorota, Peter Ryder, Aurelie, Anish, Mercy, Angela, Attia and Wei li for their timely help and lovely times together in our lab.

Many thanks to Dr Ronan Sulpice who also critically evaluated my manuscripts and gave very useful comments and suggestions.

I am very grateful to Environmental Protection Agency (EPA, Ireland) and Enterprise Ireland for funding and providing me with financial assistance (2009-PhD-ET-8).

COURSES AND SEMINARS ATTENDED

- Flocyte regional training program, February, 14-15, 2011 at Institute of Cancer Research London
- Workshop on culturing algae for biotechnology course, September, 27-28, 2011 at Scottish Association for Marine Science
- 22nd International Diatom Symposium, August, 26-31, 2012, Ghent, Belgium

Oral presentations

Simrat Kaur, Rhodri Ceredig, Dagmar Stengel and Charles Spillane (2010) Flow cytometric studies in microalgae. Plenary presentation at the 6th Annual Meeting of the Irish Cytometry Society, Dublin. 17-18 November 2010.

Simrat Kaur and Charles Spillane (2010) Algae Conversion to Biofuel: The Challenges. Invited research talk at NextGenFuels 2010, India. 30 November to 2 December.

Simrat Kaur and Charles Spillane (2012) Generation of novel microalgal lines producing high levels of nutraceuticals. Irish Plant Scientists Association Meeting, National Botanic Gardens, Dublin. 3-5 April, 2012

Simrat Kaur and Charles Spillane (2012) Lipids in the model diatom *Phaeodactylum tricornutum* and variability among mutant strains. Environ, Dublin, 8th March, 2012

Simrat Kaur, Eoghan Clifford and Charles Spillane (2013) Carbon fixation by the marine diatom *Phaeodactylum tricornutum* grown under high concentrations of air-CO_2 mixtures. Irish Plant Scientists Association Meeting, Galway. 16-17 May 2013.

Publications

Simrat Kaur and Charles Spillane. Reduction in Carotenoid Levels in the Marine Diatom *Phaeodactylum tricornutum* by Artificial MicroRNAs Targeted Against the Endogenous *PHYTOENE SYNTHASE* Gene. *Communicated to Marine Biotechnology*

ABSTRACT

Conflicting demands of food over fuel and the mushrooming need for feed and fibre are serious challenges for humankind at a time when we also need to address climate change challenges. Global demands for land based commodities will surpass increases in supply. Such divergence may bring civil unrest, hunger and malnutrition. Environmental issues associated with agriculture's environmental footprint pose challenges on a global scale including scarcity of fresh water, degradation of ecological biodiversity and the release of toxic wastes into the environment. One possible environmentally safe and sustainable solution would be the selection of alternative green energy sources that can be cultivated in marine waters or waste waters, and still offer us feed and fuel.

Microalgae are miniature biofactories that can convert sunlight and CO_2 into valuable biomass and into lipids that can be utilized as feedstock for biofuel, aquaculture feed and high value fatty acids. Marine microalgae such as diatoms represent potential targets for industrial production of useful fatty acids. In general, the fatty acids of marine microalgae are predominantly saturated and monounsaturated fatty acids, with a high level of omega-3 polyunsaturated fatty acids (PUFA). Particularly promising candidate microalgae are those that can utilize seawater, can grow at high CO_2 concentrations and can be used to produce higher-value products. The ease of growing microalgae has brought these photosynthetic machineries into the focus of intense biofuel market. We have developed strains of marine diatom *Phaeodactylum tricornutum* that differ significantly in lipid profile and fatty acids.

Diatoms are marine microalgae which are photosynthetic sinks for capturing ambient carbon dioxide. Their carbon dioxide fixation rate is maintained through CO_2 levels ranging from atmospheric concentrations to as high as 10% carbon dioxide. At present, the diatoms contribution to global photosynthetic CO_2 fixation is comparable to that of the total rainforest contribution which makes them ideal for capturing CO_2 produced by fossil-fuel combustion. Encased in nanoporous silica shells, diatoms are a group of autotrophic organisms that arose by the evolutionary phenomenon of secondary endosymbiosis. Thus, their genome is composed of a diverse repertoire of both prokaryotic and eukaryotic genes. Diatoms also display an unmatched diversity in their intricate nanofabricated siliceous cell walls which can offer new directions for development of biological membranes that can aid in the separation of CO_2 from flue gas emissions from the thermal power stations. The omega-3 fatty acid rich biomass of diatoms can provide a valuable feedstock for aquaculture.

The CO_2 biosequestration potential of the marine diatom *Phaeodactylum tricornutum* is demonstrated under high CO_2 concentrations. *P. tricornutum* showed fastest growth rate of 0.5 day^{-1} at 4% v/v CO_2 and showed maximum CO_2 removal rate of 0.379 $gC^{-1}L^{-1}$ at 2% v/v CO_2. *P.*

tricornutum also accumulated high amounts of omega-3 polyunsaturated fatty acids (PUFA) with eicosapentaenoic acid as the major omega-3.

The yield of microalgae is the paramount factor for the control of overall economics. The various factors that determine yield include growth rate, cell density and lipid content of the microalgae. Biomass yield and associated lipids which can be utilized for biofuels is under the control of complex set of environmental and genetic factors. For achieving best yield selection of potential genotypes is a prerequisite. There exists an immense genetic pool of algae; however no large-scale industrial production is possible using the wild-type strain. For genetic enhancement of lipid content, a wild strain of *P. tricornutum* was chemically mutagenised with ethylmethane sulfonate in whole-genome mutagenesis screens where new strains were identified that over-accumulated lipids and displayed altered fatty acid profiles. Two approaches were used for the selection of novel mutants from large populations of the mutagenised cells of *P. tricornutum*. The two approaches were: (1) use of an antibiotic cerulenin for the isolation of novel *P. tricornutum* mutants with altered lipid profiles; and (2) use of Fluorescence Activated Cell Sorting (FACS) to isolate individual mutant cells (from which clonal populations can be established) with the highest levels of lipids compared to the progenitor strain. Through the development of these strategies a range of novel *P. tricornutum* mutants with altered lipid properties were isolated.

The novel *P. tricornutum* strains showed 2-2.5 fold increases in total dry weight lipids over the wild type progenitor and display the same growth rates. Two of the mutant strains, designated as *Ptcer12* and *Ptcer13*, accumulated very long chain fatty acids namely erucic (C22:1) and nervonic acid (C24:1) which have important industrial applications as biolubricants, cosmetics, pharmaceuticals and in dietary therapy. The novel *P. tricornutum* mutants screened and isolated using FACS accumulated 44-50% dry weight total lipids and higher biomass productivity. To facilitate targeted genome engineering of *P. tricornutum* we also used artificial microRNAs as a tool for gene knockdown experiments in *P. tricornutum*. The *P. tricornutum* transformants that were generated expressed the mature artificial microRNAs which elicited down-regulation of an endogenous *PHYTOENE SYNTHASE* (*PSY)* gene and concomitant knockdown of carotenoid levels.

1. CHAPTER ONE

Introduction

1. GENERAL INTRODUCTION

1.1 Untapped biodiversity of microalgae

The eukaryotic algae are a polyphyletic group of organisms with members found in five eukaryotic supergroups (Figure 1) (Keeling et al., 2005). Both green and red algae are included in supergroup plantae with other members of their supergroup. These organisms derived their chloroplast genomes from primary endosymbiosis of cyanobacterium. On the other hand, the cells of chromalveolate algae including diatoms, brown algae, eustigmatophytes and most dinoflagellates engulfed a red algal genome in a process called secondary endosymbiosis (Figure 2) (Armbrust, 2009).

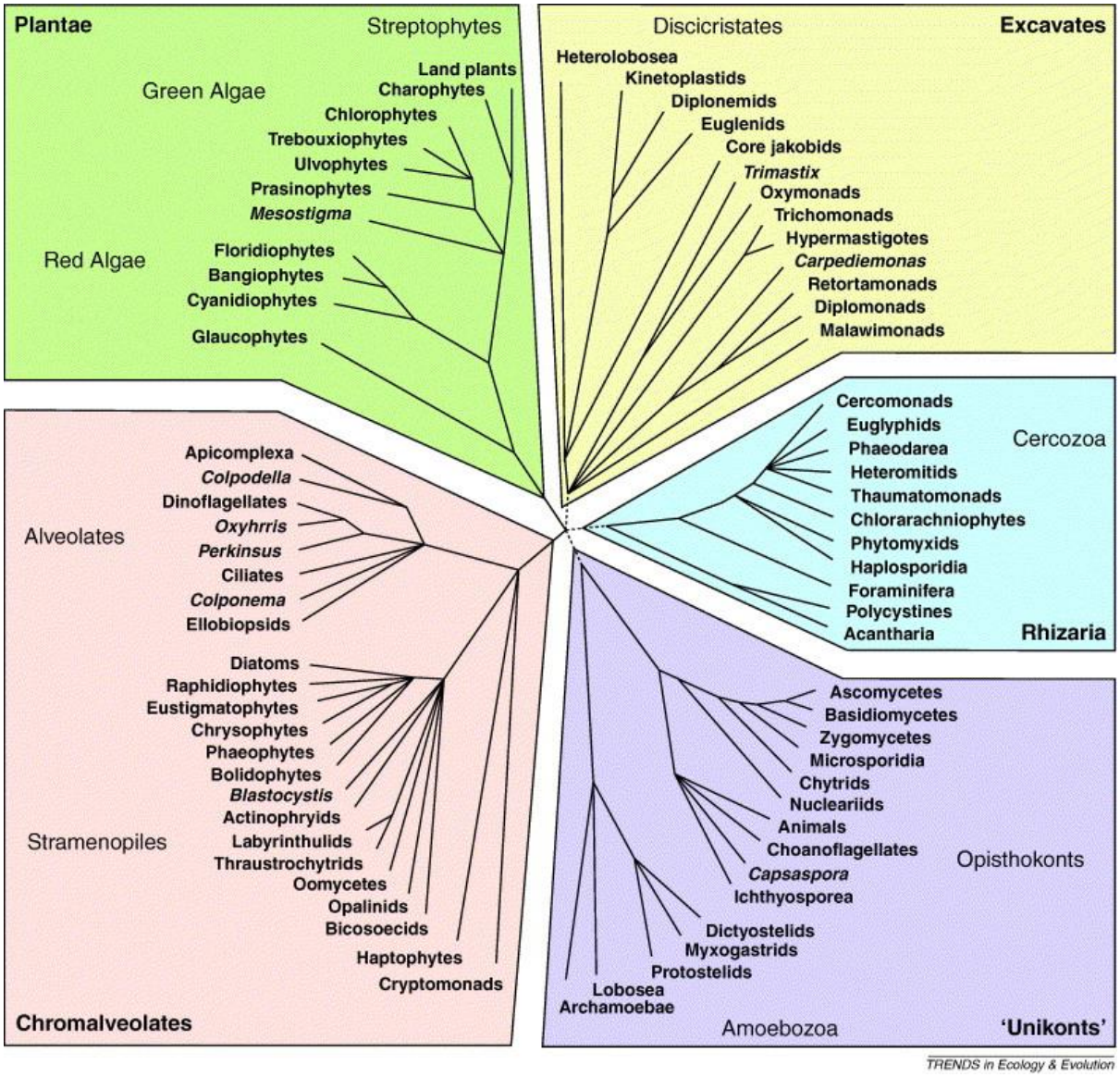

Figure 1. A possible tree of eukaryotes derived from molecular phylogenies and morphological and biochemical evidences. Tree comprised of five supergroups consisting of diverse eukaryotic life forms including algae (Keeling et al., 2005).

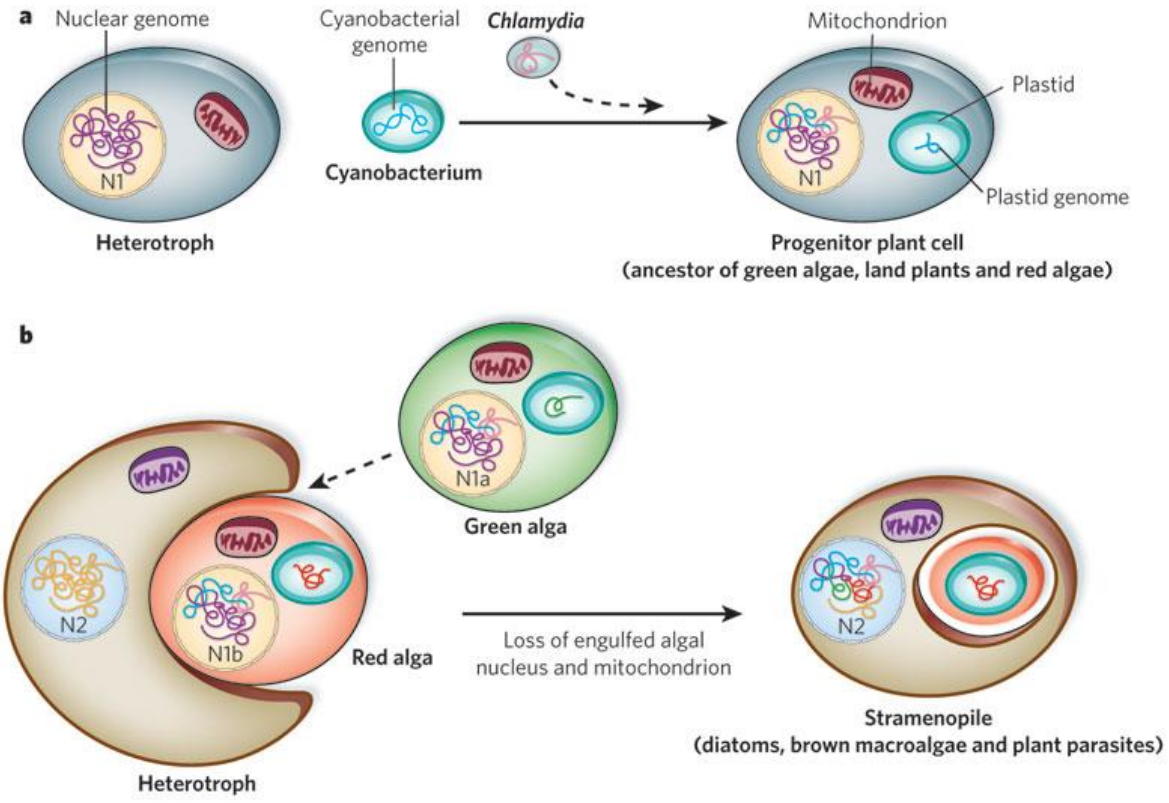

Figure 2. Diagram showing events of primary and secondary endosymbiosis that led to biogenesis of plastids in photosynthetic life forms. a) primary endosymbiosis where a cyanobacterium was engulfed into a heterotroph with transfer of most of the genome to host nucleus (N1); the cyanobacterium with few of its original genes formed the plastid in progenitor plant cell. Dashed line shows potential invasion by a chlamydial parasite. N1a and N1b show divergence of progenitor plant cell into green and red alga b) secondary endosymbiosis showing transfer of important algal nuclear and plastid genes (blue, purple and pink) to the host nucleus N2 leading to evolution of stramenopile plastid. (Armbrust, 2009).

Microalgae represent a vast and species rich group of photosynthetic and heterotrophic unicellular organisms. They have adapted to a broad array of environmental conditions such as saline, freshwater and terrestrial habitats, hot and cold springs, different mineral compositions and varied light conditions (Larkum et al., 2012). The free floating microalgae of lakes and seas are generally known as phytoplanktons. Among these phytoplanktons, the most diverse group (~200,000 species) are diatoms which are contributors of one-fifth of the photosynthesis on Earth (Armbrust, 2009). Diatoms are also the key players in the ocean carbon cycle which influence the CO_2 content of the atmosphere (Smetacek, 1999). During the Cretaceous period (100 Myr), diatoms likely played a dominant role in the carbon cycle, under atmospheric CO_2 levels five times higher than today which

also led to their diversification (Figure 3) (Armbrust, 2009). The raphid diatoms are the youngest lineage of diatoms and the most diversified (Bowler et al., 2008).

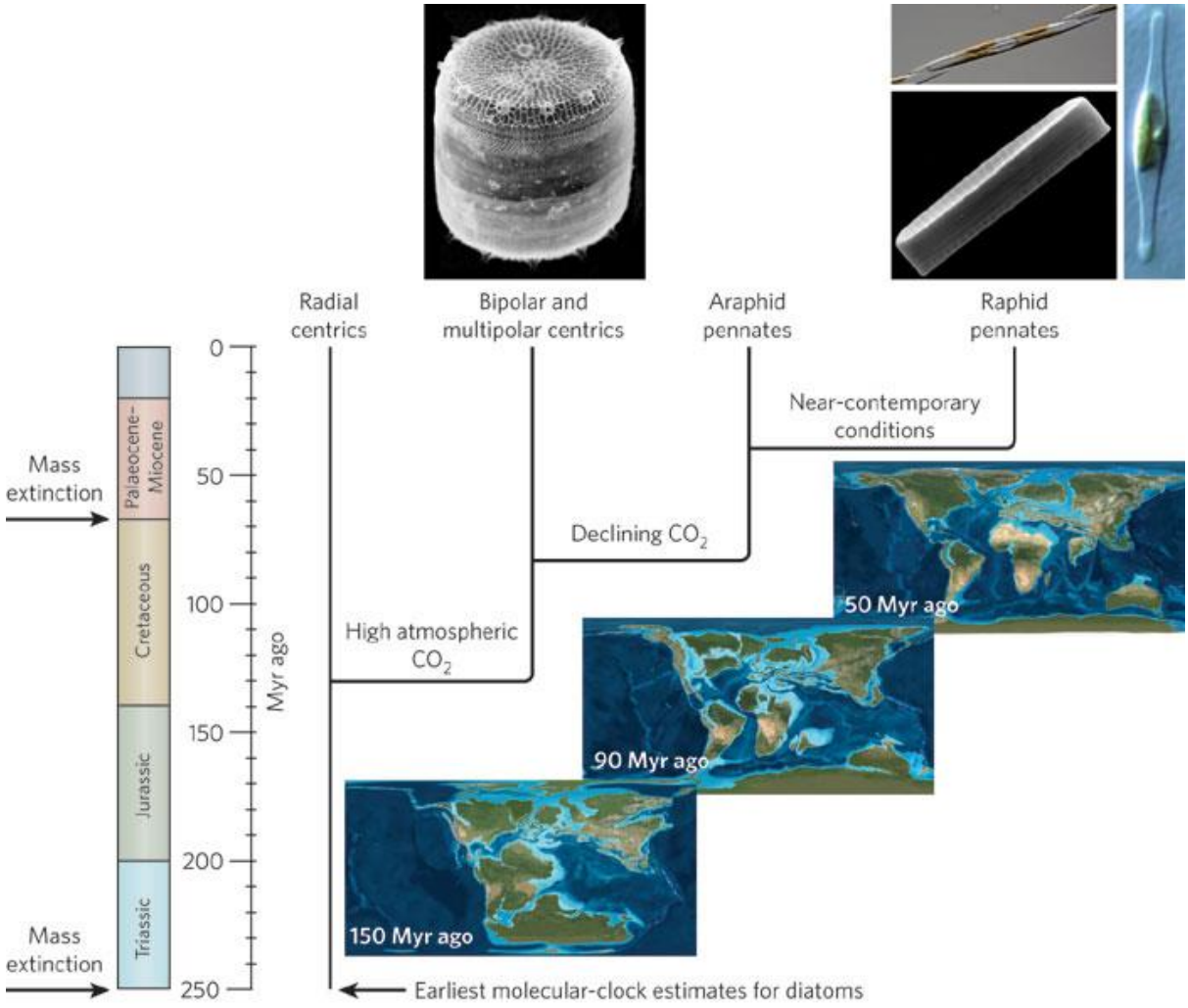

Figure 3. Diversification of four major diatom lineages and correlation with the Earth's atmospheric conditions in past geologic time periods. (Armbrust, 2009).

1.2 Domestication and genetic breeding of microalgae for lipids and fatty acids

Microalgae display high photosynthetic growth rates and are capable of accumulating oils, high value pharmaceuticals and nutraceutical products which are beneficial for mankind. Microalgae are miniature cell factories which have been commercially exploited as sources of valuable biomolecules such as proteins, pigments and fatty acids (León-Bañares et al., 2004). For lipid production, the main advantages of microalga breeding over higher plant breeding are (a) faster growth rates (b) higher oil yields, (c) seawater or brackish water cultivation on non-arable land, (d) combining of biomass production with direct bio-fixation of CO_2 and (e) modulations of biochemical composition of microalgae by varying growth conditions and genetic induction (Rodolfi et al., 2009). In addition,

microalgal oils are different from plant vegetable oils as they are rich in polyunsaturated fatty acids with four or more double bonds such as eicosapentaenoic acid (EPA, C20:5*n*-3), docosahexaenoic acid (DHA, C22:6*n*-3) (Chisti, 2007). Fatty acid chains of 18 or more carbon atoms and containing either three or more double bonds are classified as polyunsaturated fatty acids. Based on the position of the last double bond, they are grouped in two families named as omega-3 and omega-6 fatty acids. Microalgae are primary producers of polyunsaturated fatty acids (PUFA) (Figure 4) and play an important role as feedstock for aquaculture industry (Adarme-Vega et al., 2012; Adarme-Vega et al., 2014). PUFAs are derived from essential fatty acids linoleic and α-linolenic acid respectively. EPA which is an omega-3 polyunsaturated fatty is *de novo* synthesised in marine bacteria, microalgae and diatoms. These are the richest primary sources of EPA. EPA is largely found in polar lipids that constitute the cell membranes including thylakoid membranes (Desbois et al., 2009). The major dietary sources of EPA and DHA for humans are fatty fishes such as tuna, salmon and mackerel. EPA serves as an essential fatty acid for human metabolism, it maintains blood lipid equilibrium by lowering the triglyceride levels in serum which reduces the degree of platelet aggregation (Simopoulos, 1991). The advantage of diatoms derived EPA is that it will be a vegetarian source of nutrional fatty acid. Naturally existing microalgae are however not genetically programmed for overaccumulating any particular product which is desirable for commercial use. Thus, robust molecular biology tools for genetic modification are required to improve useful traits in microalgae (Kilian et al., 2011; Larkum et al., 2012).

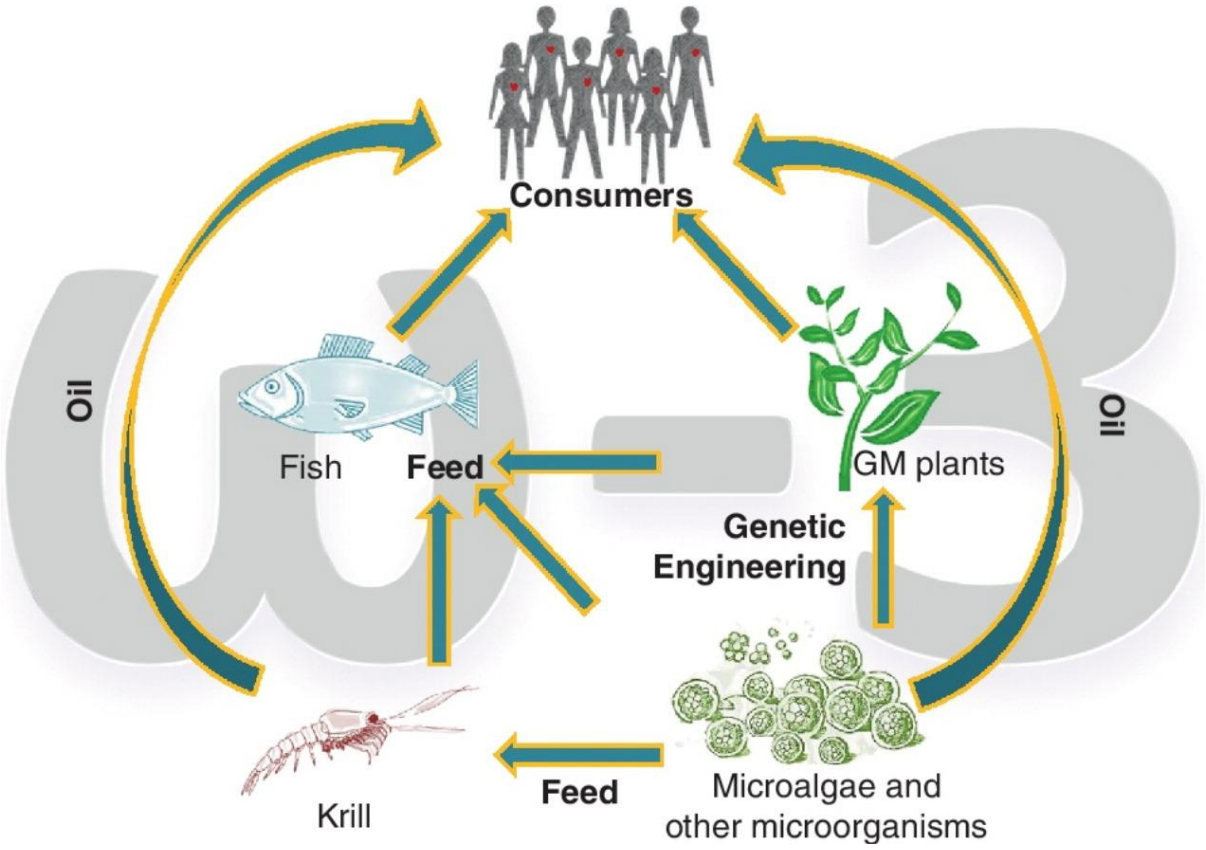

Figure 4. Diagrammatic representation showing various sources of polyunsaturated omega-3 fatty acid and how they are linked in the food chain. Microalgae being the primary source constitute important component of aquaculture feed. (Adarme-Vega et al., 2014).

1.3 Potential of microalgae for carbon dioxide biosequestration

Carbon dioxide (CO_2) accounts for 68% of the total anthropogenic greenhouse gases which are responsible for global climate change (Ho et al., 2011). For this reason, many R & D efforts have been put in to mitigating the effects of CO_2, in particular in the arena of carbon capture. There is a wide range of proposed CO_2 removal or capture solutions which are based on chemical absorbents, amine and carbonate based solvents, membranes, metal organic frameworks (MOFs) (Figueroa et al., 2008), direct oceanic injection (Ametistova et al., 2002), geologic storage (Harvey et al., 2012), and biomitigation (Kumar et al., 2011). For the deployment of any of these technologies, considerations of energy efficiency, cost effectiveness and sustainability are needed. Technologies for carbon capture from large single-point emission locations like power plants adopt three different pathways namely pre-combustion, post-combustion and oxy-combustion (see review Figueroa, et al. 2008). According to Klaus Lackner (Lackner, 2003), 'sequestration in environmentally active carbon pools (such as the oceans) seems ill advised because it may trade one environmental problem for another'. Klaus Lackner (Lackner, 2003) also concludes that photosynthesis is the only practical form of carbon capture. In addition, microalgae and cyanobacteria biomass generated during CO_2 capture can be utilized as feedstock for biofuels, nutritional foods, medication, cosmetics and aquaculture feed. Based on the above criteria, some of the microalgal and cyanobacterial species that have been considered as potentially useful for CO_2 mitigation include *Botryococcus braunii* (Yen Doan and Obbard, 2011), *Chlorella vulgaris* (Chen et al., 2010), *Chlorococcum littorale* (Ota et al., 2009), *Scenedesmus* sp. (Morais and Costa, 2007), *Chlamydomonas reinhardtii* (Packer, 2009) and *Spirulina* sp. (Morais and Costa, 2007) respectively.

1.4 Molecular strategies used for breeding of microalgae

Microalgae including diatoms have been investigated as renewable source of biofuels for over five decades and have also attracted major attention for carbon mitigation from industry sites as an add-on for biofuel production. Some microalgae can grow on saline and wastewater which helps to circumvent the need for freshwater and competition with agricultural resources for arable crops. Their unicellularity and short life cycles without any seasonal cycles can aid in miniaturization of the breeding systems which can in turn assist in reducing the economics of microalgal industrial production. Microalgae-based products that are already commercially exploited include food additives such as carotenoids, natural dyes and dietary supplements, polyunsaturated fatty acids, bioactive compounds and polysaccharides (León-Bañares et al., 2004). The unicellular nature facilitates screened with automated high throughput screening platforms. Breeding of microalgae for

commercial purposes requires genetic reprogramming of wild or natural strains for an optimised production of desired bioproducts under standard operation conditions. The microalgal species *Chlamydomonas reinhardtii* (Molnar et al., 2009) and *Phaeodactylum tricornutum* (De Riso et al., 2009) with sequenced genomes can also be more efficiently targeted for gene down-regulation through RNA interference. However, lack of genomic data and transformation techniques for many microalgal species is a limitation for developing transgenic and gene-targeting based molecular technologies in microalgae. In contrast, the random mutagenesis using UV radiations and chemicals can be applied to any microalgae to develop new strains through a "black box" forward genetics approach (Larkum et al., 2012).

1.5 Molecular breeding through whole genome mutagenesis

Mutations are heritable (mitotically or meiotically) changes in the genome of an organism which can be artificially induced by causal agents called mutagens. Some of the different mutagens widely used in genetics research include; (a) chemical mutagens like ethyl methanesulfonate (EMS) and *N*-ethyl-*N*-nitrosourea (ENU), *N*-methyl-*N*-nitrosourea (MNU), methyl methanesulfonate (MMS), 1-methyl 3-nitro 1-nitrosoguanidine (NTG), (b) physical mutagens such as UV, fast neutron bombardment, gamma and X-rays and (c) biological mutagens such as T-DNA or transposons (Maple and Moller, 2007). To date, due to the relatively limited development of molecular tools for microalgal genetics, EMS and UV mutagenesis techniques have been the main approaches for development of novel strains of microalgae for commercial biotechnological uses.

In microalgae, EMS has been successfully exploited to induce higher accumulation of metabolites like pigments and fatty acids. Induced mutations by EMS in marine microalga *Nannochloropsis oculata* have been used to enhance EPA content (Chaturvedi and Fujita, 2006). In the diatom *Cyclotella* sp. EMS was used to generate a loss of brown fucoxanthin pigment generating loss of antenna mutants (Huesemann et al., 2009). In the freshwater green microalga *Haematococcus pluvialis* EMS treatment enhanced (2.2-3.2 fold) astaxanthin accumulation (Tripathi et al., 2001). In *Nannochloropsis* sp. EMS mutants showed four-fold increase in total fatty acid content (Doan and Obbard, 2012).

Ethyl methanesulfonate (EMS) is an alkylating agent that induces chemical modification of nucleotides resulting in mispairing and base changes. Depending on the dose applied, EMS can permit saturation mutagenesis by generating a high density of irreversible mutations in the genome that can generate mutant alleles of genes. In the case of microalgae which lacking a sexual phase, the mutant alleles are likely to remain in a heterozygous state and hence any mutant effects are likely due to gain-of-function dominant effects. Such dominant or gain-of-function effects can arise due to novel versions of proteins due to alterations of specific amino acids (Maple and Moller, 2007). For instance,

dominant mutant phenotypes arising from chemical mutagenesis may be caused by missense mutations that lead to protein function modification (Medina et al., 1998).

1.6 Screening of ethyl methanesulfonate mutants using metabolic inhibitors and FACS

EMS mutagenesis can be used to generate very large populations of diverse mutant cells. Within this vast diversity the challenge is to develop selective "forward genetic" screens where individual cells displaying the desired phenotypes can be isolated from all of the other cells in the mixed mutant population. Screening of EMS mutants can be done on defined growth medium that will allow the recovery of mutants showing alterations in biosynthetic pathways. A selection method that allows only the mutants of interest to grow and ensure avoidance of false positive is necessary (Page and Grossniklaus, 2002). EMS saturation mutagenesis populations of microalgae can be screened using metabolic inhibitors such as antibiotics and herbicides and fluorescent probes. For instance, use of metabolic inhibitors such as the antibiotics cerulenin and erythromycin (Chaturvedi and Fujita, 2006) and herbicides like quizalofop (Chaturvedi et al., 2004) can allow the isolation of mutants and scoring of the mutation rate. For automated isolation of desired mutants, flouroscence activated cell sorting (FACS) is used (Figure 5).

A) Metabolic inhibutor based approaches: Antibiotic metabolic inhibitors such as cerulenin are useful for isolation of fatty acid over-producing mutants of microalgae. Use of such metabolic inhibitors provides a way to downregulate the activity of enzymes involved in a biosynthetic pathway that one intends to alter via mutagenesis. For altering levels of fatty acids in microalgae, cerulenin is used as a known inhibitor of the enzyme ketoacyl-acyl carrier protein (ACP) synthase (KAS) (Figure 6). The three different ACP enzymes involved in *de novo* fatty acid biosynthesis are important regulators of the initiation and elongation steps in the pathway. ACP synthase I (FabB) catalyse elongation of unsaturated fatty acids, synthase II (FabF) control the thermo dependent regulation of fatty acid composition and third synthase III (FabH) is involved in condensation and govern the rate of fatty acid synthesis. These condensation enzymes have similar active sites but there exists subtle structural variations that define their differential response to antibiotics which is in the order FabB > FabF >> FabH (Price et al., 2001).

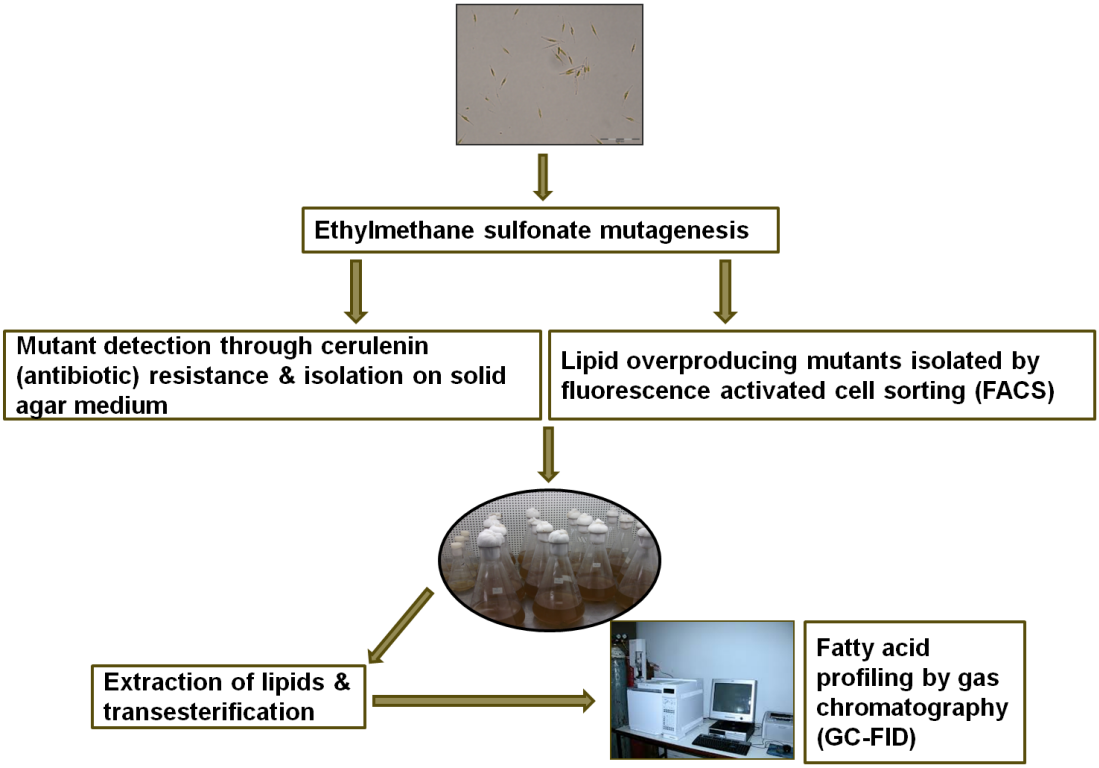

Figure 5. Schematic diagram of research methodology for ethylmethane sulfonate mutagenesis of marine diatom *Phaeodactylum tricornutum*.

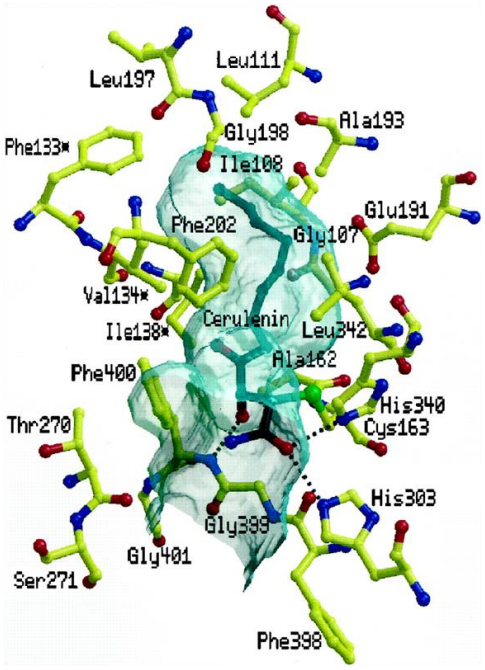

Figure 6. Cerulenin covalently binds to the active site cysteine residue of the fatty acid synthase enzyme KASII (Moche et al., 1999).

B) FACS based approaches: For rapid screening and isolation of desired mutant lines, electronic cell sorting in conjugation with flow cytometry can also be used for isolation of individual microalgal mutant cells from millions of other cells. Flow cytometric cell sorting has mainly been used to date for biodiscovery approaches of natural variants e.g. utilized as a rapid tool for isolation of different types of microalgae both from mixed culture assemblages or from natural water samples (Meiser et al., 2004). The use of FACS based approaches combined with mutagenesis developed in this PhD represents an extremely powerful approach for the generation of novel gain-of-function mutants of microalgae where potentially every base in the genome has been mutagenised in the overall mutagenised population. What is necessary for such FACS based approaches to mutagenesis breeding is a cell-autonomous reporter system which provides a fluorescence readout which is directly relevant to the trait of interest. In this PhD thesis, we have developed this approach for FACS-assisted mutagenesis breeding of *P. tricornutum* using fluorescent probes that are specific to cellular lipids (e.g. nile red and BODIPY 505/515 (Hyka et al., 2013) that can be used to act as markers to identify individual mutant cells that are hyperaccumulating lipids.

1.7 Molecular breeding through genetic engineering

Molecular biology tools are needed to standardize genetic transformation and genetic engineering of microalgae (León-Bañares et al., 2004). For model green alga *Chlamydomonas reinhardtii* and cyanobacterium *Synechococcus elongatus* genetic engineering kits are available commercially at http://www.lifetechnologies.com/ie/en/home/life-science/protein-expression-and-analysis/protein-expression/algae-engineering-kits.html. Genetic engineering of microalgae is facilitated by the access

to microalgal genome sequences of several industrially important species namely *C. reinhardtii*, *Phaeodactylum tricornutum*, *Thalassiosira pseudonana*, *Cyanidioschyzon merole*, *Psuedo-nitzschia*, *Botryococcus braunii*, *Chlorella vulgaris*, *Dunaliella salina* (Radakovits et al., 2010). Targeted gene regulation via homologous recombination is currently possible only in species undergoing sexual reproduction, such as oil producing algae *Nannochloropsis* sp. (Kilian et al., 2011) and the commercially important microalga *Schizochytrium* (Cheng et al., 2011).

1.8 Genetic engineering involving microRNA mediated gene regulation

MicroRNAs (miRNAs) are 21-24 nucleotide RNA duplex molecules involved in post-transcriptional regulation (Molnar et al. 2007). The RNA-silencing is a cascading event involving four different consensus biochemical steps (Voinnet, 2009). The first step is initiated by RNA polymerase II with the transcription of *MIR* genes that are usually located between two protein coding genes. The transcript formed in this step has a hairpin loop like structure named as pri-miRNA which in *A. thaliana* is stabilized by binding of RNA-binding protein DAWDLE (DDL). The combined action and physical interaction of C2H2-zinc finger protein SERRATE, dsRNA binding protein HYPONASTIC LEAVES1 (HYL1), double strand specific RNases of the Dicer family such as dicer like 1 (DCL1) and nuclear cap-binding complex (CBC) converts pri-miRNA to pre-miRNA. The siRNAs originating from hairpin transgenes typically contain non-coding near promoter sequences that methylates the DNA and cause chromatin modification (Ossowski et al., 2008). Thus, diced sRNA duplexes participating in the transcriptional gene silencing are retained in the nucleus. For the post transcriptional gene silencing that occurs in the cytoplasm, sRNA duplexes are exported out of the nucleus (Voinnet, 2009).

The immediate products of Dicer are short, 5' -phosphorylated dsRNAs with two nucleotide 3' overhangs (Bernstein et al., 2001). These short dsRNA intermediates are processed in both miRNA and siRNA pathways. In plants, these dsRNA or sRNA duplexes, include miRNA-miRNA* which are stabilized by methyltransferase HUA ENHANCER 1 (Yu et al., 2005). The 5' end of one of the strands of these dsRNAs has a lower thermodynamic stability which is retained by the second protein molecule called Argonaute (AGO) protein (Khvorova et al., 2003). The second strand of dsRNA is called passenger strand or miRNA* which does not take part in further processing and is rapidly degraded (Molnar et al., 2007). The plant miRNAs often starts with a U and carry a C at the last pairing nucleotide (position 19) in a 21 nucleotide miRNA-miRNA* duplex (Ossowski et al., 2008). The post-transcriptional gene silencing mediated by dsRNA duplexes occurs when the guide strand target the homologous sequences on the mRNA which causes the target mRNA destruction (Ossowski et al., 2008).

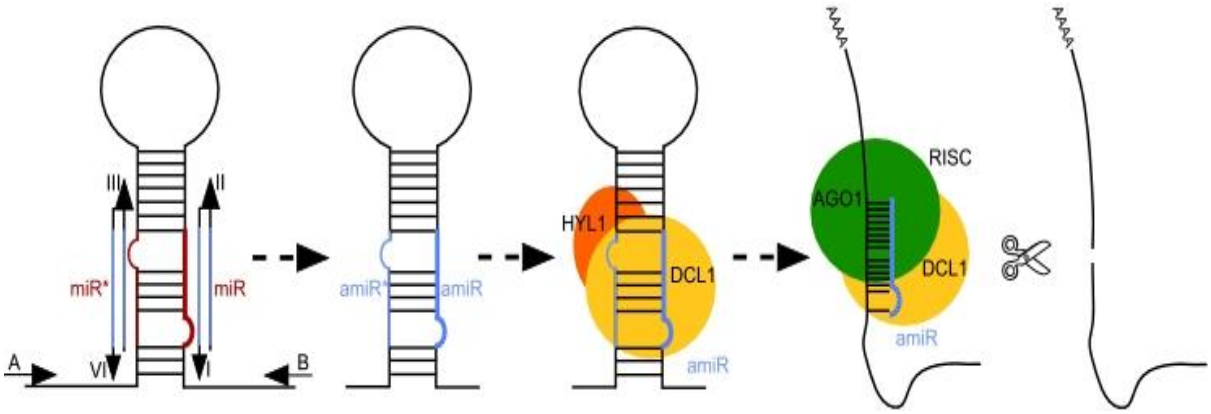

Figure 7. Diagram showing molecular strategy of engineering amiRNA sequences into the endogenous miRNA precursor and the subsequent RNA induced silencing machinery for mRNA degradation. miR- endogenous microRNA, miR*-passenger strand amiR* and amiR- artificial microRNA strands, HYL1- protein HYPONASTIC LEAVES, DCL1- dicer like 1, RISC- RNA induced silencing complex. Source- wmd3.weigelworld.org

Similar to endogenous miRNA, artificial microRNAs (amiRNAs) are also single-stranded 21 nucleotide long RNA molecules which can be designed and introduced into genomes by genetic engineering. Artificial microRNAs can be specifically designed to target mRNA of endogenous or transgenes. In *Arabidopsis*, endogenous miRNA precursor mir319a has been engineered into amiRNA by replacing the original mir319a with artificial oligonucleotides which is subsequently processed by the cellular RISC silencing machinery (Figure 7, Source-wmd3.weigelworld.org). *Arabidopsis* precursors have successfully worked in other crops such as tomato and tobacco (Alvarez et al., 2006) suggestong that the precursor backbone can be used across different taxa. To date, for microalgae artificial miRNAs have only been used for gene silencing in the green microalga *C. reinhardtii* (Molnar et al., 2009).

1.9 Breeding of pennate diatom *Phaeodactylum tricornutum* for overproduction of lipids

Diatoms are a representative algal group for exploring the biology of marine phytoplanktons (Martino et al., 2007). The pennate model diatom *Phaeodactylum tricornutum* is among the few microalgal strains for which full or near-full genomes sequences and transformation systems have been developed. This organism can typically exhibit three morphotypes namely oval, fusiform and triradiate (Figure 8). *P. tricornutum* possess a genome of 27.4 Mb size with 10,402 currently predicted genes (Bowler et al., 2008). The diatom *P. tricornutum* is a rich source of eicosapentaenoic acid. In *P. tricornutum* which does not show sexual reproduction, targeted gene regulation can be achieved via RNA interference (De Riso et al., 2009).

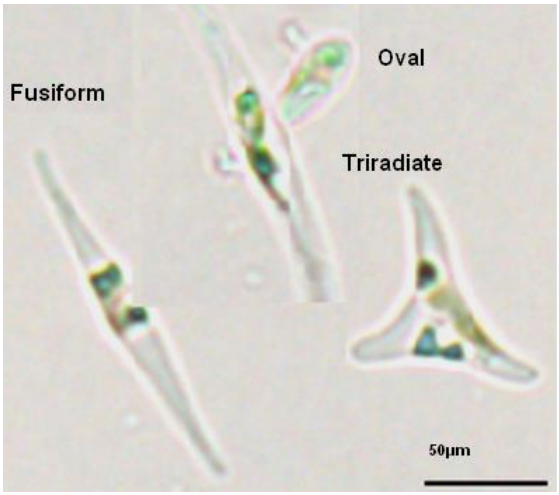

Figure 8. Three morphotypes of *P. tricornutum*.

Although *P. tricornutum* is a rich source of marine EPA, commercial production is not economically feasible with the level of bioproduction in current naturally occurring or wild-type strains. As discussed in earlier sections, whole-genome mutagenesis approaches can be used to generate strains with improved metabolite production in microalgae. Mutagenesis experiments using UV in *P. tricornutum* have generated mutants showing 44% increase in EPA content (as % of dry weight) over wild-type (Alonso et al., 1996). As discussed in section 1.4 and 1.5, lipid and fatty acid content of microalgae can be improved through EMS mutagenesis followed by the isolation of new mutants using metabolic inhibitors or directly by FACS. In this research, *P. tricornutum* was treated with mutagen EMS to generate mutant cell lines with altered cellular lipids and fatty acids profiles.

Fatty acids are building blocks for the phospholipids of cell membranes. The two types of fatty acid (FAS) biosynthesis mechanisms are type I system which is found in mammals and lower eukaryotes and type II systems, found in bacteria and plants. All plastid-containing organisms including diatoms carry out de novo biosynthesis of fatty acids within the plastid via a type II fatty acyl synthase, followed by export of fatty acids to the cytoplasm (Armbrust et al., 2004). In type II reactions, catalysis occur through a series of soluble proteins that are encoded by a discrete gene, and the pathway intermediates are transferred between the enzymes as thioesters of a holo-[acp]. The fatty acid biosynthesis is initiated upon production of an acetoacetyl-[acp], an activated molecule which is subsequently used for the elongation reactions that ultimately produce the fatty acids (Figure 9) (Fabris et al., 2012). In type II system, there are three β-ketoacyl-ACP synthases which are important regulators of the initiation and elongation steps in fatty acid synthesis pathway. The condensation reaction catalysed by the three enzymes carry out transfer of an acyl primer to malonyl-ACP and forms a β-ketoacyl-ACP that has been lengthened by two carbon atoms (Figure 9). The three synthases are synthase I (FabB), synthase II (FabF) and synthase III (FabH). In general, the enzyme encoded by FabH is responsible for initiation of fatty acid elongation by utilizing acyl-coA primers,

while the FabB/FabF products are responsible for successive rounds of elongation reactions through condensation of malonyl-ACP with different length acyl-ACPs which extend the acyl chain by two carbons (White et al., 2005). The antibiotic cerulenin was used because it targets type II fatty acid synthesis pathway and is an inhibitor of fatty acid synthase enzyme (Figure 6, section 1.6).

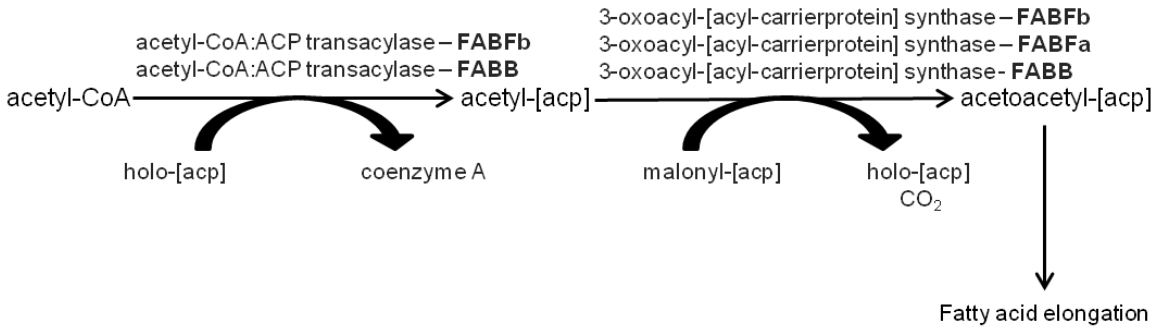

Figure 9. Diagram showing enzymatic pathway involved in the biosynthesis of fatty acids in *P. tricornutum.* The antibiotic cerulenin binds to 3-oxoacyl-acp-synthase enzyme which is coded by genes FABFb, FABFa and FABB (Source- DiatomCyc v 1.0).

Another approach of acquiring desired mutants showing overproduction of cellular lipids is by FACS. Using FACS, thousands of cells per second can be analysed based on their fluorescence intensity upon binding to the lipophilic probes such as BODIPY. The ability of flow cytometers to analyse cells at high flow rate (up to 100,000 events per second) and to detect low signals make it possible to count cells and simultaneously analyse several cell physical and chemical properties with high sensitivity and in a very short period of time. As thousands of cells per second can be screened by FACS, this allows the screening of tens of millions of cells within minutes to hour type time-scales. As the genome of *P. tricornutum* is composed of approx 27,400,000 nucleotides FACS-based mutagenesis offers the possibility of generating a population of cells (e.g. 10s of millions of cells) where each base in the *P. tricornutum* genome is mutagenised at least once.

1.10 Implications of present research for diatom biotechnology

Development of new strains or mutants that have acquired useful traits such as lipid overproduction and high value fatty acids is necessary for commercialisation of microalgal derived bioproducts. Diatom biomass has various biotechnological applications that include polyunsaturated fatty acids for pharmaceuticals and biodiesel. Diatoms that grow in saline waters and producing up to 60% of their biomass as triacylglycerols (TAGs) under certain growth conditions have been identified as potential candidates for biodiesel (Zendejas et al., 2012).

Apart from biotechnological applications, diatoms are also potential candidates for biological sequestration of high levels of CO_2. In this research, various parameters such as growth, cell density, biomass productivity, lipids and fatty acids production under high levels of CO_2 have been investigated to harness the CO_2 fixation potential of *P. tricornutum*. This research study indicates that *P.tricornutum* is a potential candidate for CO_2 biosequestration. However, the CO_2 fixation capacity of this diatom can further be increased by optimising the nutrient and light conditions. The potential applications of this research work in a diatom biotechnology or biorefinery concept is diagrammatically represented in Figure 10.

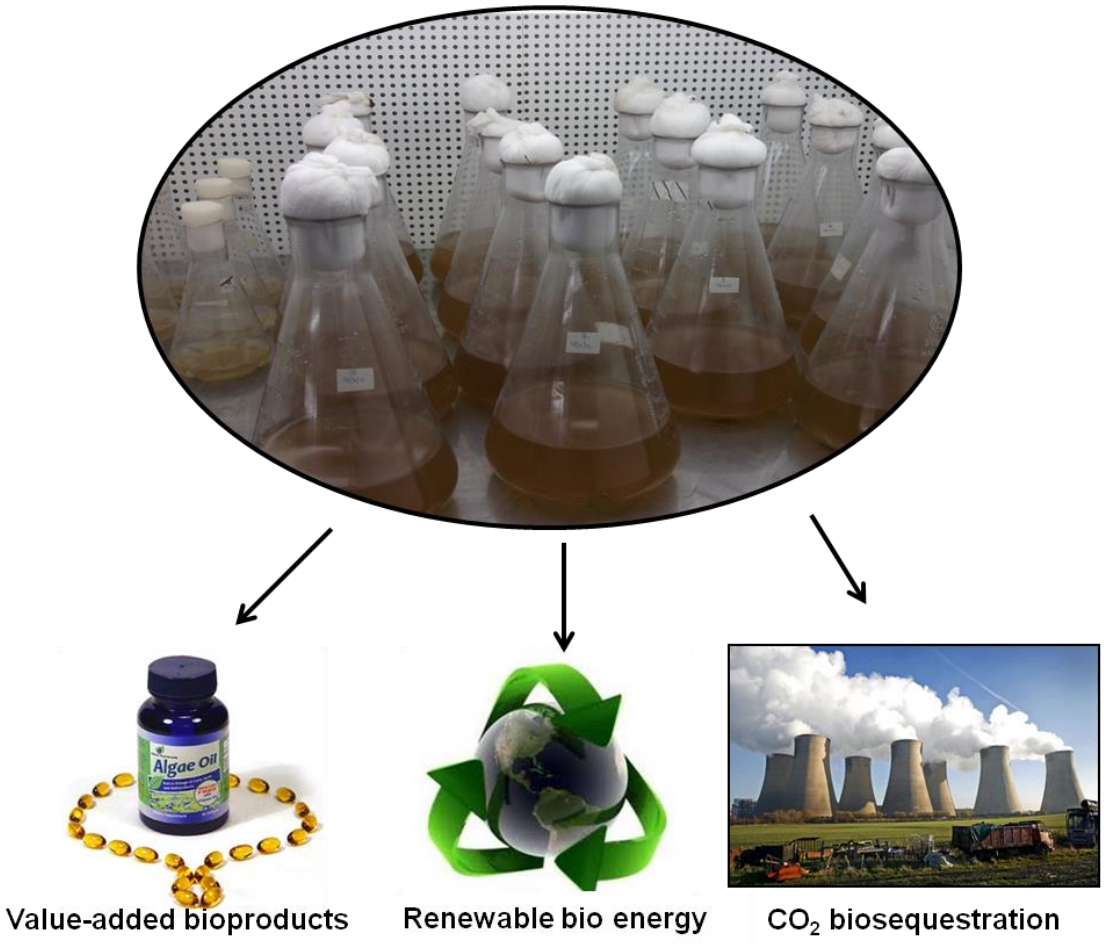

Figure 10. Diagram showing proposed biotechnological and environmental applications of breeding and domestication of new mutants of *P. tricornutum* generated in present study.

2. CHAPTER TWO

Carbon dioxide removal under elevated CO_2 concentrations by the eicosapentaenoic fatty acid-rich diatom *Phaeodactylum tricornutum*

Chapter 2 – Effect of high CO_2 on growth and oil production

ABSTRACT

The carbon dioxide biosequestration potential of the marine diatom *Phaeodactylum tricornutum* was investigated by exposing cells to high levels of CO_2 which are above the atmospheric concentrations projected by the end of this century. The CO_2 was provided by bubbling of six different concentrations of CO_2 enriched air (0.03%, 1%, 2%, 4%, 5% and 10%) at an aeration flow rate of 30 $ml.min^{-1}$. The fastest growth rate of 0.502 day^{-1} was obtained at 4% CO_2. However a severe inhibition of growth was observed at 10% CO_2. To mitigate the inhibitory effect of high CO_2 concentration the aeration flow rate was reduced to 10 $ml.min^{-1}$. The lowering of aeration flow rate significantly affected the growth rate, % CO_2 retention and CO_2 removal rates at high CO_2 concentration as analysed statistically by two-way ANOVA test. The diatom *P. tricornutum* showed maximum CO_2 removal rate of 0.379 $gC^{-1}L^{-1}$ at 2% CO_2 when bubbled with 10 $ml.min^{-1}$ aeration flow rate. Fine structural changes in the chloroplasts of cells exposed to elevated CO_2 levels were analysed which indicated that chloroplasts of cells grown at 5% CO_2 concentration decreased the size of their pyrenoids. The impact of high CO_2 growth was also observed on the production of cellular lipids and fatty acids. The highest levels of total lipids were observed at 5% CO_2 concentration. However maximum production of polyunsaturated fatty acids including eicosapentaenoic acid (2.21% dry weight biomass) was observed at 1% CO_2 with 10 $ml.min^{-1}$ aeration flow rate. Increased content of valuable bioproducts such as lipids and fatty acids has implications for enhancing the commercial value of *P. tricornutum* biomass generated during CO_2 biosequestration.

Chapter 2 – Effect of high CO_2 on growth and oil production

2.1 INTRODUCTION

Current carbon dioxide (CO_2) levels are higher than recorded for millions of years as demonstrated by paleoclimate reconstructions, which also demonstrate that global warming over past 140 years is beyond any natural climate variability (Schrag, 2007). Burning of coal, oil and gas is primarily responsible for increment of atmospheric CO_2 at 315 parts per million (ppm) in late 1950s to over 380 ppm in 2005 as shown in a classic climate experiment by Charles David Keeling (Keeling et al., 2001; Schrag, 2007). The effects of CO_2 emissions from combustion of fossil fuels are imposing a necessity to tackle climate change at global level. Carbon dioxide mitigation strategies include carbon capture and sequestration (CCS), which are typically non-biological (geologic and oceanic) processes based on engineering excellence and biological recycling of carbon (photosynthetic conversion of CO_2 into useable biomass). The biological process of photosynthesis can utilize CO_2 generated from fossil fuels burning and thus represents a post-combustion CO_2 capture (Figueroa et al., 2008), which can provides a sustainable outcome irrespective of the scale that it attains in mitigating global warming (Lehmann, 2009). Achieving the targets of 350 ppm concentrations of atmospheric CO_2, necessitates both the withdrawal of CO_2 from atmosphere in addition to the fossil fuel emissions capture (Lehmann, 2009). Conflicting demands of food over fuel and mushrooming need for feed, fibre and green chemicals are serious challenges for mankind at the time when we also need to address climate change. Global demands for these land based commodities will surpass supply which may bring civil unrest, hunger and malnutrition (Nepstad et al., 2013). Other environmental issues associated with agriculture's environmental footprint that pose challenges at global scale includes scarcity of fresh water, degradation of ecological biodiversity and release of toxic wastes in to the environment (Foley et al., 2011).

One possible environmentally safe and sustainable solution is the selection of alternative green energy source that can be cultivated in marine waters or waste waters and still offer us feed and fuel. Microalgae have been proposed as renewable and sustainable biological solution for climate change mitigation based on the following criteria: convert CO_2 into biomass (Acién Fernández et al., 2012); existence of high CO_2 tolerant natural strains (Solovchenko and Khozin-Goldberg, 2013); higher photosynthetic efficiency as compared to terrestrial plants (Packer, 2009) and biofuel crops (Kumar et al., 2010); transformation of its biomass to methane (Kumar et al., 2010), hydrogen (Benemann, 2000; Kruse and Hankamer, 2010), biodiesel (Francisco et al., 2010), bio-oil (Wang et al., 2013), human nutritional supplements and animal feed (Sijtsma and Swaaf, 2004); and bioremediation through waste water treatment (Cicci et al., 2013; Franchino et al., 2013; Pires et al., 2013; Posadas et al., 2013).

The ocean-atmosphere carbon partitioning is determined by shifting of the C:N:P stochiometry of marine primary production which is majorly derived from marine algae (Kumar et al.,

2010). Therefore, sustainability of microalgal based carbon mitigation could be achieved through combining microalgal biomass production with existing power generation and wastewater treatments infrastructures (Kumar et al., 2010).

In the current anthropocene period, CO_2 emissions associated with human activities are having strong unintended impacts on the global carbon cycle (Figueroa et al., 2008; Kumar et al., 2010; McGinn et al., 2011; Ulf, 2004). To stabilize atmospheric CO_2 concentrations, various strategies have been proposed to capture excess CO_2. One of these strategies is oceanic CO_2 sequestration in which CO_2 is either directly injected into deep ocean or is captured by biological fixation (Ulf, 2004). Microalgal photosynthesis is a biological method of CO_2 removal which has received much attention for mitigating anthropogenic climate-change (Adarme-Vega et al., 2012; Kumar et al., 2010; McGinn et al., 2011).

The study of microalgal CO_2 biofixation capabilities has to date mainly involved isolation of suitable species, photobioreactor design for optimised growth, and research into carbon concentrating mechanisms (Francisco et al., 2010; Raven et al., 2008). CO_2 sources amenable to biomitigation by microalgae include; industrial exhaust gases (typically termed 'flue gas'), solubilized carbonates, and atmospheric CO_2 itself (Kumar et al., 2010). The concentration of available CO_2 in these sources is variable and thus microalgae may be exposed to different levels of CO_2 in turn. However, atmospheric CO_2 levels are considerably lower than required for high biomass productivity as the diffusion of CO_2 into water is an inefficient process (McGinn et al., 2011). Altered carbon availability can however dramatically impact microalgal growth and biochemical composition through effects on the rate of photosynthesis. The source of carbon in aqueous environments is dissolved CO_2 which exists in equilibrium with H_2CO_3, HCO_3^- and CO_3^{2-}. Of these, the preferred chemical form for uptake by microalgae is HCO_3^- (Carvalho et al., 2006) which is the dominant form of hydrated CO_2 in aqueous microalgal culture systems between pH 6.35 and 10.33 (Van Den Hende et al., 2012).

Despite the importance of identifying the optimal microalgal species for use in carbon sequestration, only a handful of microalgal species have so far been tested for their CO_2 sequestration potential. Most of these species belong to freshwater green algae including *Chlorococcum litorrale*, *Chlorella vulgaris*, *Chlorella kesseleri*, *Scenedesmus obliquus*, *Dunaliella tertiolecta*, *Botryococcus braunii*, *Nannochloropsis oculata*, and cyanobacterium *Spirulina platensis* (Chiu et al., 2009; de Morais and Costa, 2007; Ota et al., 2009; Sydney et al., 2010; Tang et al., 2011). These studies have shown that CO_2 tolerance in microalgae is species-dependent, but also that different species show different responses to changes in culture conditions such as cell culture density, pH, nutrients and light (Van Den Hende et al., 2012). Although these elevated CO_2 levels can enhance growth rate of microalgae (Gordillo et al., 2003), higher atmospheric concentrations of CO_2 can also act as an environmental stress leading to loss of sequestration capability of algal cells (Sobczuk et al., 2000). Fossil fuel exhausts are ~12% CO_2 (Lee et al., 2002) so microalgae must be able to grow at this

concentration to be suitable for sequestering CO_2 emitted from thermal power stations. To address these conflicting requirements, we conducted a study of the CO_2 tolerance and carbon sequestration potential of a marine diatom considered to have potential as a feedstock for the commercially valuable omega-3 fatty acid, eicosapentaenoic acid.

2.2 MATERIALS and METHODS

2.2.1 Culture conditions

The diatom *Phaeodactylum tricornutum* CCAP 1055/A culture was purchased from the Culture Collection of Algae and Protozoa (CCAP), Scottish Marine Institute Oban, UK. Diatom cells were grown in F2 (Guillard, 1975) nutrient-enriched natural seawater medium in 500 ml Schott Duran pressure bottles. The cells were fed with air and five varying air-CO_2 concentrations sparged at two different flow rates of 10 ml min^{-1} and 30 ml min^{-1}. The different air-CO_2 concentrations were generated by mixing compressed air with pure CO_2 and aeration flow rates were maintained by flowmeters (Supelco Analytical, Bellefonte, PA). Complete experimental setup depicting generation of aeration mixture and sequential feeding into culture vessels is represented in Figure 11. Aeration was provided by bubbling 0.2 µm filtered air and air-CO_2 mixtures through silicone gas tubing. We used four biological replicates with an additional control culture bottle containing media without diatom cells for each of the two flow rates. To avoid sedimentation and subsequent biofouling of culture vessels with growing diatom cells, culture vessels were shaken at 150 rpm. The cultures were grown in 12:12 photoperiod with light intensity of 40.5 µmol m^{-2} s^{-1}.

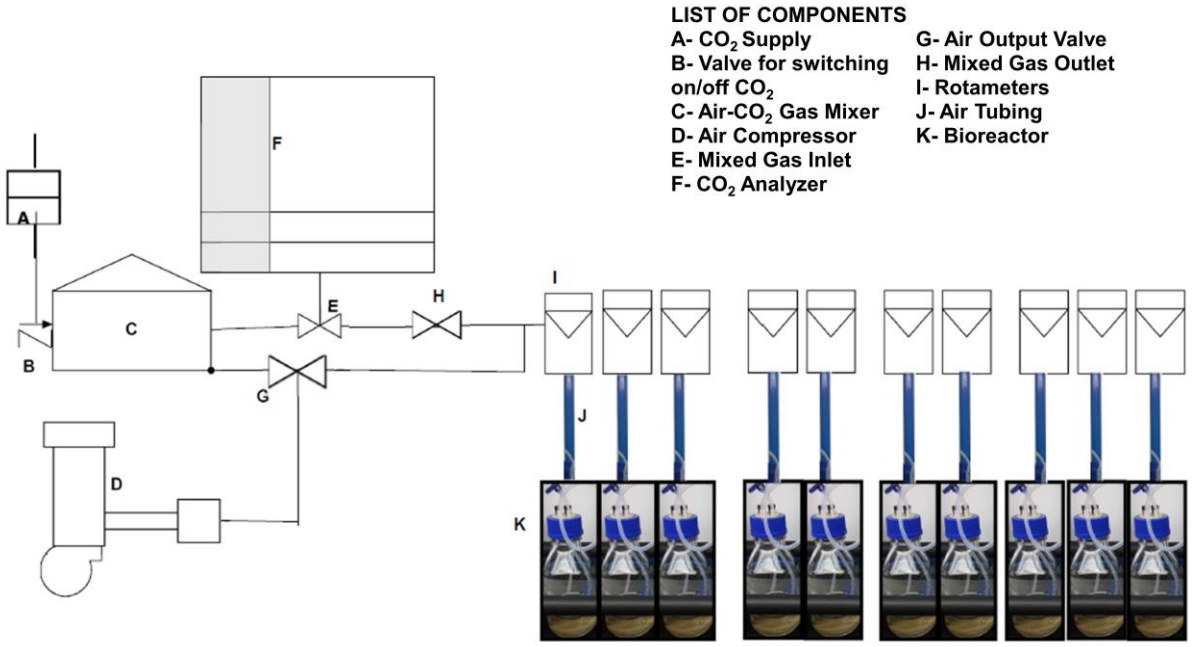

Figure 11. The Process flow chart for feeding air-CO_2 gas mix to diatom cultures at two different aeration flow rates.

2.2.2 Determination of carbon content, biomass productivity and CO_2 removal rates

For measuring percentage carbon content of diatom cells, 30 ml culture was harvested by centrifugation at 4000 rpm for 5 minutes, followed by two washes of the pellet with 0.5 M ammonium formate. The pellet was lyophilized overnight and dried by incubating for 24 hours at 105˚C and dry weight (DW) was measured on a precise weighing balance. In an equal volume (30 ml) of culture, total carbon content was measured with a BioTector TOC Analyzer (BioTector Analytical Sytems Ltd, Cork, Ireland). The percentage of carbon in biomass was expressed as total organic carbon per dry weight.

The biomass productivity was calculated using the equation: $P = X_1\text{-}X_0/T_1\text{-}T_0$ (Eq. 1), where X_0 = DW at 0 day, X_1 = DW during harvest, T_0 = day of inoculation, T_1 = day of harvest. The DW for biomass productivity was obtained from linear regression equation: y= 5E-11x + 0.002 (R^2 = 0.996) (Figure 12) obtained from relationship between cell count and dry cell weight. The value y is the DW (g) and x is the cell number. The CO_2 removal rate (R_{CO2}) expressed in g carbon per liter per day is given by the following formula: R_{CO2} = CcP (MCO_2/Mc) (Eq. 3), where Cc = carbon content (%, w/w); MCO_2/Mc = 3.6675, P = productivity.

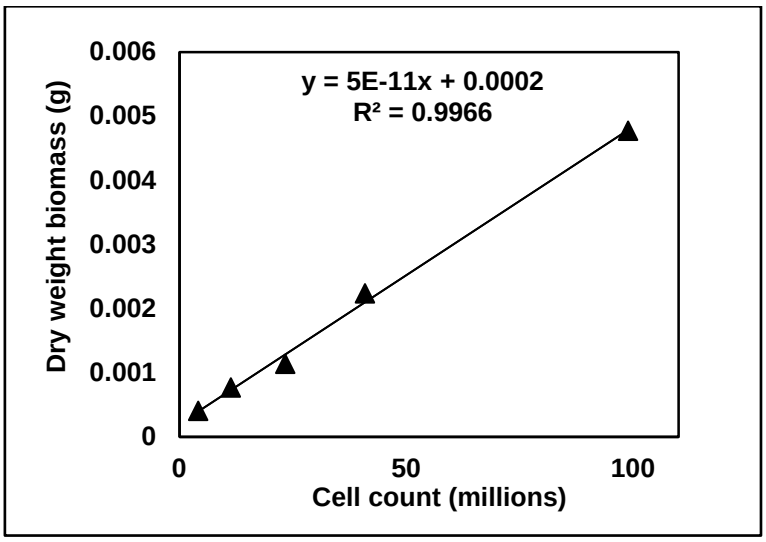

Figure 12. The relationship between cell count and dry weight biomass of *Phaeodactylum tricornutum* established by linear regression.

2.2.3 Calculation of CO_2 retention in culture vessel

To measure the effluent CO_2 concentration from diatom cultures, 10 ml of the headspace gas was taken into a syringe and 200 ul was injected into the gas chromatogram (Agilent 7890). The SP1 7890-0467 GC conditions (Agilent Technologies) was used to measure the CO_2 concentrations. The following equations and formulae were applied to calculate the % CO_2 retained in the culture vessel.

$Cin = Qin\ [CO_2]$, where Qin = flow rate of ingas (1)

$Cout = Qout [CO_2]$, where Qout = flow rate of offgas (2)

$Qin = Qout$ (3)

Deriving from the above three equations, we obtain the following formula:

% CO_2 retained = Cin-Cout/Cin x 100

2.2.4 Transmission electron microscopy

Cells for transmission electron microscopy were harvested in a 1.5 ml centrifuge tube at 3 r.c.f for 3 minutes. The pellet was suspended in the primary fixative solution containing 2% gluteraldehyde, 2% paraformaldehyde in 0.1 M sodium cacodylate/HCl buffer, pH 7.2 at 4 ˚C overnight. The solution was removed and three washes were given with 0.1 M sodium cacodylate/HCl buffer followed by two hours of secondary fixation (osmication) at room temperature in 1% Osmium tetraoxide solution prepared with sodium cacodylate buffer. The cells were further dehydrated through a series of graded alcohols i.e. 30%, 50%, 70%, 90%, 95% and pure ethanol, each for 2X 15 minutes. The pure ethanol was drawn off and replaced by propylene oxide twice for 20 minutes. Cells were initially placed in a 50:50 mixture of resin and propylene oxide for overnight followed by 5-6 hours incubation in 75:25 mixture of resin and propylene oxide. The cells were then transferred to pure resin and placed in a 65 ˚C oven for 48 hours and allowed to polymerise. After polymerisation, blocks were trimmed and sections of 1 micron thickness were cut onto glass slides and stained with 1% toluidine blue and viewed under light microscope. These sections were known as 'scout sections' as they were primarily used to ascertain tissue structure and components. Relevant regions of interest were selected for subsequent trimming and ultrathin sections of the magnitude 80-100 nm were cut and lifted onto 3mm copper grids. The grids were stained for 30 minutes in 1.5% aqueous uranyl acetate and 10 min in lead citrate. Sections were dried and viewed in the TEM.

2.2.5 Total lipids and fatty acid characterization

One week old cultures grown under different CO_2 concentrations were harvested by centrifuge at 5 r.c.f for 10 min. The pellet was freeze dried for 24 hrs and kept at -80 ºC prior to lipid extraction. Nine mg of powdered lyophilized biomass was suspended in 540 µl of a 1:1 chloroform:methanol mixture (solvent mix) in a glass vial and thoroughly vortexed for one min. The layers were separated by adding equal amounts (~180 µl) of distilled water and solvent mix. Lower layer containing lipids was transferred to new vial and residue was resuspended in 360 µl of solvent mix and incubated for 30 minutes at room temperature, followed by separation using similar volumes of water and solvent mix as taken during the first extraction. The lower layers were pooled and filtered through Whatman 1 filter paper. The solvent was evaporated and dried extract was weighed on a precise balance and expressed as total lipids (Ryckebosch et al., 2012).

Extracted total lipids were transmethylated using a protocol slightly modified from (Ryckebosch et al., 2012). Dried lipids were dissolved in one volume of toluene and two volumes of 1% sulphuric acid in methanol. Tridecaenoic acid (C13:0) was used as an internal standard for calculating the amounts of fatty acid. The mixture was incubated initially for one hour at 80 ºC followed by overnight incubation at 50 ºC. The following morning, a 5% NaCl solution was added to the methanolic mixture and fatty acid methyl esters (FAME) were extracted in hexane. For GC-FID analysis, 5 µl of FAME was injected at 220 ºC. The starting oven temperature of 140 ºC was initially maintained for 5 minutes and ramped at 4 ºC to the final temperature of 240 ºC and analysed by flame ionisation detector at 260 ºC. Supelco FAME mix containing 36 different fatty acids was used to identify the fatty acids.

2.2.6 Statistics

The data analysis was performed on Minitab statistical software package v. 16.2.4 (Minitab Inc.). The statistical significance of the interactive effect of aeration flow rates at different levels of CO_2 concentrations was tested by two-way ANOVA at a significance level of $P < 0.05$. In all experiments, mean values were compared by one-way ANOVA (Tukey, $P < 0.05$).

2.3 RESULTS

2.3.1 Effects of high CO_2 concentrations on growth rates and biomass productivity

Diatom cells were grown till the mid-exponential stage under six different air-CO_2 mixtures namely compressed air (0.038%), 1%, 2%, 4%, 5% and 10% (v/v). The growth rate, biomass productivities, CO_2 removal rate, total lipids and fatty acid production were assessed at two different aeration flow rates viz 10 ml.min^{-1} and 30 ml.min^{-1}. The observed specific growth of 0.502 day^{-1} rate was highest at 4% CO_2 (Table 1). Compared to ambient air-CO_2 concentration, the 3.5% increase in growth rate at 4% CO_2 led to enhancement of 16.1% and 17.6 % in cell density and biomass productivity respectively. At the aeration flow rate of 30 ml.min^{-1}, we observed decrease ($P < 0.00$) in the growth rates at 5% and 10% CO_2 (Table 1). The inhibitory effect at higher (10%) CO_2 levels (Figure 13) was mitigated by a threefold reduction (10 ml.min^{-1}) in the aeration flow rate. The aeration flow rate induced increase in the growth rates at higher CO_2 level indicated an interaction between the two physical parameters which was significant at level $P < 0.00$ (Table 1).

The reduction in growth rate of microalgae is mainly attributed to the fact that high concentrations of CO_2 lower the pH of cultivation medium (Tang et al., 2011). The inverse relationship of increasing CO_2 concentrations and decreases in pH could adversely affect microalgal physiology (Kumar et al., 2010). The pH values for diatom cultures grown under different CO_2 conditions were recorded at the day of harvest (Figure 14). Higher CO_2 concentrations led to the

acidification of cultures which dropped to pH 6.5 at 10% CO_2 aerated with flow rate of 30 $ml.min^{-1}$ (Figure 14).

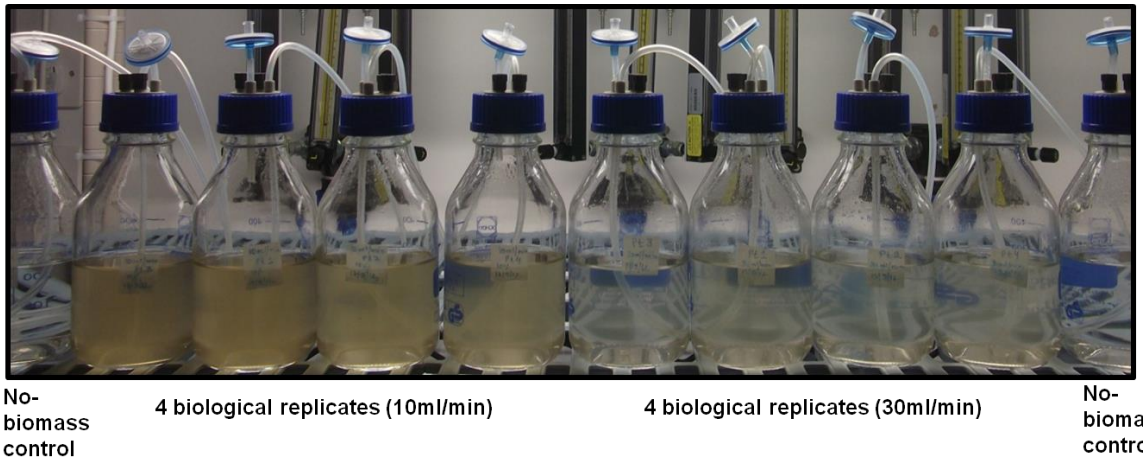

Figure 13. Comparison between growth of diatom cultures at 10% CO_2 under different aeration rates viz. 10 ml/min and 30 ml/min.

Aeration flow rate	% CO_2 (v/v)	Growth rate (day^{-1}) N = 3	Productivity ($g.L.day^{-1}$) N = 3	% CO_2 retained N = 3	R_{CO2} ($gC.L^{-1}day^{-1}$) N = 3	Cell density ($cells.L^{-1}$) N = 3
30 ml.min^{-1}	0.038	0.45 + 0.04 ab	0.14 + 0.00 c	25.7 + 2.6 ab	0.20 + 0.00 c	2.6 x 10^9 b
	1	0.39 + 0.04 bc	0.23 + 0.014 a	35.7 + 3.1 a	0.33 + 0.02 a	4.5 x 10^9 a
	2	0.49 + 0.03 ab	0.22 + 0.03 ab	24.4 + 4.4 ab	0.32 + 0.05 ab	3.6 x 10^9 ab
	4	0.50 + 0.03 a	0.16 + 0.03 bc	13.7 + 2.5 b	0.23 + 0.04 bc	3.1 x 10^9 b
	5	0.38 + 0.02 c	0.13 + 0.02 c	15.3 + 1.9 b	0.16 + 0.02 c	2.6 x 10^9 b
	10	0.12 + 0.02 d	0.01 + 0.00 d	23.4 + 10.4 ab	0.07 + 0.00 d	1.8 x 10^8 c
10 ml.min^{-1}	0.038	0.48 ± 0.05 a	0.10 + 0.00 bc	72.6 + 1.6 a	0.15 + 0.00 bc	1.9 x 10^9 bc
	1	0.34 ± 0.07 a	0.21 + 0.06 ab	53.7 + 1.3 b	0.31 + 0.10 ab	4.2 x 10^9 a
	2	0.45 ± 0.03 a	0.20 + 0.06 ab	44.3 + 2.7 c	0.38 + 0.10 a	4.0 x10^9 ab
	4	0.44 ± 0.01 a	0.13 + 0.02 abc	34.7 + 0.9 d	0.20 + 0.03 bc	2.6 x 10^9 abc
	5	0.44 ± 0.03 a	0.17 + 0.01 ab	40.6 + 5.7 cd	0.28 + 0.04 ab	3.3 x 10^9 ab
	10	0.34 ± 0.07 a	0.04 + 0.01 c	46.9 + 3.8 bc	0.07 + 0.01 c	7.5 x 10^8 c
Two-way Analysis of variance						
Aeration flow rate		NS	NS	$P < 0.00$	NS	NS
% CO_2		$P < 0.00$	$P < 0.000$	$P < 0.00$	$P < 0.00$	$P < 0.00$
Aeration flow rate x % CO_2		$P < 0.00$	NS	$P < 0.00$	$P < 0.04$	NS
Factor mean						
30 ml.min^{-1}		0.39	0.15	23.06	0.21	2.7 x 10^9
10 ml.min^{-1}		0.41	0.14	48.84	0.23	2.8 x 10^9

Table 1. Growth rates, biomass productivity, % CO_2 retention, CO_2 removal rates and cell density of *P. tricornutum* cells grown at different CO_2 concentrations sparged with two different aeration flow rates. Mean values at different % CO_2 levels within columns for same aeration flow rates marked by different alphabets are significantly different as tested by Tukey post hoc test at $P < 0.05$ level. Interactive effects of factors shown by p values obtained from two-way ANOVA; NS: non-significant effect.

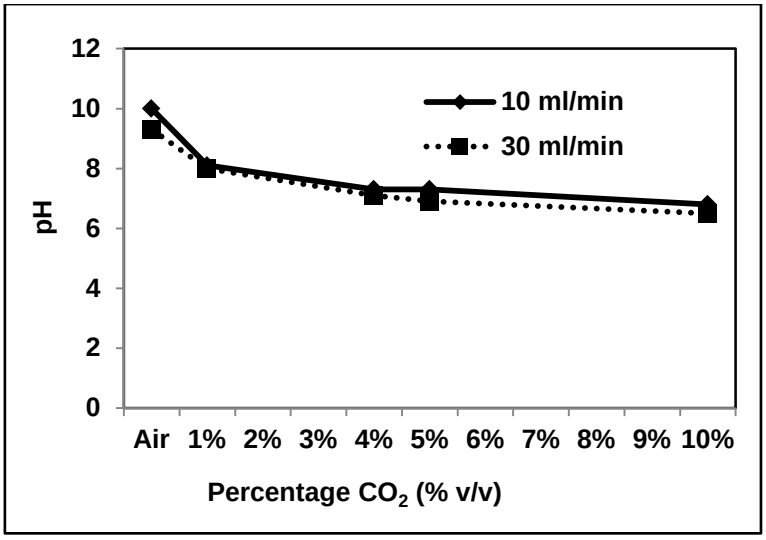

Figure 14. pH of *P. tricornutum* cultures measured at the end of seven days growth in different concentrations of CO_2 aerated at flow rates of 10 ml min^{-1} and 30 ml min^{-1} .

2.3.2 Effects of high CO_2 concentrations on CO_2 removal rates of *P. tricornutum*

The CO_2 removal rate by microalgae is a measure of the rate at which they can capture CO_2 and assimilate carbon into biomass; this is affected by many factors (Chiu et al., 2009). As we detected an interaction between aeration flow rate and *P. tricornutum* growth rate under elevated CO_2, we investigated the impact of aeration rates on the mass transfer of inorganic carbon into diatom biomass at different CO_2 levels. The CO_2 removal rate of *P. tricornutum* with 2% CO_2 was 0.379 g C L^{-1} day^{-1}, which was similar to the value obtained with 5% CO_2 at 0.279 g C L^{-1} day^{-1} suggesting that *P. tricornutum* maintains capability to capture CO_2 under increasing CO_2 levels (Table 1). The biomass productivity obtained at 2% CO_2 for *P. tricornutum* was 0.199 g L^{-1} day^{-1} (Table 1) which would yield around 200 g m^{-2} day^{-1}. It has been suggested that increasing the microalgal productivity to 50 $g.m^{-2}.day^{-1}$ would potentially increase the annual consumption of CO_2 to 3.73 Gton CO_2 (Stuart, 2011). There was significant decline in CO_2 removal rate at 10% ($P < 0.00$). The concentration of CO_2 in the headspace of the culture bottles was measured to calculate the fraction of inlet CO_2 that was retained by the culture system. The highest fraction of ingas CO_2 was retained at 0.038% CO_2 concentration (Table 1). The residence time of gas mixture is inversely proportional to the aeration flow rate, thus we observed a significant increase in the percentage of CO_2 retained within the culture system as we lowered the aeration flow rate (Table 1, $P < 0.00$). The interactive effects of aeration flow rates and different CO_2 concentrations were assessed by performing two-way ANOVA statistical tests. There was an increase ($P < 0.00$) in % CO_2 retained by the diatom cultures aerated with lower aeration flow rate but corresponding increases in the CO_2 removal rates were not observed (Table 1). It is possible that light availability and/or nitrogen may be limiting factors.

2.3.3 Effects of high CO_2 concentrations on ultrastructure of *P.tricornutum*

The light microscopic observation of cells grown under different aeration conditions showed no morphological variations. The cells were all in fusiform stage and no polymorphism were observed under CO_2 conditions. To study the influence of elevated CO_2 on the photosynthetic apparatus of *Phaeodactylum* we examined its chloroplast structure. Figure 3 show the electron micrographs of ambient air (0.038%) and 5% CO_2 grown cells of *P. tricornutum*. Number of serial sections observed in present study also (Figure 15 D-E) revealed a typical spatial relationship between mitochondria and chloroplasts of *P. tricornutum* (Prihoda et al., 2012). The chloroplasts of *P. tricornutum* are typical secondary plastids which are surrounded by four membranes; the outer envelope is termed as chloroplast endoplasmic reticulum (CER) which is continous with nuclear envelope (Prihoda et al., 2012). There is a characteristic 'girdle lamella' that runs in parallel with membranes; the girdle lamella and thylakoids are found in bundles of three and are not partitioned between stack and unstacked grana as found in green algae and higher plants (Figure 15) (Prihoda et al., 2012). Pyrenoids in the chloroplasts of cells in both ambient air and 5% CO_2 were intersected by thlakoid membrane (Figure 15). Cells grown under ambient air showed comparatively larger pyrenoids than in the chloroplasts of cells grown at 5% CO_2 (Figure 15 A-F). Elevated CO_2 can provoke significant structural changes in land plant chloroplasts (Griffin et al., 2001). We then tested whether elevated CO_2 was adversely affecting the chloroplast structure of *P. tricornutum*, but it appeared unaltered in *P.tricornutum* under high CO_2 (Figure 15). The transmission electron microscopic study showed that chloroplasts of cells grown at 5% CO_2 have more inter-thylakoid stromal space than cells grown at ambient (0.038%) CO_2 levels. No change in number of pyrenoids per cell was observed with increasing CO_2 level (Figure 15).

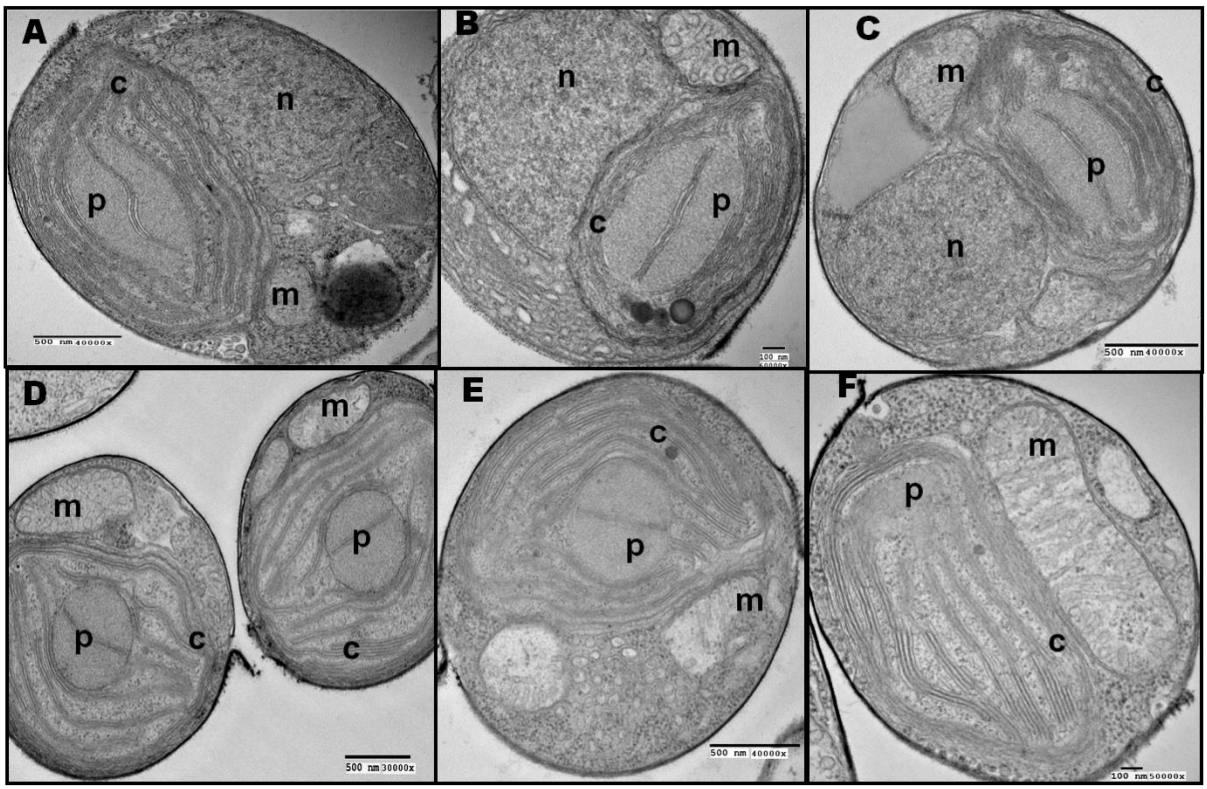

Figure 15. Electron micrographs of *P. tricornutum* cells grown in ambient air and 5% CO_2. A-C Transverse sections of cells grown under ambient air. D-E Transverse section of cells grown in 5% CO_2. F Longitudinal section of a cell grown under 5% CO_2. Chloroplast (c), mitochondrion (m), pyrenoid (p), nucleus (n).

2.3.4 Effect of CO_2 on total lipids and fatty acids in *P. tricornutum*

In addition to efficiently capturing CO_2, microalgal biorefineries will need to incorporate sequestered carbon into metabolites, including fatty acids of potential commercial value as biodiesel, pharmaceutical and nutraceutical products (Cohen et al., 2000; Ota et al., 2009; Xu et al., 2006). We investigated the effect of increased CO_2 fixation on lipid and fatty acid composition in mid-stationary phase cells of *P. tricornutum.* Strikingly, we discovered that growth at elevated CO_2 concentrations led to significant increases in total lipid content (Table 2). Although several major fatty acids (including palmitic (16:0), palmitoleic (16:1) and cis-5,8,11,14,17 eicosapentaenoic (20:5n3) acid) were found at all CO_2 concentrations, cells grown with 1% and 4% CO_2 aeration mixtures accumulated significantly increased concentrations of eicosapentaenoic acid (20:5) (Table 2). Eicosapentaenoic acid (also called EPA) is an omega-3 fatty acid which is of particular commercial value. In our study, EPA represents the largest proportion of the major fatty acids synthesized by *P. tricornutum* when grown at high CO_2 (Figure 16). This agrees with models which predict that low CO_2 leads to increased synthesis of saturated fatty acids in microalgae, while elevated CO_2 favours the accumulation of polyunsaturated fatty acids, or PUFAs (Ota et al., 2009; Tang et al., 2011). Compared

to the reported values of EPA content under different culture conditions (Table 3), we obtained 2.21% dry weight EPA at 1% CO_2.

Fatty acid	*% dry weight biomass in 10ml.min^{-1} aeration cultures*						*% dry weight biomass in 30ml.min^{-1} aeration cultures*						*Two-way ANOVA (P values)*[a]		
	Air	1%CO_2	2%CO_2	4%CO_2	5%CO_2	10% CO_2	Air	1%CO_2	2%CO_2	4%CO_2	5%CO_2	10% CO_2	AR	%CO_2	AR vs % CO_2
C6:0	0.04 ± 0.02 a	0.04 ± 0.02 a	0.03 ± 0.00 a	0.04 ± 0.00 a	0.03 ± 0.00 a	0.038 ± 0.00 a	0.03 ± 0.01 a	0.03 ± 0.00 a	0.04 ± 0.01 a	0.03 ± 0.00 a	0.03 ± 0.00 a	0.037*	N.S	N.S	N.S
C8:0	0.05 ± 0.02	0.07 ± 0.03	0.04 ± 0.00	0.06 ± 0.00	0.05 ± 0.00	0.061 ± 0.00	0.04 ± 0.01	0.06 ± 0.01	0.07 ± 0.02	0.05 ± 0.00	0.05 ± 0.00	0.014*	N.S	N.S	N.S
C14:0	0.07 ± 0.00 b	0.37 ± 0.03 a	0.14 ± 0.05 ab	0.21 ± 0.06 ab	0.13 ± 0.05 b	n.d	0.17 ± 0.09 ab	0.19 ± 0.11 ab	0.22 ± 0.03 b	0.14 ± 0.09 b	0.12 ± 0.02 b	n.d	N.S	0.002	0.01
C16:0	0.16 ± 0.12 b	0.74 ± 0.07 a	0.36 ± 0.12 ab	0.57 ± 0.15 ab	0.38 ± 0.13 ab	n.d	0.38 ± 0.20 ab	0.39 ± 0.22 ab	0.41 ± 0.24 ab	0.39 ± 0.25 ab	0.38 ± 0.06 ab	n.d	N.S	0.005	0.005
C16:1	0.31± 0.07 c	1.38 ± 0.11 a	0.86 ± 0.01 ab	1.1 ± ab	0.75 ± 0.05 bc	n.d	0.78 ± 0.10 bc	0.87 ± 0.39 b	0.98 ± 0.13 ab	0.87 ± 0.00 bc	0.63 ± 0.01 bc	n.d	N.S	0.002	0.007
C17:1	n.d	0.14 ± 0.00 abc	0.08 ± 0.02 abc	0.22 ± 0.02 a	0.15 ± 0.00 abc	0.11*	0.09± 0.00 bc	0.10 ± 0.04 bc	0.14 ± 0.01 abc	0.21 ± 0.04 a	0.17 ± 0.00 ab	n.d	N.S	0.002	N.S
C18:0	n.d	0.03*	n.d	n.d	0.03 ± 0.00	n.d	0.019*	0.03*	n.d	0.03*	0.03 ± 0.00	n.d			
C18:1	n.d	0.03 ± 0.00	n.d	0.03*	0.03*	n.d	0.03 ± 0.01	0.03*	n.d	0.03 ± 0.00	n.d	n.d			
C18:2n6c	n.d	0.09 ± 0.00 a	0.07 ± 0.00 a	0.09 ± 0.01 a	0.06 ± 0.00 a	n.d	0.07 ± 0.00 a	0.06 ± 0.02 a	0.07 ± 0.01 a	0.07 ± 0.00 a	0.057 ± 0.00 a	n.d	0.04	N.S	N.S
C18:3n3	n.d	0.03*	n.d	0.04 ± 0.01	0.04*	n.d	n.d	n.d	n.d	0.04 ± 0.01	n.d	n.d			
C20:5	0.48± 0.01 cd	2.21 ± 0.14 a	0.811± 0.22 bcd	2.01 ± 0.09 a	1.44 ± 0.02 abc	1.358*	1.36 ± 0.13abcd	1.54 ± 0.67 ab	1.76 ± 0.19 ab	1.15 ± 0.14 ab	1.307 ± 0.02abcd	0.111*	N.S	0.002	0.002
C23:0	n.d	0.11 ± 0.00 ab	0.07 ± 0.02 b	0.14 ± 0.00 a	0.10+ 0.00 ab	n.d	0.07 ± 0.00 b	0.09 ± 0.03 ab	0.11 ± 0.01 ab	0.12 ± 0.004 ab	0.113 ± 0.00 ab	n.d	N.S	N.S	N.S
C24:0	n.d	0.14 ± 0.01 a	0.07 ± 0.02 a	0.13 ± 0.01 a	0.08 ± 0.00 a	n.d	0.07 ± 0.01 a	0.09 ± 0.03 a	0.12 ± 0.01 a	0.10 ± 0.00 a	0.08 ± 0.00 a	n.d	N.S	N.S	0.05
SFA	0.43 ± 0.04 cd	1.53 ± 0.11 a	0.83 ± 0.15 bcd	1.28 ± 0.07 ab	0.92 ± 0.02 abc	0.181 ± 0.12 d	0.96 ± 0.09 abc	0.99 ± 0.43 abc	1.07 ± 0.13 abc	1.03 ± 0.13 abc	0.86 ± 0.01 bc	0.051*	0.00	0.00	0.00
PUFA	0.480 ± 0.01 bc	2.37± 0.23 a	1.37± 0.47 abc	2.12 ± 0.07 a	1.52 ± 0.05 abc	1.358*	1.43 ± 0.13 abc	1.62 ± 0.72 abc	1.84 ± 0.21 a	1.65 ± 0.13 ab	1.36 ± 0.02 abc	0.111*	N.S	0.005	0.01
MUFA	0.31 ± 0.07 cd	1.63 ± 0.16 a	0.97 ± 0.02abcd	1.33 ± 0.05 ab	0.92 ± 0.07 bcd	0.110*	0.91 ± 0.11 bcd	0.99 ± 0.47 abc	1.12 ± 0.14 ab	1.11 ± 0.04 ab	0.81 ± 0.00 bcd	0.174*	N.S	0.001	0.006
Others	0.19± 0.01 c	1.73 ± 0.04 a	0.66 ± 0.14 bc	1.76± 0.11 a	1.34 ± 0.04 ab	0.664 ± 0.43 bc	1.09 ± 0.08 abc	1.21 ± 0.56 ab	1.43 ± 0.24 ab	1.33 ± 0.00 ab	0.88 ± 0.13 abc	0.285*	N.S	0.001	0.001
Total lipids (%)	10.56 ± 2.35 ab	12.22 ± 0.00a	7.78 ± 0.00b	10.56 ± 0.78ab	14.44 ± 0.00a	10.556 ± 0.78ab	16.66 ± 3.14	17.22 ± 2.35	13.33 ± 1.5	11.66 ± 2.3	14.44 ± 4.7	7.00 ± 1.41	0.01	0.01	0.04

Table 2. Percentage of dried weight total lipids and total extracted fatty acids from *P. tricornutum* cells grown at different CO_2 concentrations sparged with two different flow rates. Data is mean of 3 biological replicates and coefficient of variance was tested by performing ANOVA on both aeration treatments separately. Mean values that are indicated with different letters are significantly different.

Strain name	Cultivation conditions			EPA content		Reference
	Culture mode	Reactor vessel	Trophic conditions/other factors	% dry weight	% fatty acid	
Phaeodactylum tricornutum Bohlin UTEX 640	Batch	1L Flask	Autotrophic with CO_2 supplementation	3.8	-	(Alonso et al., 1996)
Phaeodactylum tricornutum Bohlin UTEX 640	Continuous	Flat panel airlift loop reactor	autotrophic with 1.25% CO_2	5.0	33	(Meiser et al., 2004)
Phaeodactylum tricornutum WT	Batch	-	-	0.7-1.7	-	(Medina et al., 1998)
Phaeodactylum tricornutum WT	Batch	-	air supplemented with CO_2	1.8-3.3	-	(Medina et al., 1998)
Phaeodactylum tricornutum	Batch	Glass vessel	mixotrophic with glycerol	2.2	-	(Lebeau and Robert, 2003)

Table 3. Reported values of EPA content in different strains of *P. tricornutum* grown under varied culture conditions.

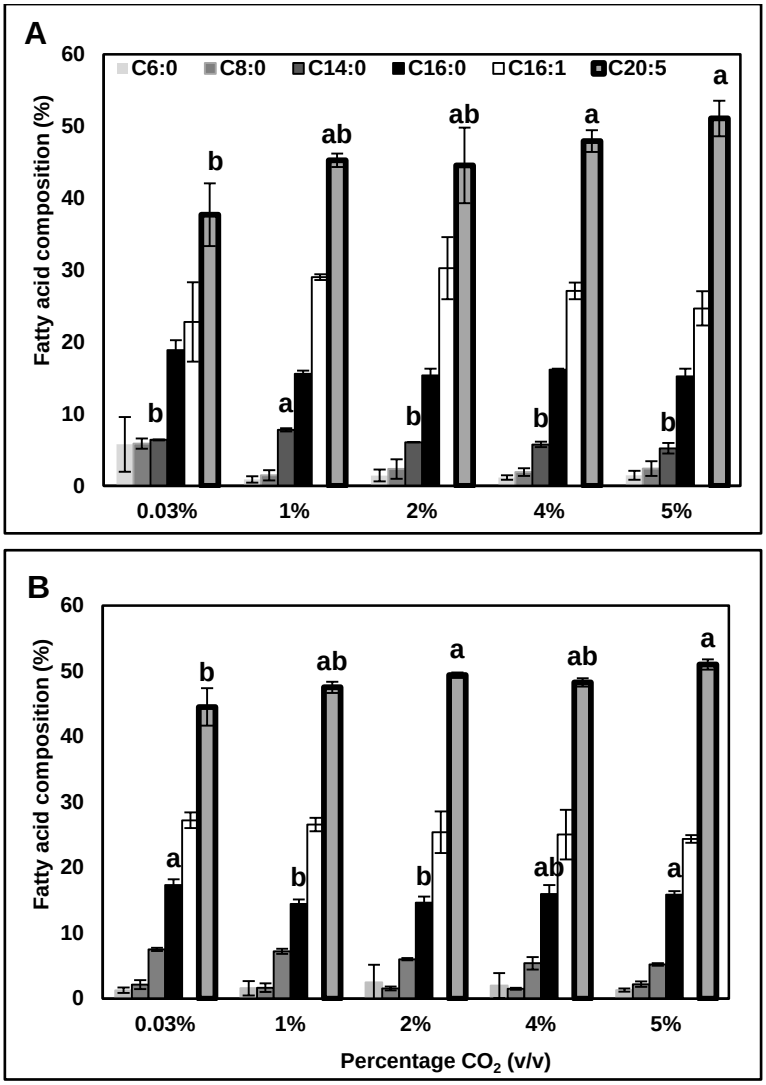

Figure 16. Percentage of major fatty acids in *P. tricornutum* cells grown at different CO_2 concentrations aerated at flow rates of 10 ml min^{-1} (A) and 30 ml min^{-1} (B). Error bars shows standard deviation of three biological replicates. One-way ANOVA is applied on four independent biological replicates of each treatment and means that do not share a letter are significantly different.

2.4 DISCUSSIONS

The burning of fossil fuels produce about 10-12% CO_2 which can be used for the cultivation of microalgae (Morais and Costa, 2007) . However a high CO_2 concentration above 5% v/v may adversely affect growth of some microalgal species (Adarme-Vega et al., 2012). For example, reduction in growth rate of the centric diatom, *Thalassiosira pseudonana*, occurs at CO_2 levels elevated to 0.076% v/v (i.e. 760 ppm) (Crawfurd et al., 2011). Therefore, to test CO_2 tolerance in *P. tricornutum*, the diatom cells were grown under higher levels range from 0.038-10% CO_2. To be efficient for CO_2 sequestration, microalgae need to have a fast growth rate under gas-feeds containing such high CO_2 concentrations. Some economically important microalgal candidate species such as *Dunaliella salina* exhibit an average specific growth rate of 0.237 day^{-1} under 6.3% (v/v) CO_2 in a

bubble column reactor (Harter et al., 2013). In this study,, the marine diatom *P. tricornutum* comparatively show a higher growth rates under 5% -10% CO_2 levels in conditions similar to the study of Haerter et al (2013).

P. tricornutum fed with 2% CO_2 yield approximately 0.2 g of biomass per liter per day and consume 0.379 g CO_2 per liter per day i.e for generating 1 kg biomass it can capture 1.895 kg of CO_2. Therefore to capture 1 tonne of CO_2 per annum via a system operating at a capture rate of 138.3 grams L^{-1} $year^{-1}$ we would require diatom cell suspension volume of at least 7219 litres. The green alga *Scendesmus obtusiusculus* grown at 10% CO_2 show a maximum CO_2 fixation rate of 970 g m^{-3} day^{-1} (Toledo-Cervantes et al., 2013). The other microalgae that have been investigated for carbon dioxide fixation are *Botryococcus braunii, Spirulina platensis* and *Chlorella vulgaris* which showed CO_2 fixation rates of 496.98, 318.61 and 251.64 mg L^{-1} day^{-1} respectively (Sydney et al., 2010).

For microalgal carbon capture and recycling to have impact it will have to be scaled up to deal with the levels of CO_2 emissions from single-site CO_2 emitters such as cement factories. This can be exemplified as: a cement factory with an output of 1000 tonnes per annum of clinker could generate emissions of 860,000 tonnes of CO_2 per annum. Clearly *P. tricornutum* based carbon capture systems with a capacity of 138.3 grams L^{-1} $year^{-1}$ would need to be a massive volumetric scale for significant carbon capture from such single-site CO_2 emitters. For example, the figures suggest that, for this rate of capture to have an impact on an 860,000 tonne CO_2 cement factor emittor would require volumetric scales of 6.2 X 10^9 litres. While these calculations are simplistic they serve to act as a reality check on the scale-up for impact challenge that microalgal based carbon capture recycling systems face. However, it is clear that while impacts on CO_2 capture may be negligible at these rates of capture, there is strong potential for locating microalgal based biorefineries at or close to high CO_2 emissions sites as *P. tricornutum* can function as a bio-factory for high value bioproducts such as poly unsaturated fatty acids including eicosapentaenoic acid.

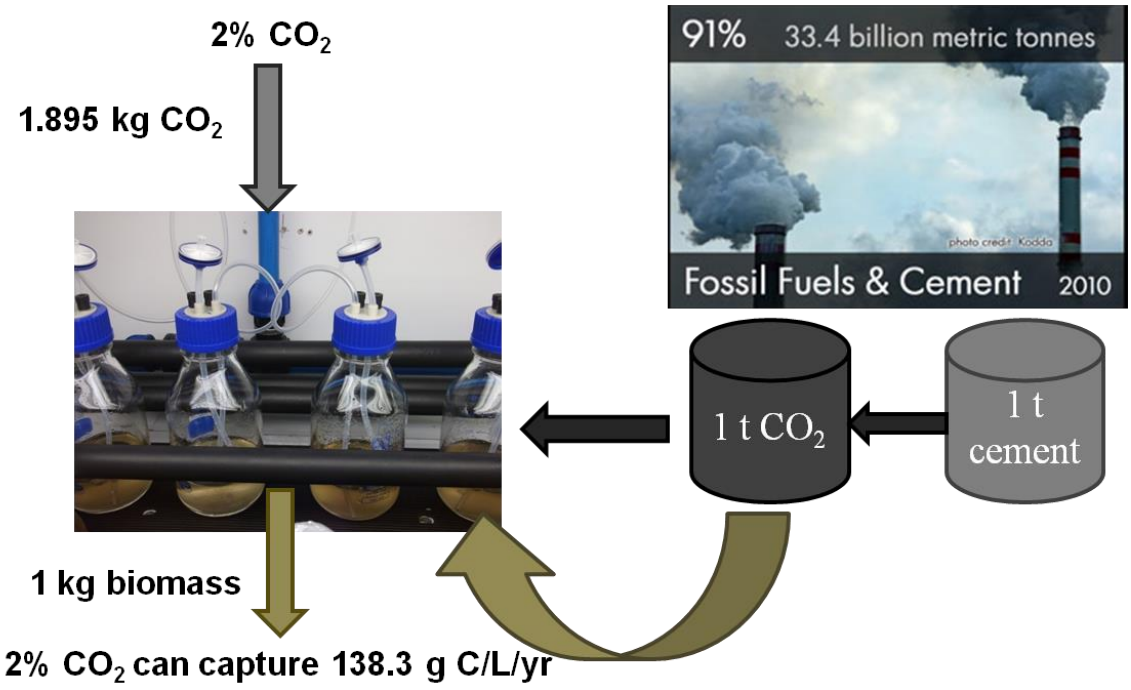

Figure 17. *P. tricornutum* based CO_2 capture system for generation of biomass rich in fatty acids.

2.5 CONCLUSIONS

The cultivation method developed in the present study provides a basis for investigation of the CO_2 acclimation and sequestration potential of diatom *P. tricornutum*. Growth and CO_2 assimilation performance of the marine diatom *P. tricornutum* were tested under increasing CO_2 levels in ambient air. *P. tricornutum* grown under ambient air can also grow well in the aerated system with higher levels of 5-10% CO_2. Achieving the optimal biomass productivity and CO_2 removal rate in batch cultivation, the diatom could be cultured with higher CO_2 levels with a lower aeration flow rate. The highest CO_2 removal rate of 0.379 g L^{-1} day^{-1} was obtained at 2% CO_2 when fed with an aeration flow rate of 10 $ml.min^{-1}$. Apart from CO_2, another important nutrients are nitrogen and phosphorous which can enhance the carbon fixation capability of diatom. Our findings suggest that microalgae adapted for sequestration of concentrated CO_2 streams could be a valuable source of EPA and other valuable commercially valuable PUFAs which are enhanced under high CO_2 conditions. As CO_2 is one of the major components of flue gas, *P. tricornutum* (with an ability to tolerate 10% CO_2) must be tested for flue gas to fully utilize its potential to moderate the anthropogenic effects of greenhouse gas emissions.

3. CHAPTER THREE

Ethylmethane sulfonate (EMS) mutagenesis combined with antibiotic selection for generation of high lipid mutants of *Phaeodactylum tricornutum*

Chapter 3 – EMS mutagenesis with cerulenin selection

ABSTRACT

Ethylmethane sulfonate (EMS) treated populations of *Phaeodactylum tricornutum* were selectively screened under the selective pressure of the antibiotic cerulenin to generate novel mutants with altered lipids and fatty acids profiles. Three novel cerulenin resistant mutants namely *Ptcer12, Ptcer13* and *Ptcer14* displayed 2-2.5 fold increases in total dry weight lipids over wild type progenitor strain without any effect on growth rate and biomass productivity. All three mutants displayed heterogeneous array of lipid types with significant differences in amounts of the triacylglycerols (TAGs) and phosphotidylcholine. In particuar, some TAG lipid classes namely TAG 48:3, 50:3, 50:4, 50:6, 52:7, 56:3 and 58:7 were only found in mutant strains and not in wild type. The mutant *Ptcer14* accumulated (21% over wild type) more TAGs with a concomitant decrease in the levels of phospholipids. The mutants *Ptcer12* and *Ptcer13* accumulated very long chain fatty acids such as erucic (C22:1) and nervonic acid (C24:1) which account for 0.02% and 0.03% of dry weight biomass respectively. The P*tcer* mutants showed overexpression of fatty acid synthase FABB and FABFa.

Chapter 3 – EMS mutagenesis with cerulenin selection

3.1 INTRODUCTION

Whole genome mutagenesis offers a strain improvement method for microalgae which can generate strains that are regulated as non-genetically modified organisms (non-GMOs). Mutagenesis approaches can be implemented even with sparse knowledge about the biochemical pathways for the synthesis of desired bioproduct is required for mutagenesis. Forward genetic mutagenesis screens allow to artificially induce genetic variation and mutagenized plants are screened for phenotypes of interest.

There are two classes of mutagens namely physical like ultraviolet, gamma and X-rays and chemical such as ethyl methanesulfonate (EMS) and nitrosomethyl guanidine (NTG). In 1959 it was demonstrated that EMS has mutagenic properties using the T4 viral system (Flibotte et al., 2010). EMS mutagenesis is most widely used chemical mutagenesis technique which has high mutagenicity. EMS mutagenesis is the process by which heritable alterations in the genome of an organism are produced. The chemical principle is alkylation of guanine bases resulting in base mispairing. An alkylated G will pair with T and result in G/C to A/T transition that ultimately results in amino acid change or deletion (Figure 18). The advantages are generation of high density of non-biased irreversible mutations in the genome that permits saturation mutagenesis. It generates loss-of-function alleles as well as novel mutant phenotypes, which include dominant or gain-of-function versions of proteins typically due to alterations of specific amino acids (Maple and Moller, 2007). For example, carotenoid-less phenotype of *Chlamydomonas reinhardtii* (McCarthy et al., 2004) and eicosapentaenoic fatty acid lacking mutants of green alga *Nannochloropsis* have been generated through EMS mutagenesis (Schneider et al., 1995). For microalgae, EMS has been used for improving useful traits for commercial applications such as higher accumulation of astaxanthin and polyunsaturated fatty acid (Chaturvedi and Fujita, 2006; Tripathi et al., 2001). Random whole genome mutagenesis approaches have been applied for strain improvement in various microalgal species for enhancing lipids, fatty acids, CO_2 tolerance and carotenoids (Table 4).

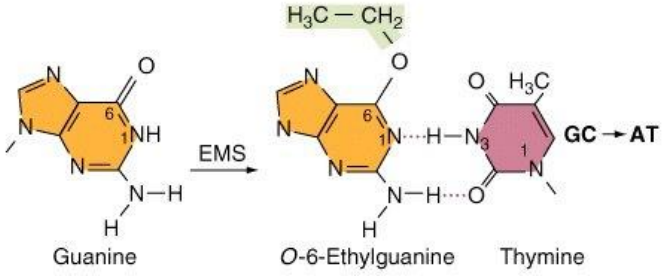

Figure 18. Mechanism of action of ethylmethane sulfonate. Alkylation of 6' -O position in guanine results in pairing of alkylated guanine with thymine instead of cytosine causing GC to AT transition.

Strain name	Method of mutagenesis	Cellular traits		Change w.r.t wild type	Reference
		Metabolites	Others		
Chlamydomonas reinhardtii	EMS, UV	pigments	white phenotype	decrease in chlorophyll a, increase in α-Tocopherol	(McCarthy et al., 2004)
Chlorella ellipsoidea	ENU	-	CO_2 insensitive	stable photosynthetic rates under high CO_2	(Ochiai et al., 2007)
Nannochloropsis oculata	EMS	EPA	-	29% increase	(Chaturvedi and Fujita, 2006)
Haematococcus pluvialis	UV, EMS	astaxanthin	-	2.2-3.2 fold increase	(Tripathi et al., 2001)
N. oculata	MNU	PUFA	thermo tolerance	108-120% increase	(Chaturvedi et al., 2004)
Nannochloropsis	EMS	total fatty acids	-	~ 4 fold increase	(Doan and Obbard, 2012)
Phaeodactylum tricornutum	UV	EPA	-	37-44% higher	(Alonso et al., 1996)
Chlorella sp.	UV, EMS	lipids	-	10-37% higher	(Manandhar-Shrestha and Hildebrand, 2013)
Nannochloropsis	EMS	EPA	-	deficient	(Schneider et al., 1995)
Haematococcus pluvialis	UV, EMS, NTG	carotenoids, astaxanthin	-	23-59% increase	(Sandesh Kamath et al., 2008)
C. reinhardtii	EMS		H_2-production, O_2 tolerance	10 times more O_2 tolerance	(Flynn et al., 2002)

Table 4 Genetic improvement for useful traits of microalgal strains through random mutagenesis approaches. EMS- ethylmethane sulfonate, UV- ultraviolet radiation, ENU- *N*-ethyl-*N*-nitrosourea, MNU- *N*-methyl-*N*-nitrosourea, NTG-1-methyl 3-nitro 1-nitrosoguanidine, EPA- eicosapentaenoic acid, PUFA- polyunsaturated fatty acid.

Following mutagenesis the challenge is to develop a selection system to isolate the desired mutant from all other non-desired mutants and wild type cells. Desired mutants can be acquired by several screening protocols such as antibiotic selection and fluorescence based methods (Doan and Obbard, 2012). Antibiotics such as cerulenin can be used for regulating de novo fatty acid biosynthesis in microalgae (Chaturvedi and Fujita, 2006). The key regulating enzyme of fatty acid synthesis called the β- ketoacyl-acyl carrier protein (ACP) synthase is a known target for cerulenin which forms a covalent adduct with the active site cysteine (Figure 19) (Price et al., 2001). In the present study, EMS mutagenesis was carried out with subsequent antibiotic selection using cerulenin to isolate and generate novel mutants of *P. tricornutum* with an improved cellular lipid profiles.

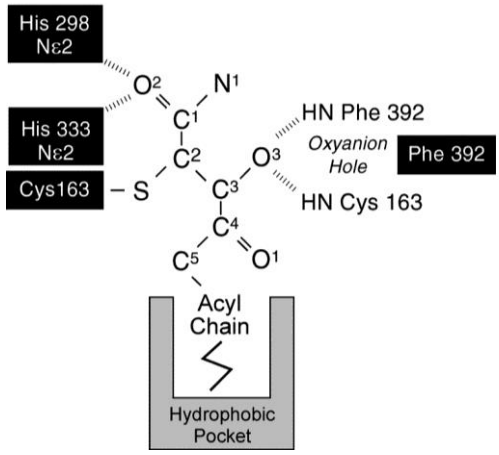

Figure 19. Binding of cerulenin to β- ketoacyl-acyl carrier protein (ACP) synthase I (FabB). The hydrophobic cavity that accommodates fatty acid chain of the acyl-enzyme intermediate is occupied by cerulenin. The C-2 of cerulenin forms a covalent bond with the active site cysteine (Price et al., 2001).

3.2 MATERIALS and METHODS

3.2.1 Diatom strain and culturing

The CCAP 1055/A strain of *Phaeodactylum tricornutum* was obtained from Culture Collection of Algae and Protozoan (CCAP), Dunstaffnage Marine Laboratory, Oban, Argyll, UK. Cultures were grown in F2 (Guillard, 1975) medium prepared in GF/F filtered natural sea water at 17 ˚C in 12:12 day/light under intensity of white fluorescent lights. The cultures were grown in Erlenmeyer flasks (50 – 500 ml) with 20 to 300 ml F2 medium and were shaken at 120 rpm on an orbital shaker.

3. 2.2 Cerulenin toxicity assay

Cerulenin was tested for toxic effects at different concentrations, namely: 0, 1, 5, 20, 40, 60 and 80 μM. For testing the toxicity effect of different cerulenin concentration, 50 μl inoculums culture

containing 1 X 10^4 diatom cells were inoculated on 1% F2 cerulenin agar plates. After 3 weeks, colonies were counted using Gene Tool, GeneSnap (Syngene, Cambridge, England).

3.2.3 Ethyl methano sulfonate (EMS) mutagenesis and mutant screening

Diatom cells growing at exponential growth phase at cell density of 1 X 10^6 were treated with different doses of EMS viz. 100, 150 and 200 mM for 2 hours in darkness at 17˚C with shaking at 1000 rpm in Thermomixer compact (Eppendorf). Three replicates were maintained for each concentration level. After EMS treatments, the cells were washed with 5% sodium thiosulfate to neutralise the EMS, followed by two washings with the sterile F2 medium. After washings the cells were resuspended in the F2 medium. Aliquots of cells were used for the cell viability assay using propidium iodide (PI) and for mutant isolation under antibiotic (cerulenin) selection. The %cell lethality was scored against untreated cell populations (control) using the following formula.

$$\% \text{ lethality} = \frac{(\text{dead cells})_{EMS} - (\text{dead cells})_{control}}{(\text{dead cells})_{control}} \times 100$$

3.2.4 Growth measurements and biomass productivity of EMS mutants

The biomass productivity was calculated using the equation: $P = X_1\text{-}X_0/T_1\text{-}T_0$, where X_0 = dry weight (DW) at 0 day, X_1 = DW during harvest, T_0 = day of inoculation, T_1 = day of harvest. The DW for biomass productivity was obtained from linear regression equation: $y= 0.0197x + 0.0005$ ($R^2 = 0.997$) obtained from relationship between optical density at 750 nm (OD_{750}) and dry cell weight. The value on y axis is the DW (g) and on x axis is the optical density OD_{750} (Figure 20).

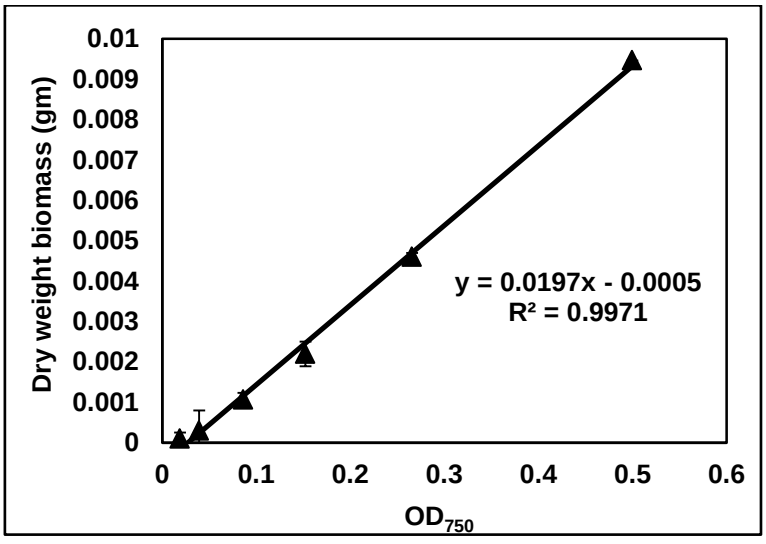

Figure 20. Correlation equation between dry weight biomass and OD_{750} for measuring the biomass productivities.

3.2.5 Lipidomic analysis

The extractions for lipidomic analysis were performed according to (Giavalisco et al., 2011). Briefly, metabolites were extracted from frozen diatom pellet with -20˚C methanol: methyl-tert-butyl-ether: water (1:3:1) with shaking for 30 min at 4˚C, followed by 10 min incubation in ultrasonication bath. 650 ul of ultra performance liquid chromatography (UPLC) grade methanol: water 1:3 was added and vortexed followed by centrifuge for 5 min at 4˚C in a table top centrifuge. The upper phase containing lipids was isolated and dried and used for lipidomic analysis with Waters Acquity UPLC system (Waters, http://www.waters.com) using a C8 reversed-phase column (100 mm X 2.1 mm X 1.7 µm particles). Water with 1% 1 M NH_4Ac, 0.1% acetic acid and acetonitrile: isopropanol (7:3) containing 1% 1 M NH_4Ac, 0.1% acetic acid were used as mobile phases. A 2 µl sample was injected and gradient of 1 min 45% A, 3-min linear gradient from 45% A to 35%A, 8 min linear gradient from 25% A to 11% A, 3min linear gradient from 11% A to 1%A was eluted with a flow rate of 400 $\mu l.min^{-1}$. The mass spectrum was acquired with Exactive mass spectrometer (Thermo-Fisher) (Giavalisco et al., 2011).

3.2.6 Extraction of total lipids and gas chromatography analysis

Optimized analytical procedure of Ryckebosch et al (2011) was followed for extraction of lipids from the lyophilized diatom cells. Briefly, known amount of lyophilized microalgae was mixed with chloroform-methanol 1:1 in a glass vial and vortexed. Equal volume of solvent mixture and water was added to separate the aqueous methanolic layer and lipidic chloroform layer by centrifuge at 2000 rpm for 10 min. Lower layer was transferred into another vial and cell pellet was reextracted in the solvent mixture followed by layer separation. The two chloroform layers were pooled and filtered through anhydrous sodium sulphate using Whatman No. 1. The chloroform was evaporated in a stream of nitrogen gas and dried extract was weighed and expressed as % total lipids.

Transesterification on dried lipids was performed according to (Ryckebosch et al., 2011). Briefly, to 1 mg of dried lipids, 100 microlitres of toluene and 200 microlitres of 1% sulphuric acid in methanol were added and incubated at 80 ˚C for one hour followed by overnight incubation at 50 ˚C. The additional incubation at 80 ˚C was our modification to the protocol of Ryckebosch et al (2011). To separate the layers, 500 microlitres of 5% aqueous sodium chloride was added and fatty acid methyl esters (FAME) were extracted using 300 microlitres of hexane.For quantification of FAME, tridecanoic acid (C13:0) was used as internal standard.

The gas chromatographic analysis was performed by injecting 1µl of FAME into the GC machine at 220 ºC. The initial oven temperature of 140 ºC was maintained for 5 minutes and ramped at 4 ºC to the final temperature 240 ºC. The peaks were identified by flame ionisation detector (FID) at 260 ºC. Supelco FAME mix containing 36 different fatty acids was used for peak identifications.

3.2.7 Genomic DNA library preparation and whole genome sequencing

The KAPA library preparation kit from Illumina was used to construct library from fragmented dsDNA via four main steps:

1. End repair: It produced blunt-ended, 5′- phosphorylated fragments.

2. A-tailing: To add dAdenine monophosphate (AMP) to the 3′ -ends of the dsDNA library fragments.

3. Adaptor ligation: For ligating dsDNA adaptors with 3′ -dThymidine monophosphate (TMP) overhands to library fragments.

4. Library amplification: It involved PCR amplification of library fragments carrying appropriate adaptor sequences on both ends.

The steps were followed according to the manual instructions of KAPA Library Preparation Kit – Illumina (KAPA Biosystems, Boston, Massachusetts, US).

3.2.8 Genome mapping, polymorphism identification and estimation of EMS mutation frequency

The read files in fastq format provided from sequencing were mapped using the software Burrows-Wheeler Aligner (bwa) with default parameter settings (Li and Durbin, 2009). The reads were mapped on the reference genome of *Phaeodactylum* Phatr2.0 (http://genome.jgi.doe.gov/Phatr2). The genome coverage was extracted using genomecov script of bedtools (Quinlan and Hall, 2010). To identify single nucleotide polymorphism (SNP), we used samtools mpileup (Li et al., 2009) and created a vcf file (variant call format) for each genome. Then we used the wild type vcf file as a reference to identify polymorphism due to EMS in mutant strain *Ptcer14*. We removed all polymorphism identified in both wild type and mutant using bedtools intersect (Quinlan and Hall, 2010).

To identify which genes are affected by SNPs, the gene structure reference file was used for *Phaeodactylum* (Phatr2_geneModels_FilteredModels2.gff, http://genome.jgi.doe.gov/Phatr2) and we genes containing snps were identified using bedtools intersect for the mutant strain. The mutation frequency due to EMS was identified using genomes of WT and mutant strain *Ptcer14*. The number of SNPs identified divided by the size of the reference genome and multiplied by 10,000 give a mutation per kilo-base metric.

3.2.9 Statistical Analysis

The data analysis was performed on Minitab statistical software package v. 16.2.4 (Minitab Inc.). In all experiments, mean values were compared by one-way ANOVA (Tukey, $P < 0.05$).

3.3 RESULTS

3.3.1 Cerulenin sensitivity of wild type strain

The sensitivity of the wild type *Phaeodactylum tricornutum* towards the antibiotic cerulenin was determined by growing cells on agar supplemented with different concentrations of cerulenin (0- 80 µM). Number of colonies obtained decreased as the concentration of cerulenin increased and no colonies could grow at 80 µM (Figure 21). Thus, 80 µM was selected and used as lethal dose for screening and isolating resistant mutants.

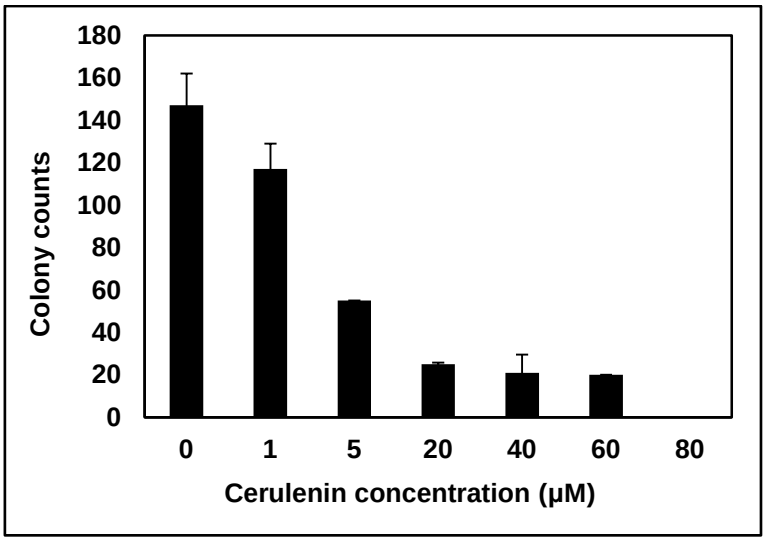

Figure 21. Effect of cerulenin on growth of wild type *P. tricornutum.* Error bars on mean values represent standard deviation of three replicates.

3.3.2 Isolation of EMS mutants under cerulenin selection pressure

Exponentially growing cultures of *P. tricornutum* treated with ethylmethane sulfonate (EMS) showed 66.6% lethality at 200 mM EMS (Figure 22) which was selected as mutagenesis dose. The lethal dose of EMS was 250 mM for *P. tricornutum* (Figure 22). Consideration for percentage lethality upon chemical mutagenesis in microalgae varies from 25-88% (Sakaguchi et al., 2011; Schneider et al., 1995). A total of 2×10^4 untreated and mutagenised cells were plated onto the cerulenin agar medium. After three weeks of growth on antibiotic selection medium colonies were counted. The frequency of cerulenin resistant mutants was recorded as 0.15×10^{-6}. This represents the *in vitro* frequency or the number of mutant cells and is different from mutation events. Hence, we have recorded only favorable mutations that lead to a cerulenin resistance phenotype. The resistant colonies were isolated from the agar medium and were re grown in liquid medium supplemented with cerulenin. The colonies that

survived the second round of re-selection were selected for further analysis. The selected mutants were grown as batch cultures for the lipid and fatty acid analysis.

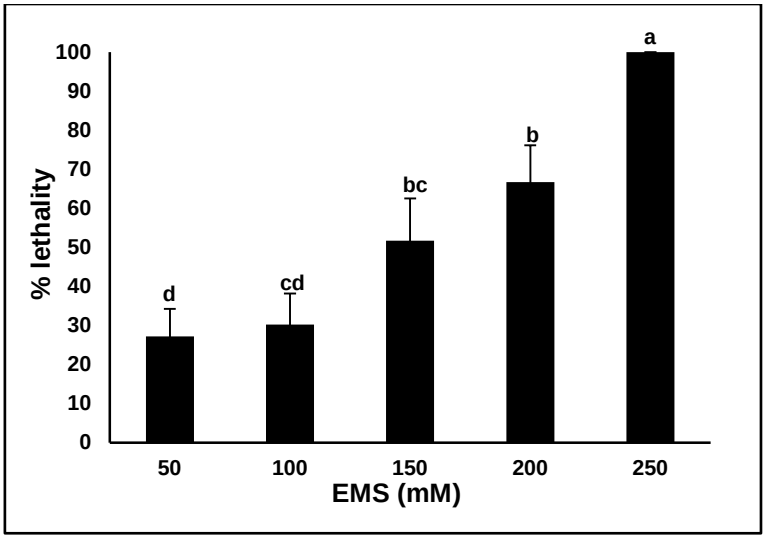

Figure 22. Effect of different concentrations of EMS on wild type cells of *P. tricornutum.* Analysis of variance was analyzed by one-way ANOVA and means that are shown with different alphabets are significantly different as tested by Tukey post hoc test. Error bars show standard deviations of three replicates.

3.3.3 Total lipids and growth characteristics of cerulenin resistant mutants

EMS induced random mutagenesis under the selection pressure of antibiotic cerulenin resulted in 14 independent tolerant mutant strains of *P.tricornutum* (Figure 23). To compare the accumulation of lipids in wild type and mutants, cells were grown upto the stationary phase in the absence of antibiotic cerulenin. The three cerulenin tolerant mutant strains designated as *Ptcer12*, *Ptcer13* and *Ptcer14* out of the total fourteen mutants displayed an increase in cellular lipid levels as high as 40% of dry weight biomass. The enhanced levels of lipids with respect to wild type strain in the three mutants *Ptcer12*, *Ptcer13* and *Ptcer14* were shown to be stable even after duration of one year. Monitoring of the specific growth rate in the absence of cerulenin revealed that *Ptcer13* showed a higher specific growth rate compared to the wild type (Figure 24). There were no observed differences in growth rates of wild type, *Ptcer12* and *Ptcer14* (Figure 24). Similar biomass productivities were observed for the wild type and *Ptcer* mutants (Figure 25).

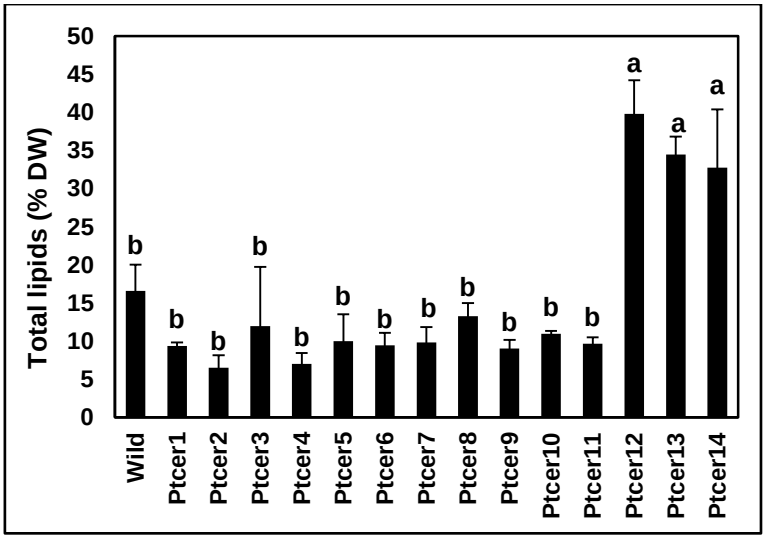

Figure 23. Dry weight (DW) total lipids of wild type and cerulenin resistant mutant cell lines. Analysis of variance was analyzed by one-way ANOVA and means that are shown with different alphabets are significantly different as tested by Tukey post hoc test. Error bars show standard deviations of three replicates.

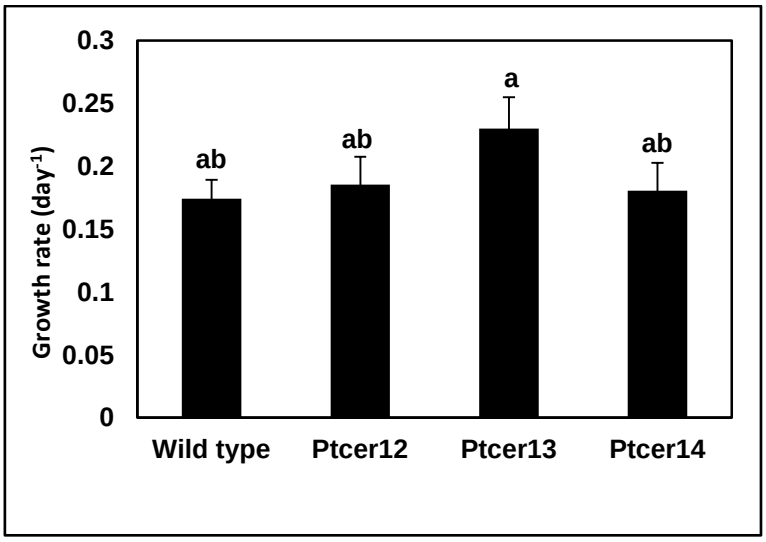

Figure 24. Comparison between growth rates of wild type (WT) and mutant strains of *P. tricornutum*. Means were analysed by one-way ANOVA and level of significance was tested by Tukey post hoc test and shown with different alphabets. Error bars show standard deviations of three replicates.

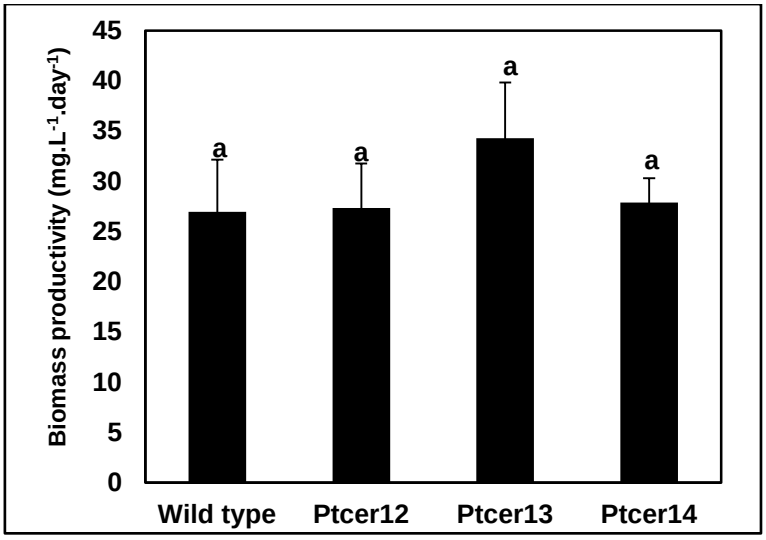

Figure 25. Comparison between biomass productivity of wild type and mutant strains of *P. tricornutum*. Means were analysed by one-way ANOVA and level of significance was tested by Tukey post hoc test and shown with different alphabets. Error bars show standard deviations of three replicates.

3.3.4 Lipidomic analysis

Qualitative analysis of the various classes of lipids in *Phaeodactylum tricornutum* was performed by annotating peaks from the MTBE-based extraction protocol (Giavalisco et al., 2011). *Phaeodactylum tricornutum* accumulated different classes of lipids namely phospholipids, glycolipids, non-polar lipids and betaine lipids. Diacylglycerol (DAG) and triacylglycerols (TAGs) constituted the non-polar or storage lipids (Figure 26). Heterogeneity in the lipidomic signatures showed that all three mutant strains are different from each other and to wild type strain (Figure 24). The TAGs of *P.tricornutum* mainly consists of unsaturated fatty acids. The only two saturated TAGs namely TAG 48:0 and TAG 50:0 found in *P. tricornutum* were abundant in *Ptcer14* (Figure 26). The pigment pheophytin was only found in mutant strains and highest in *Ptcer13* (Figure 26). Despite the observed differences among the different strains some generalized trend was also reflected from the lipidomic analysis. TAG and diacylglyceryltrimethylhomoserine (DGTS) lipids were amongst the major classes of lipids synthesized by *P. tricornutum* (Figure 27). The mutants *Ptcer12* and *Ptcer14* accumulated highest amounts of TAGs as compared to wild-type and *Ptcer14* synthesized lowest amounts of PCs (Figure 28). Of the various classes of lipids only TAGs and PCs were significantly changed in the mutant strains.

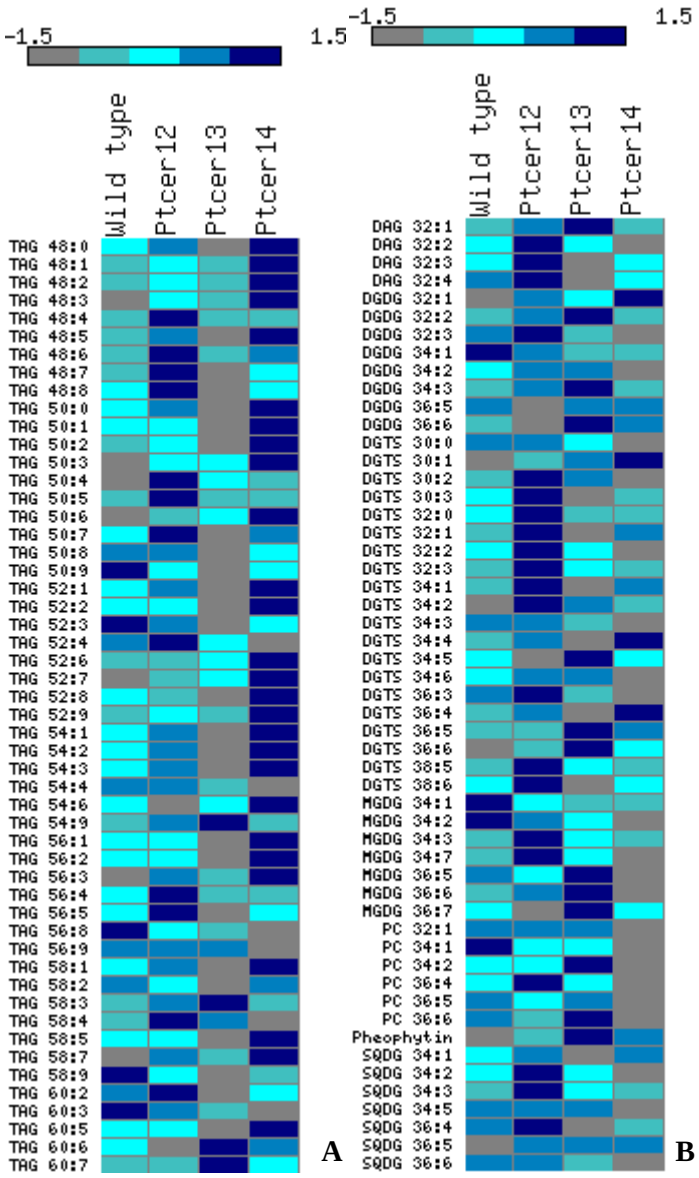

Figure 26. Heat map showing variations in composition of lipids detected in wild type and four cerulenin resistant mutant cell lines. A) Different types of triacylglycerols (TAGs), B) Other classes of lipids- diacylglycerols (DAG), digalactosyldiacylglycerols (DGDG), diacylglyceryltrimethylhomoserine (DGTS), monogalactosyldiacylglycerols (MGDG), Phosphotidylcholine (PC), sulfoquinovosyldiacylglycerols (SQDG).

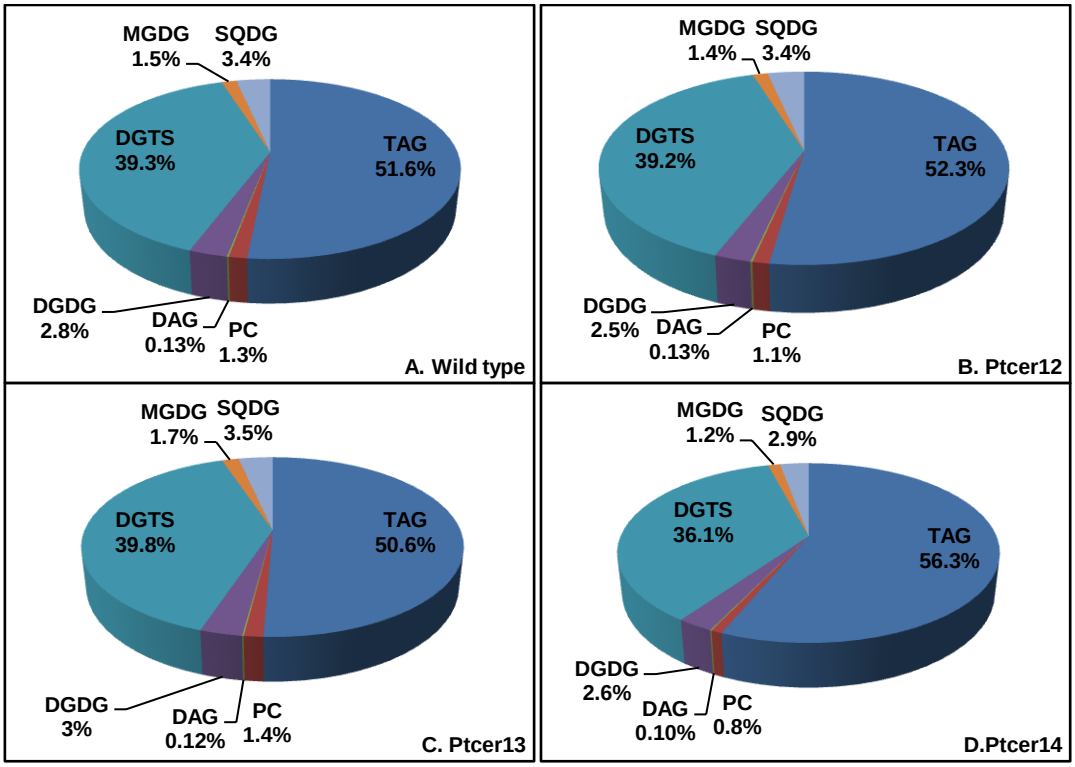

Figure 27. Distribution of lipid classes in wild-type and cerulenin resistant mutants. diacylglycerols (DAG), digalactosyldiacylglycerols (DGDG), diacylglyceryltrimethylhomoserine (DGTS), monogalactosyldiacylglycerols (MGDG), Phosphotidylcholine (PC), sulfoquinovosyldiacylglycerols (SQDG).

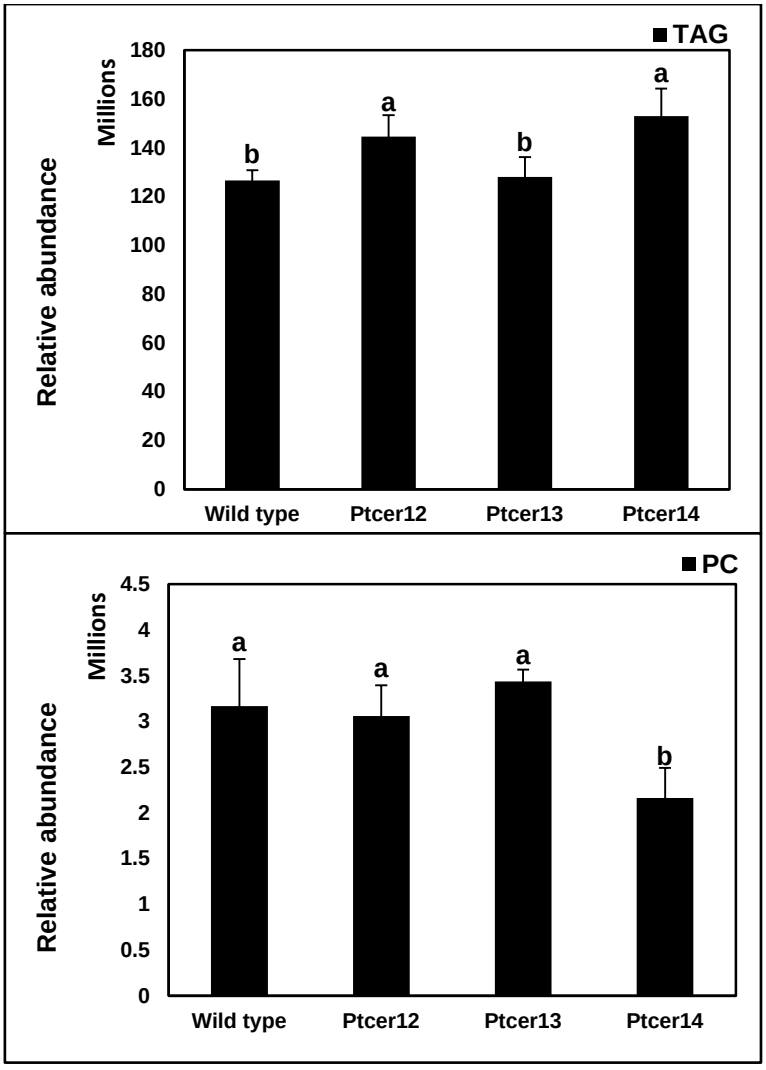

Figure 28. Relative abundance of triacylglycerols (TAGs) and phosphotidylcholine (PC) in wild type and mutant strains. Means were analysed by one-way ANOVA and level of significance was tested by Tukey post hoc test and shown with different alphabets. Error bars show standard deviations of three replicates.

3.3.5 Fatty acid profiling

The EMS mutants generated under cerulenin selection pressure showed both quantitative and qualitative heterogeneity in fatty acid profiles (Table 5, Figure 29-30). The mutant *Ptcer12* accumulated a greater number of fatty acids and thus showed the most diverse fatty acid profile among all the studied strains (Table 5). *Ptcer12* was the only strain that synthesized very long chain unsaturated fatty acids namely erucic acid (C22:1) and nervonic acid (C24:1), albeit at low levels.

Ptcer12 also accumulated highest amounts of EPA as percentage of dry weight biomass (Table 5). Compared to wild-type accumulation of short chain fatty acids namely caproic acid (C6:0) and caprylic acid (C8:0) remain unchanged in *Ptcer14* and reduced in both Ptcer12 and Ptcer13 (Table 5). The commercially valuable fatty acids such as oleic acid (C18:1), linolenic acid (C18:2),

linolenic acid (C18:3), γ-linolenic (C18:3 n6) and eicosapentaenoic acid (C20:5) showed variation among the wild-type and mutants. Occurrence of palmitoleic acid (C16:1), which is a dominant monounsaturated fatty acid found in diatoms (Mansour et al., 2005) was not significantly different among all the strains of *P. tricornutum* (Table 5).

Myristic (C14:0), palmitic (C16:0), palmitoleic (C18:1) and eicosapentaenoic acid (C20:5) were the major fatty acids accumulated by *P. tricornutum* (Figure 29). Proportions of major fatty acids among wild type and mutant strains varied. *Ptcer14* accumulated more EPA than palmitic and palmitoleic acids (Figure 29). *Ptcer12* and *Ptcer13* accumulated highest levels of oleic acid (Figure 30). The oleic acid content of *Ptcer12* and *Ptcer13* is around 4.4-4.6% of total fatty acids (Figure 30), which is two-fold increase over the wild type. Thus, mutagenesis can be easily used as an approach to develop tailor-made microalgal oils displaying different properties that can be exploited for wide number of applications. Comparing polyunsaturated fatty acids in wild type and mutants, *Ptcer14* showed a higher proportions of both linolenic (C18:2) and linolenic (C18:3) acids (Figure 30).

Fatty acids	Amount (% dry weight)			
	Wild-type	Ptcer12	Ptcer13	Ptcer14
Caproic C6:0	0.025 ± 0.002a	0.019 ± 0.001ab	0.018 ± 0.000b	0.024 ± 0.002a
Caprylic C8:0	0.039 ± 0.004a	0.031 ± 0.001bc	0.028 ± 0.002c	0.04 ± 0.002a
Myristic C14:0	0.521 ± 0.09ab	0.603 ± 0.07a	0.425 ± 0.07ab	0.303 ± 0.03b
Palmitic C16:0	1.352 ± 0.16ab	1.888 ± 0.08a	0.920 ± 0.10b	0.730 ± 0.11b
Palmitoleic C16:1	2.524 ± 0.58ab	2.803 ± 0.16ab	1.965 ± 0.43ab	1.347 ± 0.43b
Heptadecanoic C17:0	0.059 ± 0.01	0.0512 ± 0.003	0.054 ± 0.004	0.040 ± 0.004
Oleic C18:1	0.220 ± 0.000ab	0.380 ± 0.004a	0.305 ± 0.05ab	0.157 ± 0.06b
Linoleic C18:2	0.131 ± 0.03	0.145 ± 0.01	0.114 ± 0.00	0.09 ± 0.01
Linolenic C18:3	0.068 ± 0.03	0.077 ± 0.01	0.076 ± 0.01	0.064 ± 0.001
γ-linolenic C18:3n6		0.022 ± 0.006	0.020 ± 0.003	
Eicosatrienoic C20:3n3		0.020 ± 0.00	0.016	
Eicosapentaenoic C20:5	1.03 ± 0.02ab	1.215 ± 0.11a	1.028 ± 0.01ab	0.928 ± 0.06ab
Erucic C22:1		0.022 ± 0.002		
Nervonic C24:1		0.032 ± 0.002		

Table 5. Fatty acid profiles of wild-type and cerulenin resistant mutant strains of *P. tricornutum*. Means were analysed by one-way ANOVA and level of significance was tested by Tukey post hoc test and shown with different alphabets. Error bars show standard deviations of three replicates.

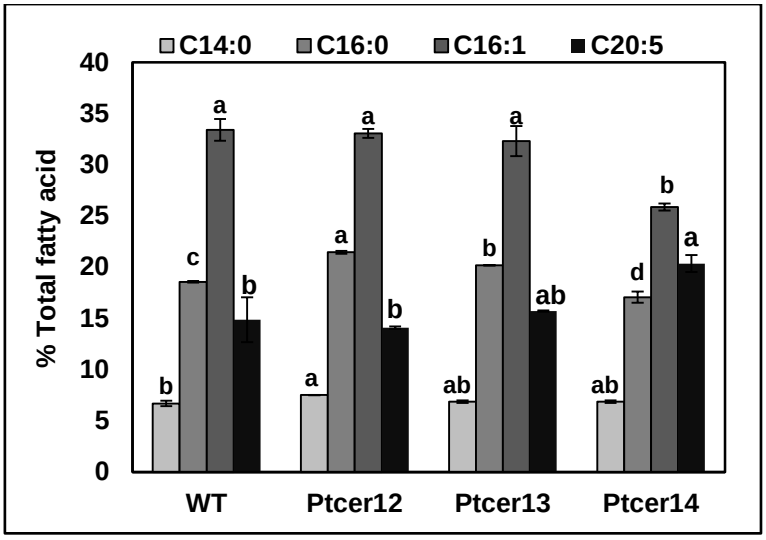

Figure 29. Percentages composition of major fatty acids accumulated in total fatty acids biosynthesized by wild-type and mutants of *P. tricornutum*. Means were analysed by one-way ANOVA and level of significance was tested by Tukey post hoc test and shown with different alphabets. Error bars show standard deviations of three replicates.

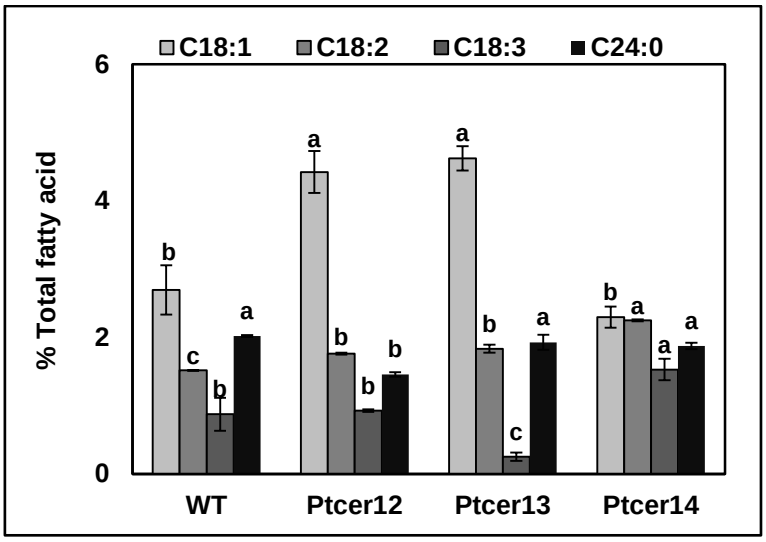

Figure 30. Percentages composition of minor fatty acids accumulated in total fatty acids biosynthesized by wild-type and mutants of *P. tricornutum*. Means were analysed by one-way ANOVA and level of significance was tested by Tukey post hoc test and shown with different alphabets. Error bars show standard deviations of three replicates.

3.3.6 Misregulation of fatty acid synthase genes

The levels of mRNA of three important genes involved in the fatty acid biosynthesis initiation II pathway was monitored. It is possible that cerulenin resistant mutants can be derived due to suppressor mutations in the fatty acid synthase gene or the pathway resulting in cerulenin resistance. Additional mechanisms can be posited to explain the antibiotic resistance in cerulenin resistant *Ptcer*

mutants. For instance, an increase in expression levels of relevant genes encoding enzyme oxoacyl-acp synthase which is inhibited by antibiotic cerulenin. We have tested this hypothesis and demonstrate overexpression of genes encoding 3-oxoacyl-acp synthase in the selected *Ptcer* mutants that have shown increments in levels of total lipids. Overexpression of the target gene could provide an explanation for counteracting the inhibition by antibiotic (Figure 31). An increased expression of synthase I (FABB) that catalyses elongation of unsaturated fatty acids could explain the enhancement in proportions of oleic and linolenic acids in *Ptcer13* (Figure 30). Synthase II (FABF) is also involved in the regulation of fatty acids through elongation of palmitoleic acid and all three mutants have shown an increase over the wild type FABFa expressions levels (Figure 31). The disparity in the extent of increase in long chain unsaturated fatty acid content in mutant, despite unchanged level of FABB could be explained by genome sequencing as explained in section 3.3.7. However, further study on transcriptome analysis of genes involved in biosynthesis of lipids is needed.

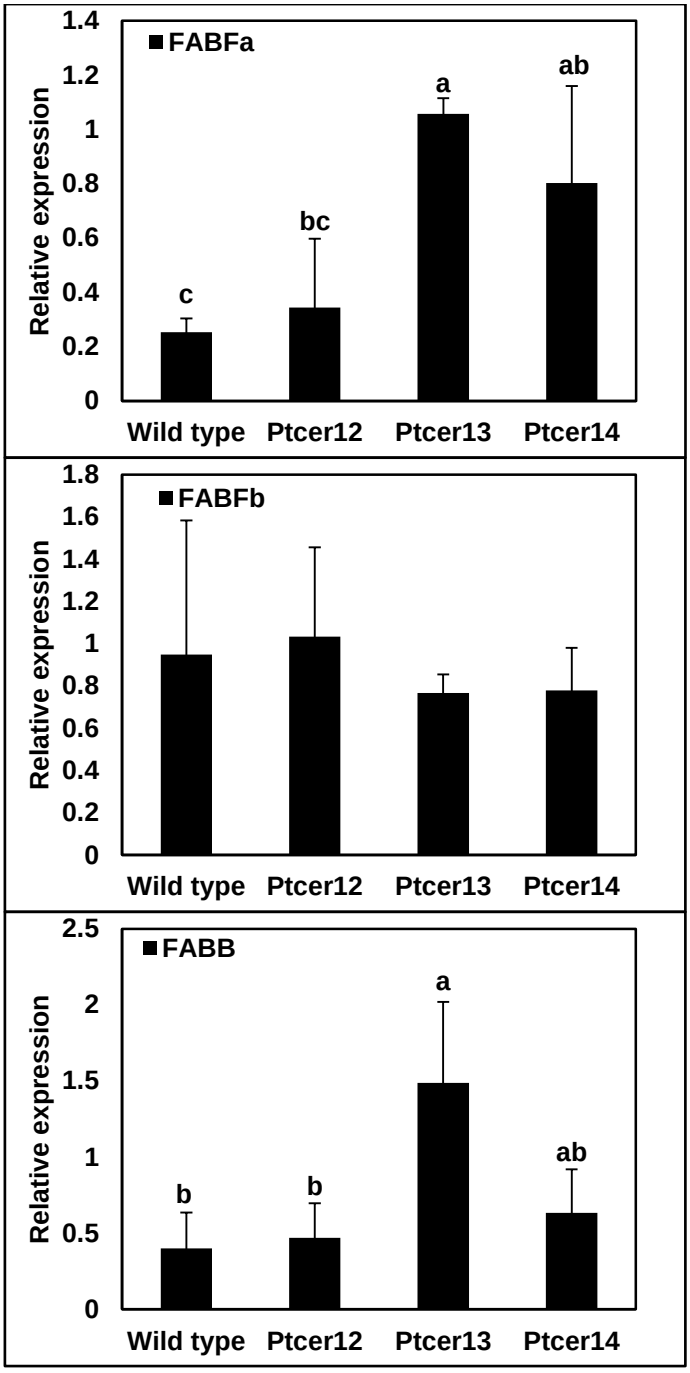

Figure 31. Graphs showing quantitative dysregulation in expressions of A) FABFa, B) FABFb and C) FABB genes. Data is mean of 3 biological replicates and coefficient of variance was tested by performing ANOVA. Error bars show standard deviation and are indicated with different alphabets that show significant differences.

3.3.7 Mutation discovery by whole genome sequencing

The high lipid producing mutant *Ptcer14* was randomly chosen for whole genome sequencing to estimate the EMS mutation frequency. The genome of mutant *Ptcer14* showed large number of mutations compared to wild type genome (Table 6). A total of 8554 single nucleotide substitutions were detected in *Ptcer14* both in coding and non-coding regions of the genome. The fatty acid biosynthesis initiation II pathway produces an acetoacetyl-[acp] activated molecule that is used for subsequent elongation reactions, which finally produce the fatty acids. The reactions in initiation II pathway are catalysed by individual enzymes that are encoded by a discrete gene. The genes involved in this pathway namely FABFa, FABFb and FABB (Figure 32). Formation of long chain polyunsaturated fatty acids involves various desaturases and elongases (Figure 33). In *Ptcer14* three genes involved in the initiation and formation of polyunsaturated fatty acids showed SNPs which were FABB, PTD5 and PTD6 (Table 6).

Mutant strain	**Total mutations/genome**	**Mutations/kb**	**Total genes showing mutations**	**Average genome coverage (WT: 114X)**	**Candidate genes with mutations**
Ptcer14	**8554**	**0.329**	**807**	**80X**	**Δ6-desaturase, Δ5-desaturase, *PTD6, FABB***

Table 6. Summary of mutations screened by whole genome sequencing of cerulenin resistant EMS mutant of *P. tricornutum.*

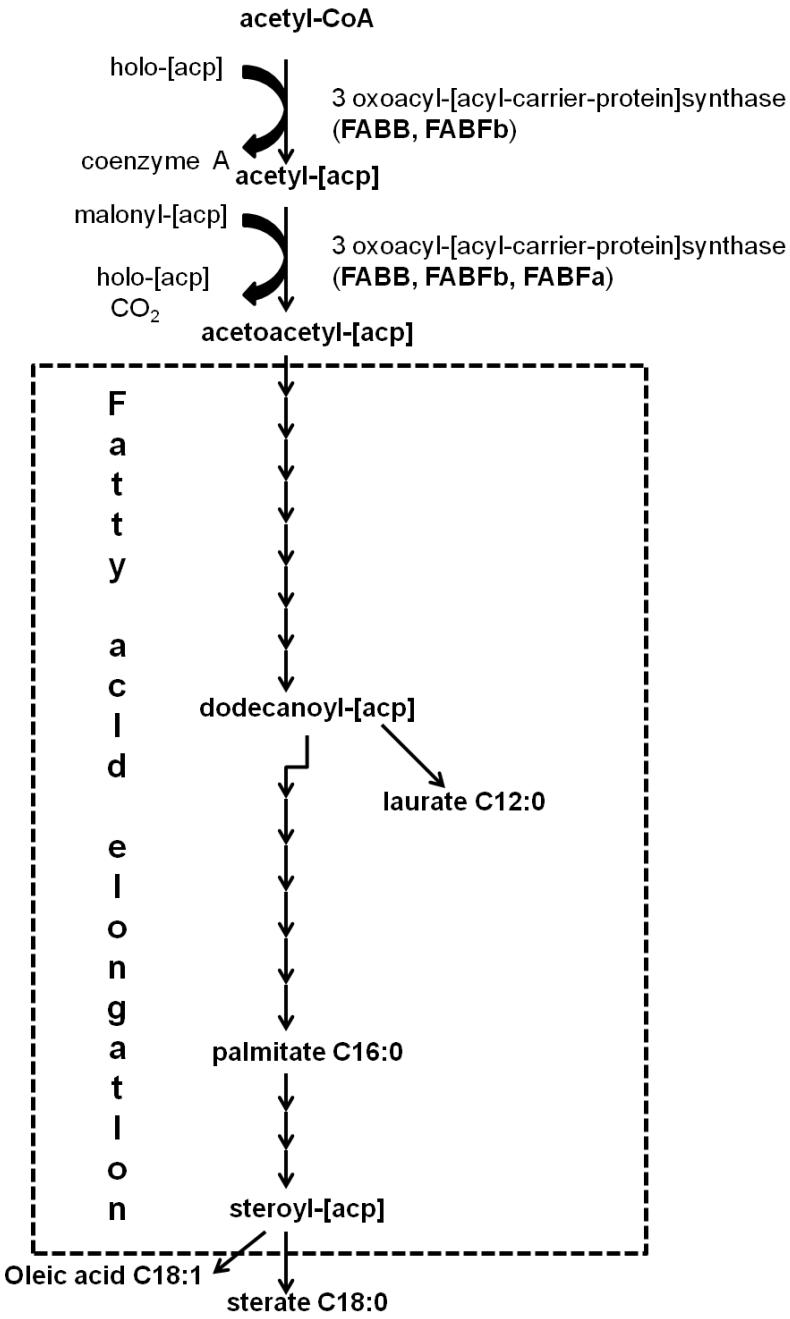

Figure 32. Fatty acid biosynthesis initiation II and elongation pathway in *P. tricornutum*. The initiation II reactions are catalysed by individual soluble proteins acetyl-CoA:ACP transacylase and synthase each encoded by FABFa, FABFb and FABB genes. The dotted box represents reactions involved in fatty acid elongation and formation of saturated fatty acids.

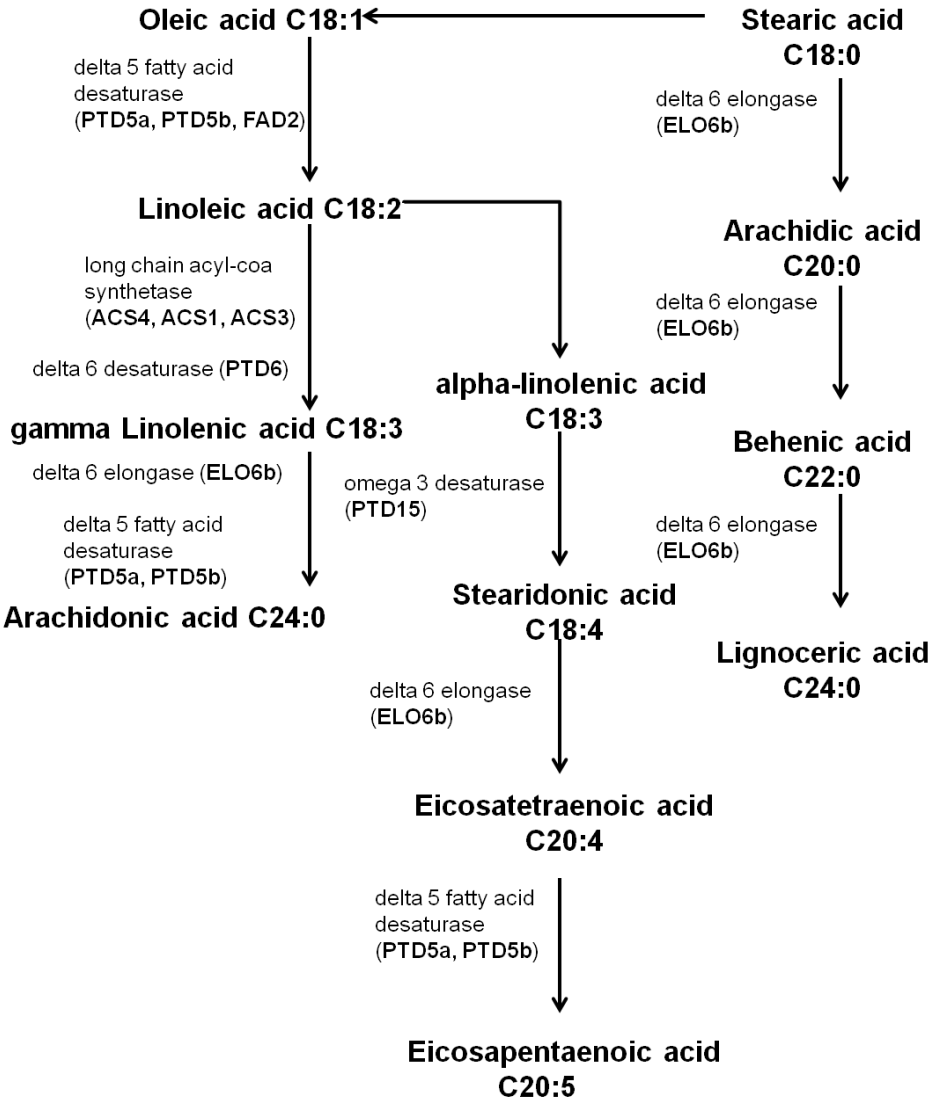

Figure 33. Pathway proposed for biosynthesis of very long chain and polyunsaturated fatty acids in *P. tricornutum*. The very long chain lignoceric acid is formed by series of reactions catalysed by delta 6 elongase encoded by gene ELO6b. The formation of polyunsaturated fatty acids involves delta 5 and delta 6 desaturases encoded by genes PTD5 and PTD6. Adapted from (Li et al., 2014).

3.4 DISCUSSIONS

The use of random mutagenesis as a tool for manipulating levels of cellular metabolites such as lipids, polyunsaturated fatty acids and pigments has been exploited only for few microalgae namely *Chlamydomonas* (McCarthy et al., 2004), *Nannochloropsis* (Chaturvedi et al., 2004; Doan and Obbard, 2012), *Chlorella* (Manandhar-Shrestha and Hildebrand, 2013) and *Haematococcus* (Sandesh Kamath et al., 2008). Hitherto, there is no report of EMS induced random mutagenesis in marine diatom *P. tricornutum*. Isolation of EPA over producing genetic mutants of *Phaeodactylum*

tricornutum has previously been reported by use of ultraviolet radiations (Alonso et al., 1996) without selection pressure.

In the present study, EMS was used for whole genome random mutagenesis of *P.tricronutum* and mutants were selected based on their antibiotic resistance. The antibiotic resistance insures genetically tractable mutants which can easily be isolated from the nutrient agar supplemented with antibiotic. The average mutation rate scored by counting cerulenin resistant colonies was estimated to be 1.5 in 10^7. This is comparable to mutational frequency reported for spontaneous resistant mutants in other microalgae such as *Chlamydomonas reinhardtii* (1 in 10^7) (Hartnett et al., 1987), and *Nannochloropsis oculata* (5-10 in 10^7) (Chaturvedi et al., 2004).

The main objective of EMS mutagenesis was to obtain mutants that display enhancements in total lipid content. Therefore, the antibiotic cerulenin which inhibits the enzyme involved in de novo synthesis of fatty acids, the building blocks of all lipids was used for selection of mutants. Cerulenin inhibits the enzyme β-ketoacyl-ACP synthase which catalyse the condensation reaction wherein it transfers an acyl primer to malonyl-ACP to form β-ketoacyl-ACP which is extended by 2 C atoms (Price et al., 2001) and is an important regulator of lipid metabolism. The resistant mutants in this study showed a 2.5 fold increase in the levels of lipids compared to the wild type. Apart from random mutagenesis, there are several other approaches to augment cellular lipids in microalgae. In *P.tricornutum* the enhancement of cellular lipids due to changes in growth conditions could only reach levels of 16% dry weight (Adarme-Vega et al., 2012). Thus, impact of growth conditions such as nutrient stress on EMS mutants developed in this study would be interesting to observe any further increases in lipid levels. Lipids in *P. tricornutum* are comprised of various classes like phosphatidylcholines (PCs) and galactolipid species namely, monogalactosyldiacylglycerols (MGDGs), digalactosyldiacylglycerols (DGDGs) and sulfoquinovosyldiacylglycerols (SQDGs) which are used in cell membranes. The thylakoid membrane of diatoms contain anionic SQDG and phosphatidylcholine (Prihoda et al., 2012). The other lipids such as triacylglycerols or TAGs represent energy storage form which is more than two fold greater than starch and is highly important bio molecule for conversion to biodiesel (Siaut et al., 2011). The *de novo* biosynthesis of triacylglycerol requires two substrate pools namely diacylglycerols (DAGs) and phosphotidylcholine (PC). Phosphotidylcholine is abundant phospholipids in both animal and plants and are key building blocks of membrane bilayers. For biodiesel applications, phospholipids are not suitable species as phosphate obstructs the transesterification process and thus the yield of biodiesel is reduced to less than 70% (MacDougall et al., 2011). Interestingly, an enhancement of TAGs in *Ptcer14* was observed with a concomitant decrease in PC levels which is an important factor for biodiesel application.

The lipids are composed of fatty acids which play important roles in energy storage, membrane transport, and chemical precursors in many materials (Ota et al., 2009). The different

classes of fatty acids are saturated, monounsaturated and polyunsaturated depending on the number of double bonds. The algal lipids have high quantities of fully saturated fatty acids namely palmitic (C16:0) and stearic (C18:0) which play an important role in terms of biofuels (Talebi et al., 2013). The mutant strain *Ptcer12* accumulates the highest amount of palmitic acid. For biodiesel application, the ideal fatty acid methyl esters profile exhibit low degree of polyunsaturated fatty acid and high amount of palmitic and oleic acids (Pereira et al., 2013).Microalgae are the primary producers of omega-3 long chain polyunsaturated fatty acids (LC-PUFA) which have various health benefits. Based on total lipid content, omega-3 LC-PUFA content and ease of cultivation, the microalgae *Nannochloropsis* and *Phaeodactylum* are promising candidates for commercialization (Ryckebosch et al., 2012).

The less abundant classes of very long chain fatty acids such as erucic and nervonic acids are important bioindustrial and bionutritional oils. The new mutant *Ptcer12* accumulated these two less abundant classes of VLCFA. The other microalgal strain that synthesize nervonic acid is *Mychonastes afer* HSO-3-1 which accumulates 3.8% of total fatty acids (Yuan et al., 2011). Industrial applications of erucic acid include lubricant, detergent, cosmetics and in pharmaceuticals; whereas nervonic acid (which is abundant in myelin sheath of nerve fibre) is useful in dietary therapy for proper neurological functions and thus has potential nutritional applications (Cook et al., 1998; Taylor et al., 2010). The manufacturing and marketing of tailored oil is expanding recently, for example the collaborative deal between Solazyme and Sasol to supply algae-based erucic acid (http://www.che.com/only_on_che/latest_news/Solazyme-to-supply-algal-oil-to-Sasol_10862.html). The microalgae rich in oleic acid have potential to act as a renewable and sustainable source for skin care products. The leading anti-aging skincare brand namely Algenist (http://www.algenist.com/why-algenist/patented-breakthrough-ingredient) exploits the use of oleic acid rich microalgae oil in formulating advanced anti-aging repairing oil. Previous report on improvement of *P. tricornutum* by UV mutagenesis showed merits in terms of dry weight content of EPA but not as percentage of total fatty acids (Alonso et al., 1996). In this PhD study, EMS mutants showed differences both in terms of dry weight content and as percentage of total fatty acids particularly for palmitic, palmitoleic acid and EPA.

3.5 CONCLUSIONS

Numerous ways by which production of valuable fatty acids can be enhanced for commercial utilization include screening of oleaginous microalgal strains, genetic improvement, culture conditions optimization and developing high efficiency photobioreactor. This study employed whole genome mutagenesis as a method of genetically improving a wild strain of diatom *Phaeodactylum tricornutum* for augmentation of cellular lipids and valuable fatty acids. The improved new strains that were isolated using the selective pressure of the antibiotic cerulenin showed elevated levels of total lipids, heterogeneous lipidomic signatures and modified fatty acid profiles. Compared to wild type progenitor, the three novel mutant strains namely *Ptcer12*, *Ptcer13* and *Ptcer14* accumulated 2-2.5 fold amounts of dry weight lipids. Over accumulation of triacylglycerols with concomitant decrease in production of phospholipid in mutant strain *Ptcer14* makes it a potential feedstock strain for biodiesel. Synthesis of significantly higher ($P < 0.002$) levels of oleic acid was observed in mutant strains *Ptcer12* and *Ptcer13*. Oleic acid possesses anti-aging repairing properties and is a commercially useful fatty acid. The two very long chain monounsaturated fatty acids namely erucic (C22:1) and nervonic acid (C24:1) that have important industrial implications were only produced by *Ptcer12*, albeit at low levels. As demonstrated in this study, the use of antibiotic selection pressure cerulenin resulted in successful generation of resistant mutants showing augmented lipid profiles, which have not been previously available in this diatom.

4. CHAPTER FOUR

High lipid mutants of *Phaeodactylum tricornutum* generated by saturation mutagenesis combined with fluorescence activated cell sorting (FACS)

Chapter 4 – EMS mutagenesis with flow cytometry

ABSTRACT

Random whole mutagenesis offers a powerful approach for increasing the levels of commercially important bioproducts in microalgae. Saturation whole-genome mutagenesis coupled with fluorescence activated cell sorting allows rapid isolation of desired mutants from a population of millions of cells in a few hours. Using a mutagenised population of approximately 75 million cells, we performed fluorescence activated cell sorting (FACS) based single cell sorting in 96 well plates to generate clonal oleaginous mutants of *Phaeodactylum tricornutum*. From the 75 million cells screened by FACS, we obtained oleaginous mutants that displayed 44-50% dry weight total lipids and higher biomass productivity. The oleaginous mutants accumulated higher amounts of eicosapentaenoic acid (EPA) which is commercially valuable polyunsaturated fatty acid. This study demonstrate the application of lipophilic dye BODIPY for the development of cytometric based single cell isolation method which is faster than the traditional technique of antibiotic selection for oleaginous diatoms.

4.1 INTRODUCTION

Marine microalgal mutant lines generated through random whole-genome mutagenesis can form the basis for improved feedstock for aquaculture practices as they can generate high biomass, produce large amounts of lipids and can synthesize various useful fatty acids (Doan and Obbard, 2012). Random whole-genome mutagenesis on millions of cells can induce different point mutations in different cells that can be used as a basis to generate mutants with desirable characteristics for various strains of microalgae and cyanobacteria (Tillich et al., 2012). Random whole-genome mutagenesis of large populations of cells when coupled with high throughput cell-sorting platforms such as FACS, allow screening for cells hyperproducing commercially important molecules such as triacylglycerols (TAGs) in microalgae (Manandhar-Shrestha and Hildebrand, 2013). Flow cytometry (FACS) based approaches allow isolation of overproducer sub-populations from a heterogeneous microalgal cultures that can be cultivated again for further analysis and cultivation (Hyka et al., 2013). Successive cell sorting using flow cytometry (from cell populations with very limited genetic variation consisting only of three strains) led to doubling of intracellular lipid content (to 55%) in marine *Nannochloropsis* sp after only three rounds of consecutive cell sorting (Yen Doan and Obbard, 2011).

Microalgal lipid bodies contain TAGs which are suitable for conversion to fatty acid methyl esters or biodiesel. TAGs are easily stained using lipophilic dyes such as Nile Red (9-diethylamino-5H-benzo-aphenoxazine-5-one) and BODIPY 505/515 (4,4-difluoro-1,3,5,7-tetramethyl-4-bora-3a,4a-diaza-s-indacene) for fluorescence analysis of intracellular lipids in microplates, which allows identification of overproducer microalgal and diatom strains (Wong and Franz, 2013). The TAGs of diatoms are rich in nutritional fatty acids such as eicosapentaenoic acid, which is important bioactive compound and has proven beneficial for treatment of coronary heart diseases (Pérez-López et al., 2014).

Diatoms produce up to 60% of their cellular mass as TAGs under some growth conditions, and are potentially carbon neutral feedstock for biodiesel production (Zendejas et al., 2012). TAGs from algal lipids contain unsaturated fatty acids which are good alternative source of fish oils. The marine diatom *Phaeodactylum tricornutum* synthesizes a high abundance of polyunsaturated fatty acid namely eicosapentaenoic acid (EPA) which is around 44.7% of total TAGs (Rezanka et al., 2012). For conversion of TAGs into biodiesel, the total fatty acid composition of *P. tricornutum* is important as it affects the fuel properties of the derived biodiesel (Zendejas et al., 2012). Genetic manipulation of *P. tricornutum* improves the biofuel quality by increasing accumulation of short chain fatty acids such as lauric acid (C12:0) and myristic acid (C14:0) (Radakovits et al., 2011). In the

present study, we employed whole genome saturation mutagenesis on large populations of cells combined with FACS isolation of cells hyperproducing fatty acids as a method for genetic improvement of *P. tricornutum* to enhance production of cellular lipids and alter fatty acid profiles.

4.2 MATERIALS and METHODS

4.2.1 Diatom strain and culturing

The CCAP 1055/A strain of *Phaeodactylum tricornutum* was obtained from Culture Collection of Algae and Protozoan (CCAP), Dunstaffnage Marine Laboratory, Oban, Argyll, UK. Cultures were grown in F2 (Guillard, 1975) medium prepared in GF/F filtered natural sea water at 17 ˚C in 12:12 day/light under intensity of white fluorescent lights (for recipe see Appendix I). The cultures were grown in Erlenmeyer flasks (50 – 500 ml) with 20 to 300 ml F2 medium and were shaken at 120 rpm on an orbital shaker.

4.2.2 Ethyl methane sulfonate (EMS) mutagenesis

A total of 1 x 10^6 cells per ml growing in exponential phase (~5-7 days) were subjected to random mutagenesis with 200mM EMS in darkness at 17 ˚C with constant shaking at 1000 rpm. After incubation of 2 hours exposed cells were centrifuged and 5% sodium thiosulfate was added to the cell pellet to neutralise and wash off the excess EMS. Additional two washings with were also performed. Washed cells were resuspended in sterilised F2 medium and were grown under normal culture conditions prior to cell sorting by flow cytometry.

4.2.3 Fluorescence activated cell sorting and growth screening

Mutagenised cells of *P. tricornutum* were sorted using a high speed BD FACS Aria II cells sorter equipped with 488 nm blue laser and 100 μm nozzle. A 15 ml volume of cells at concentration of 5 X 10^6 cells per ml (a total of approx 75 million cells) were stained with 2 μM BODIPY 505/515 (4,4-Difluoro-1,3,5,7-Tetramethyl-4-Bora-3a-Diaza-s-Indacene) (Cooper et al., 2010) for 96 well plate single cell sorting. Artificial sea water of pH 8.0 and salinity 30 was used as sheath fluid. While sorting, the sample and collection temperature was maintained at 17 ˚C and cells were agitated at 300 rpm. Cells were observed on dot plots of side scatter (SSC-A) vs forward scatter (FSC-A) and autofluorescence of unstained cells was measured at 695/40 nm (PerCp Cy5.5 channel) (Figure 34a). BODIPY fluorescence was measured at 530/30 nm (AF 488-A channel) (Figure 34b). For sorting, gates were established on SSC vs FSC plots and were kept constant throughout the sorting procedure (Figure 34). Four individual 96 well plate sorts, namely: 30 cells/well, 10 cells/well, 3 cells/well and 1 cells/well were performed in triplicates to calculate the sort cloning efficiency. Sterile conditions were maintained throughout the sorting procedure. Following sorting, individual sort plates were kept under normal growth conditions and cell proliferation in plates were observed after 15 days under Olympus CKX41inverted microscope. Total number of positive responses (BODIPY positive sorted

cells) obtained per dose and 3 replicates for each of the 96 well plate sorts was calculated using L-Calc™ software (StemCEll Technologies Inc, Version 1.1.1 2005). To select the highest growing clones from 1 cell/well sort 96 well plates, we seeded equal volume of culture from original sort plate into new 96 well plates containing sterile F2 medium. The growth rates were calculated by daily measurements of OD750. The first screening for growth was performed for 8 days and we calculated specific growth rate using the following formula $\mu = \ln (OD_n/OD_0)/ (t_n-t_0)$ where OD_n and OD_0 are optical densities at nth and 0 day respectively.

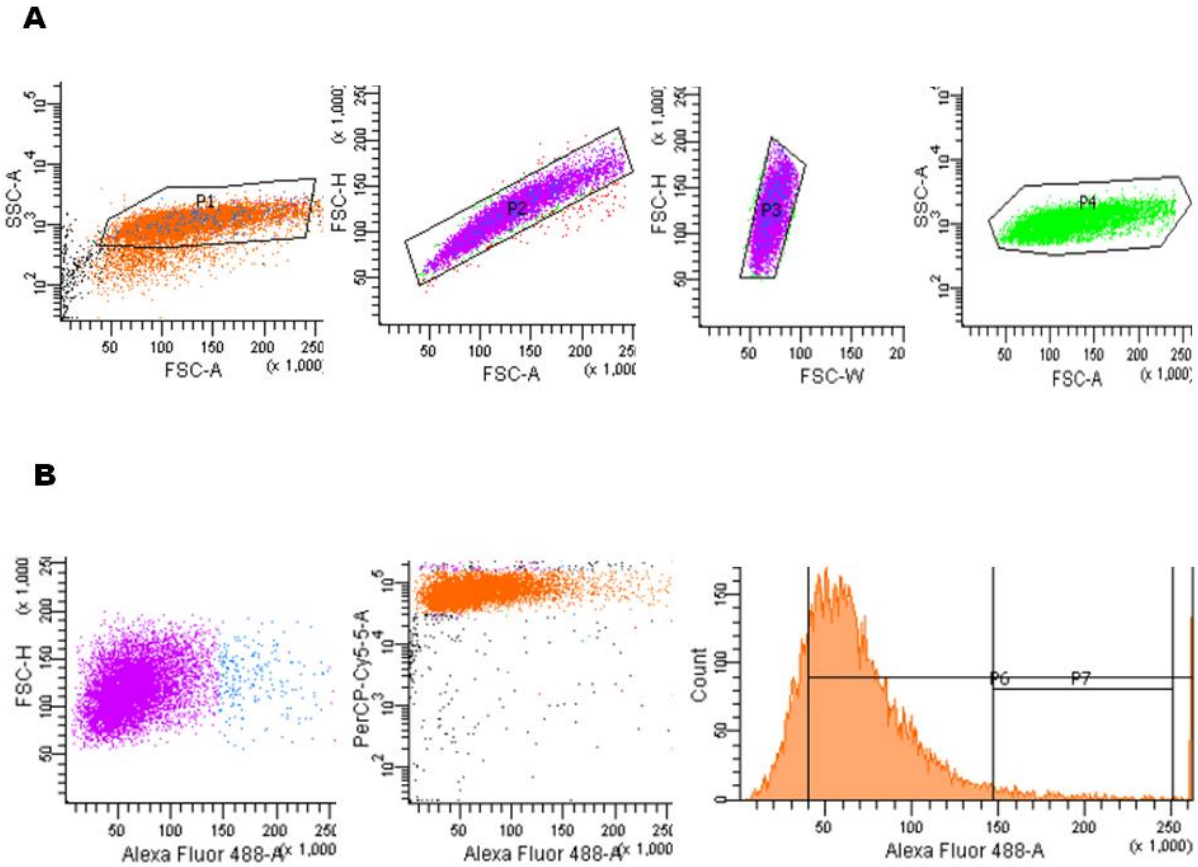

Figure 34. Dot-plots of flow cytometry analysis with the gated region of BODIPY stained diatom populations which are distinguished by their size (FSC), granularity (SSC), chlorophyll content (PerCP-Cy5-5-A), and BODIPY staining (Alexa Fluor).

4.2.4 Total lipids and FAME analysis

Optimized analytical procedure of Ryckebosch et al (2011) was followed for extraction of lipids from the lyophilized diatom cells. Briefly, known amount of lyophilized microalgae was mixed with chloroform-methanol 1:1 in a glass vial and vortexed. Equal volume of solvent mixture and water was added to separate the aqueous methanolic layer and lipidic chloroform layer by centrifuge at 2000 rpm for 10 min. Lower layer was transferred into another vial and cell pellet was reextracted in the solvent mixture followed by layer separation. The two chloroform layers were pooled and filtered through anhydrous sodium sulphate using Whatman No. 1. The chloroform was evaporated in a stream of nitrogen gas and dried extract was weighed and expressed as % total lipids.

Transesterification on dried lipids was performed according to Ryckebosch et al (2011). Briefly, to 1 mg of dried lipids, 100 microlitres of toluene and 200 microlitres of 1% sulphuric acid in methanol were added and incubated at 80 ˚C for one hour followed by overnight incubation at 50 ˚C. The additional incubation at 80 ˚C was our modification to the protocol of Ryckebosch et al (2011). To separate the layers, 500 microlitres of 5% aqueous sodium chloride was added and fatty acid methyl esters (FAME) were extracted using 300 microlitres of hexane.

For Gas chromatography analysis, 5 microliter of FAME was injected at 220 ºC. The starting oven temperature of 140 ºC was initially maintained for 5 minutes and ramped at 4 ºC to the final temperature of 240 ºC and analysed by flame ionisation detector (FID) at 260 ºC. Supelco FAME mix containing 36 different fatty acids was used to identify the fatty acids detected in diatom samples.

4.2.5 Genomic DNA library preparation and whole genome sequencing

The KAPA library preparation kit from Illumina was used to construct library from fragmented dsDNA via four main steps as described earlier in section 3.2.7. The bioinformatic analysis of genome sequencing including SNP identification and EMS mutation frequency of WT and mutant *EmPt2A6* was performed in same manner as described in section 3.2.8.

4.2.6 Statistical analysis

The data analysis was performed on Minitab statistical software package v. 16.2.4 (Minitab Inc.). In all experiments, mean values were compared by one-way ANOVA (Tukey, $P < 0.05$).

4.3 RESULTS

4.3.1 Growth competitiveness among singly sorted mutagenised cells

Four different sorting formats viz. 30 cells/well, 10 cells/well, 3 cells/well and 1 cells/well were tested to estimate the sorting frequency. The sorting frequency is defined as number of positive responses (growth) obtained per dose (cells/well) for total number of replicates tested. The frequency of 1 in 2 was obtained for the BODIPY stained mutagenised cell population of *P. tricornutum*. The positive

response or growth depend on the number of selected cells (BODIPY +ve) placed in each well. In 1 cell/well sort format we obtained 27% negative response (Figure 35, Table 6). The cells were grown in well plates in smaller volumes without any agitation due to which some cells sank down at the bottom of well. The curve tails off rather than go through the origin suggest that the culture system was not 100% optimal as they were growing in well plates and not culture flasks (Figure 35). Random mutagenesis followed by fluorescence activated cell sorting resulted in large number of single cell clones (~96^3) per sorting format. For establishing mutant clonal population that originated form a single cell, we maintained surviving cells from 1 cell/well plates. Initial screening of single cell sort was performed by sub culturing into fresh F2 96 well plates and OD750 measurements were recorded daily for 8 days using a plate reader. In addition to dry weight lipid screening, isolation of improved strains requires that growth of mutants be competitive (Manandhar-Shrestha and Hildebrand, 2013), therefore we aimed for selecting oleaginous mutants that also possess high growth rates so that they are competitive with wild type. Growth rate was measured for each well and comparison is shown in heat maps constructed from three replicate 96 well plates (Figure 36). In heat maps, wells coded with fluorescent green colour (Figure 36) showed highest growth rates and were selected for lipid screening.

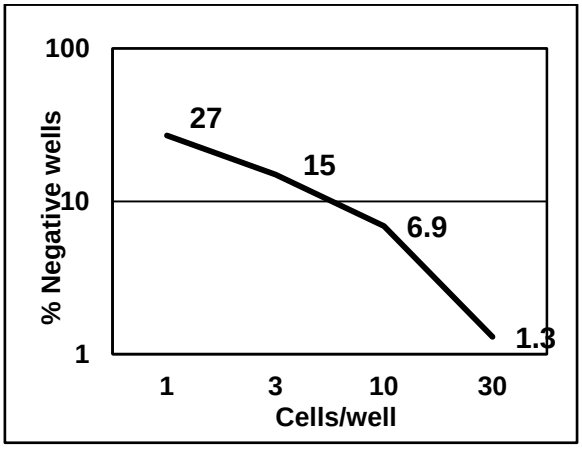

Figure 35. Sorting efficiency of *P. tricornutum* cells subjected to fluorescence activated cell sorting in a 96 well plate format.

Dose (number of cells sorted/well)	Number of wells with surviving cells	Number of wells
30	**284**	**288**
10	**268**	**288**
3	**243**	**288**
1	**210**	**288**

Table 6. Post sorting analysis for survival frequency of cells sorted in four different sorting formats viz. 30 cells/well, 10 cells/well, 3 cells/well and 1 cell/well.

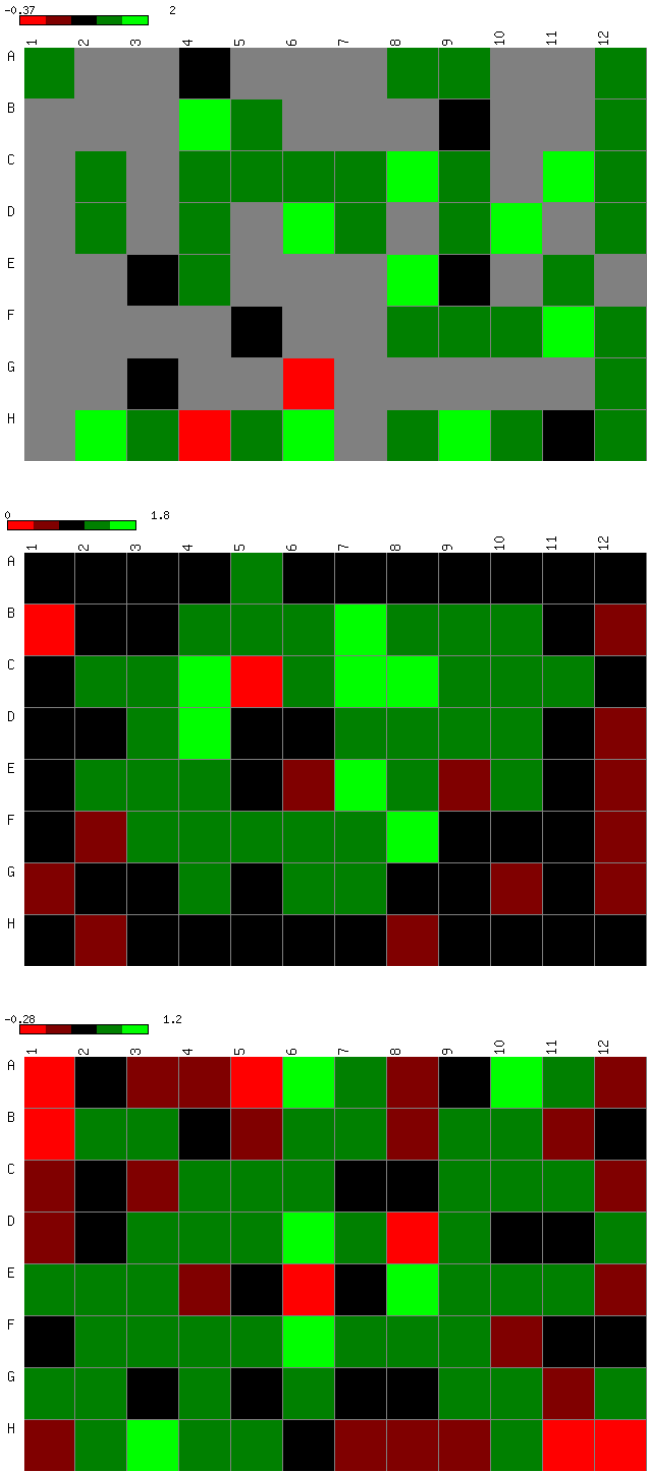

Figure 36. Heat maps showing average growth rates of singly sorted cells. Color code- in red- lowest growth rate, fluorescent green- highest growth rate.

4.3.2 Growth comparisons in high lipid producing mutant strains of *P. tricornutum*

After the first round of growth rate screening, batch cultures were set up to compare the total lipids of fast growing sorted clones and the wild type progenitor culture. Growth rates were compared in flask cultures of wild type and mutant clones (Figure 37). Differences were observed in the levels of total lipids of wild type and mutants (Figure 38). The lipids in *P. tricornutum* generally accounts for 19-25% of dry weight biomass (Gatenby et al., 2003; Ryckebosch et al., 2011). The three most promising lipid hyperaccumulating mutants *EmPt1F11*, *EmPt1F10* and *EmPt2F6* we generated showed 50%, 44.5% and 44.25% respectively lipids per dry weight. Other mutants namely *EmPt2A10*, *EmPt2A6* and *EmPt3D4* showed similar levels (37%) of lipid levels (Figure 38). Eight of the mutants *EmPt1D10, EmPt1C9, EmPt3C8, EmPt1E8, EmPt3C4, EmPt1B4, EmPt3B4* and *EmPt1D6* showed no significant difference relative to the wild type lipid levels (Figure 38). When biomass productivities of our selected high lipid mutants were compared with wild type, the mutant strain *EmPt1F10* showed the highest productivity (Figure 39). A 3-fold increase in microalgal lipid content is induced by change of growth conditions such as nutrient deprivation.

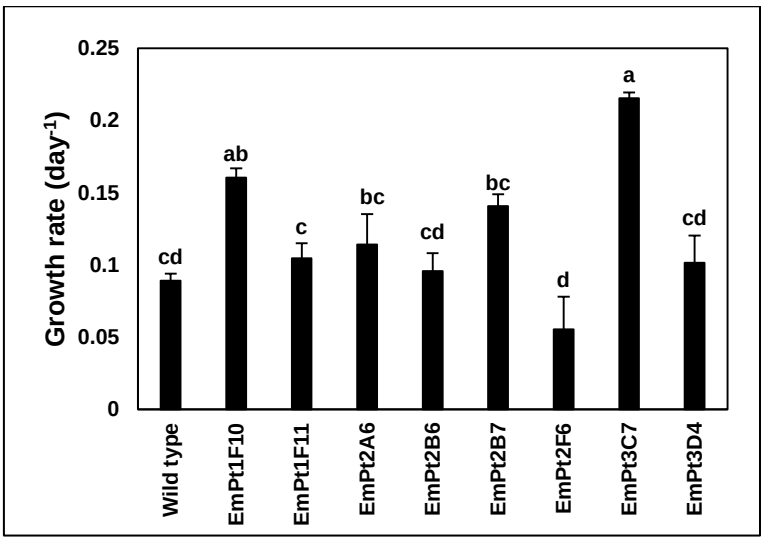

Figure 37. Growth rates of wild type and mutants of *Phaeodactylum tricornutum* grown under batch cultures. Means of three replicates were compared by one-way ANOVA and Tukey post-hoc test was used to check the level of significance. Different alphabets are used where the means are significantly different.

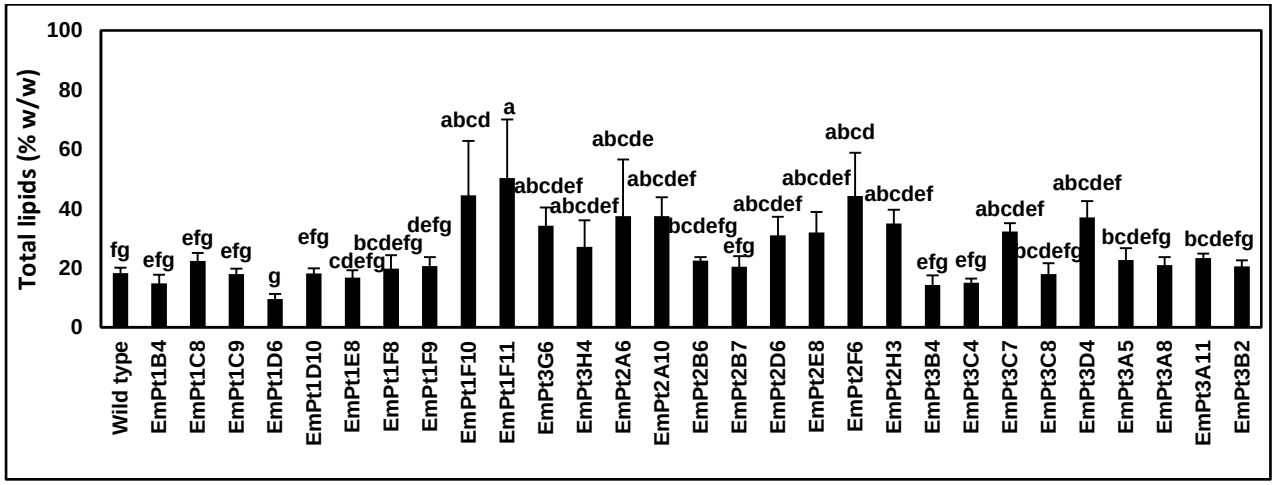

Figure 38. Comparison of total lipid content of wild type and singly sorted mutant populations of *P. tricornutum*. Means were compared by one-way ANOVA; level of significance was tested by Tukey post-hoc test. Means shown with different alphabets are significantly different.

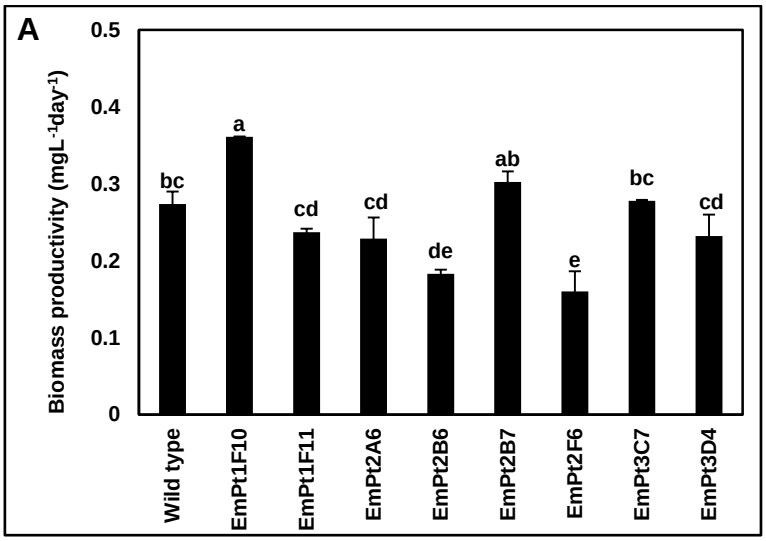

Figure 39. Biomass productivities of wild type and mutants of *Phaeodactylum tricornutum*. Means of three replicates were compared by one-way ANOVA and Tukey post-hoc test was used to check the level of significance. Different alphabets are used where the means are significantly different.

4.3.3 Alterations of fatty acid profiles in the novel *P. tricornutum* mutant strains

Analysis of FAME composition is critical for evaluating the economic potential of diatom oil. As fatty acids have varied applications, to select best candidate for any particular use one needs to investigate both quantitative and qualitative differences among the mutants. FAME profiling revealed the differences in the abundance of different fatty acids synthesized by the new mutant strains that were changed with respect to the wild type. The highest proportions of myristic acid (C14:0) and C17:0 were observed in mutants *EmPt1F11*, *EmPt2B6* and *EmPt3C7* (Figure 40A). The total fatty acid composition of *P. tricornutum* contains various other mono- and polyunsaturated fatty acids such as oleic (C18:1), linolenic (C18:2) and linolenic acids (C18:3) which are difficult to separate from EPA during purification (Ibáñez González et al., 1998). In this context, we have generated novel mutants namely *EmPt1F11*, *EmPt2B6* and *EmPt3C7* which are lacking in PUFA C18:2 (Figure 40B) and thus could be advantageous for downstream processing of diatom oil. The fatty acid composition on dry weight basis of the wild type and selected high lipid mutants is presented in Table 7. The three major fatty acids synthesized by *P. tricornutum* were palmitic (C16:0), palmitoleic (C16:1) and EPA (Table 7). *EmPt2A6* accumulated the highest dry weight percentage of palmitic acid and EPA, whereas increased levels of palmitoleic acid were found in *EmPt2B7* (Table 7).

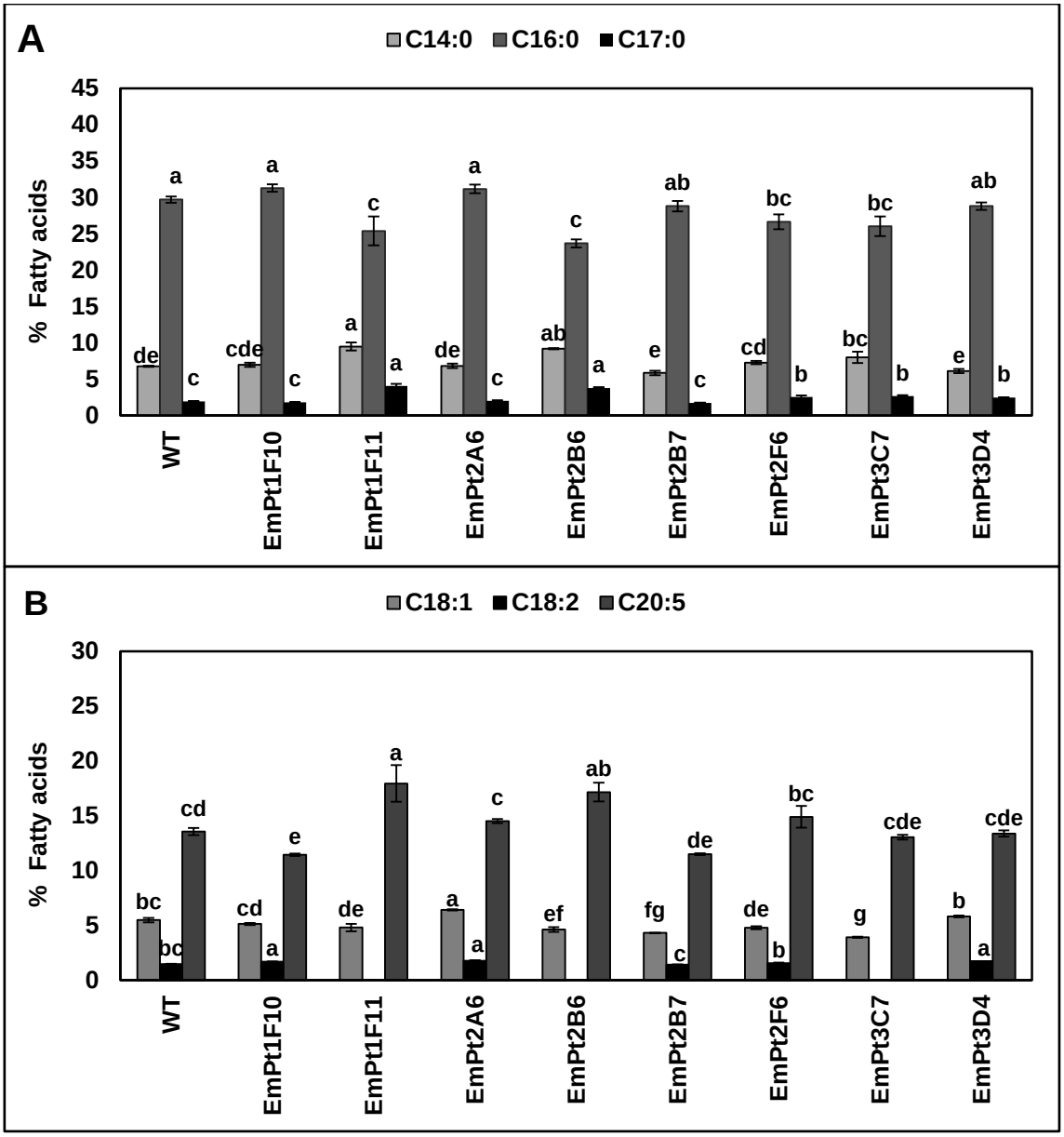

Figure 40. Proportions of various fatty acids expressed as percentage of total fatty acids. A) Percentage of saturated fatty acids found in total fatty acids. B) Percentages of unsaturated fatty acids in total fatty acids. Means of three replicates were analysed for variance by one-way ANOVA and levels of significance were tested by Tukey post-hoc test. Means with different alphabets are significantly different.

Fatty acids	% dry weight								
	Wild type	**EmPt1F10**	**EmPt1F11**	**EmPt2A6**	**EmPt2B6**	**EmPt2B7**	**EmPt2F6**	**EmPt3C7**	**EmPt3D4**
Caproic (C6:0)	0.26	0.28 ± 0.006	0.22 ± 0.03	0.26 ± 0.001	0.27 ± 0.03	0.30 ± 0.000	0.31 ± 0.07	0.33 ± 0.08	0.29 ± 0.05
Caprylic (C8:0)	0.09 ± 0.004	0.09 ± 0.000	0.09 ± 0.000	0.08 ± 0.002	0.08 ± 0.003	0.09 ± 0.01	0.09 ± 0.004	0.10 ± 0.01	0.08 ± 0.003
Myristic acid (C14:0)	0.66 ± 0.05	0.67 ± 0.06	0.54 ± 0.07	0.70 ± 0.14	0.49 ± 0.11	0.67 ± 0.12	0.65 ± 0.07	0.56 ± 0.07	0.48 ± 0.07
Palmitic acid (C16:0)	2.92 ± 0.22ab	3.17 ± 0.34ab	1.51 ± 0.17d	3.26 ± 0.62a	1.28 ± 0.32d	3.31 ± 0.54a	2.47 ± 0.27abc	1.88 ± 0.21cd	2.28 ± 0.30bcd
Palmitoleic (C16:1)	3.77 ± 0.29abc	4.03 ± 0.40ab	1.96 ± 0.23d	3.61 ± 0.66bc	1.61 ± 0.39d	4.89 ± 0.63a	3.46 ± 0.37bc	2.81 ± 0.28cd	2.85 ± 0.36cd
Heptadecanoic acid (C17:0)	0.17 ± 0.01	0.20 ± 0.01	0.26 ± 0.03	0.24 ± 0.007	0.20 ± 0.05	0.21 ± 0.03	0.24 ± 0.03	0.20 + 0.00	0.20 + 0.02
Oleic acid (C18:1)	0.53 ± 0.02b	0.55 ± 0.04b	0.31 ± 0.02c	0.73 ± 0.06a	0.25 ± 0.06c	0.49 ± 0.07b	0.46 ± 0.03b	0.29 ± 0.01c	0.46 ± 0.05b
Linoleic acid (C18:2)	0.15 ± 0.008ab	0.18 ± 0.02ab	n.d	0.21 ± 0.005a	n.d	0.17 ± 0.02ab	0.15 ± 0.01b	n.d	0.15 ab
Eicosapentaenoic acid (C20:5)	1.33 ± 0.14ab	1.12 ± 0.13ab	1.02 ± 0.20b	1.47 ± 0.31a	0.93 ± 0.26ab	1.32 ± 0.18ab	1.34 ± 0.17ab	0.92 ± 0.08b	1.05 ± 0.10ab

Table 7. Percentage dry weight composition of various fatty acids in wild type and mutants of *P. tricornutum*. Means were compared by one-way ANOVA and Tukey post-hoc test. Mean values shown with different alphabets are statistically different.

4.3.4 Rate of EMS mutations

The whole genome sequences of wild-type strain and a randomly selected mutant strain were compared to estimate the rate of EMS mutations in the high lipid producing strain *EmPt2A6* (Table 8). The paired-end sequencing technology from Illumina was used. The EMS mutant strain *EmPt2A6* was sequenced at depth of 118X coverage. A total of 5925 mutations were found per 27Mb genome of *EmPt2A6* (Table 8).

Mutant strain	Total mutations/genome	Mutations/kb	Total genes showing mutations	Average genome coverage (WT: 114X)	Genes with mutations
EmPt2A6	**5925**	**0.227**	**910**	**118X**	**Δ6-desaturase, FABB, ACC, FABFb and long chain acyl-coa aynthetase**

Table 8. Summary of mutations screened by whole genome sequencing of EMS mutant of *P. tricornutum.*

4.4 DISCUSSIONS

Chemical mutagenesis using ethylmethane sulfonate (EMS) is an effective method to achieve mutations in microalgae. The marine diatom *Phaeodactylum tricornutum* with a genome size of 27 Mb was treated with an optimized dose of 200 mM EMS. The in situ measurements of cellular lipids with the use of flow cytometry and lipophilic probe (BODIPY) to monitor enhanced levels of lipids within individual EMS mutagenised cells is an efficient and rapid technique to isolate oleaginous mutants. BODIPY has a high oil/water coefficient which allows membrane permeability and labelling of lipid components of live cells. The excitation of BODIPY is by a blue 488 nm laser with maximum emission in green spectrum at 515 nm, which has no spectral overlap with algal chloroplasts (Cooper et al., 2010). The strain selection procedure using EMS mutagenesis and flow cytometry was applied to the diatom *P. tricornutum* which resulted in 20-50 % enhancement in the cellular lipids.

This study demonstrate successful application of the combination of whole genome mutagenesis of large mutagenized populations (75 million cells) and FACS-based cell sorting which allowed 20% to 50% increase in lipid levels of *P. tricornutum.* Mutagenesis approaches combined with FACS have been previously implemented to generate green algal oleaginous mutants. For example, use of FACS in *Nannochloropsis* increased the wild type dry weight lipid level from 34% in the progenitor strain to 50.8% in the mutant MT-15 (Doan and Obbard, 2012).

Diatoms such as *Thalassiosira pseudonana* and *P. tricornutum* have been investigated by researchers as potential feedstocks for biodiesel production due to their desired lipid composition (Zendejas et al., 2012). In terms of biodiesel application of diatom oil, an estimated 25-30% lipid content of biomass has been considered potentially feasible (Valenzuela et al., 2013). In *P.tricornutum* lipid content is induced from 8.12% to 16.8% of dry weight under different culture conditions (Adarme-Vega et al., 2012). The mutants *EmPt1F11*, *EmPt1F10* and *EmPt2F6* isolated in this research study showed more than 2 fold increases over the wild type without any change in the culture conditions or nutrient deprivation.

Increased accumulation of short chain fatty acids such as lauric acid (C12:0) and C14:0 is a desirable trait for biofuel production from microalgae (Radakovits et al., 2011). In contrast to the targeted genetic engineering approach random whole genome saturation mutagenesis coupled with FACS provides a powerful high throughput approach for altering the levels of desired fatty acids.*Phaeodactylum tricornutum* is an important source of polyunsaturated fatty acid eicosapentaenoic acid (EPA), which is an essential fatty acid for human dietary uptake. The major dietary source of EPA is marine fish fed on microalgae, diatoms and bacteria (Kuhnt et al., 2012). Studies have also shown the beneficial effects of *Phaeodactylum* feeding in poultry hen which led to an increase in EPA content in the egg yolk (Lemahieu et al., 2013). The combination of UV mutagenesis and flow cytometry sorting in alga *Isochrysis affinis galbana* led to an increase in total fatty acid from 262 mgTFA to 409 mgTFA (Bougaran et al., 2012).

To determine the rate of EMS mutations, paired-end whole genome sequencing of wild type strain and a randomly selected mutant isolated using FACS were performed. The deep sequencing offers an unprecedented view of the whole genome and can describe the spectrum of mutations induced by the mutagen. A total of 910 genes showed mutations and several of these genes encode enzymes for fatty acid biosynthesis pathways. The biosynthesis of EPA in *P. tricornutum* involve two important enzymes called Δ5 and Δ6-desaturase which take part in both ω-3 and ω-6 pathways (Domergue et al., 2002). The genome sequencing of *EmPt2A6* revealed mutations in Δ6-desaturase which is required for desaturation of linoleic acid (C18:2) and linolenic acids (C18:3) in the ω-3 and ω-6 pathways for EPA biosynthesis. The overaccumulation of C18:2 in *EmPt2A6* can be explained by the occurrence of mutations in Δ6-desaturase which regulate the desaturation of C18:2 to EPA.

4.5 CONCLUSIONS

The wild type progenitor CCAP 1055/A strain of *Phaeodactylum tricornutum* showing 20% dry weight lipids was subjected to random saturation mutagenesis with ethylmethane sulfonate to generate large mutant populations (e.g. 75 million cells). From these large populations single cell fluorescence activated cell sorting (FACS) was used as a forward genetics strategy to isolate lipid novel hyperaccumulation mutants. The novel mutants isolated in 96 well plates were screened for

competitive growth and were analysed for total lipids. The lipid hyperaccumulation mutants showed 44-50% dry weight total lipids, which is more than a 2 fold increase over the wild type progenitor strain CCAP 1055/A. Two of the mutants *EmPt1F11* and *EmPt2B6* also accumulated a higher percentage of eicosapentaenoic acid (EPA). Compared to wild type, the highest content of palmitoleic acid (C16:1) (4.86% dry weight) was also observed in the mutant strain *EmPt2B7*. Overall this study demonstrates a proof of principle for the power of forward genetic approaches in microalgae that combine saturation mutagenesis of large population sizes with FACS based single cell sorting to isolate novel mutant strains that can hyperaccumulate lipids and other valuable bioproducts.

5. CHAPTER FIVE

Reduction in carotenoid levels in the marine diatom *Phaeodactylum tricornutum* by artificial microRNAs targeted against the endogenous *PHYTOENE SYNTHASE* gene

Chapter 5 – artificial microRNA mediated gene silencing

ABSTRACT

MicroRNAs are key regulators of gene expression in eukaryotes where they can function to down-regulate expression levels or functioning of mRNAs that are targetted by mature miRNAs displaying sequence homology. The "active" mature miRNA forms are short RNAs which are processed from longer precursor miRNA molecules that have a stem-loop structure. While artificial miRNAs have been developed for gene knockdown experiments in a range of eukaryotes, it is not known whether artificial or endogenous miRNAs can functionally knockdown mRNA levels in the model marine diatom *Phaedodactylum tricornutum*. Here, we investigate the potential use of artificial microRNAs (amiRNAs) for targetted gene knockdowns in *P. tricornutum*, by generation of transformants harbouring a transgene cassette for the generation of amiRNAs designed to target the endogenous *PHYTOENE SYNTHASE* (*PSY*) gene. In *P. tricornutum*, the amiRNA stem loop precursor was processed to produce a mature amiRNA that successfully targeted the *PSY* mRNA and reduced *PSY* mRNA levels. As the PSY gene is a key component of the carotenoid biosynthetic pathway, the levels of carotenoids in the *P. tricornutum* amiRNA knockdown lines was reduced relative to untransformed control lines. This study demonstrates that artificial miRNAs can be successfully deployed for gene knockdown experiments in the model diatom *P. tricornutum*, providing a powerful tool for future metabolic engineering and synthetic biology experimentation in this model marine diatom.

Chapter 5 – artificial microRNA mediated gene silencing

5.1 INTRODUCTION

MicroRNAs (miRNAs) are 21-24 nucleotide RNA molecules involved in post-transcriptional regulation (Molnar et al. 2007). MiRNAs are processed from a precursor (pre-miRNA) molecule that has a characteristic hairpin secondary structure by an RNAaseIII-like endonuclease called Dicer (Mathelier and Carbone, 2010). MiRNAs bind to target RNA transcripts and can direct RNA cleavage and translational inhibition of mRNA as a means of regulating gene expression (Khraiwesh et al., 2008). MiRNAs arose early in eukaryotic evolution and have played a key role in gene expression regulation since the emergence of multicellularity. In the plant kingdom, many miRNAs are evolutionarily conserved, typically begin with a U at the 5' end of the RNA molecule and are transcribed from independent miRNA genes (Reinhart et al., 2002).

Phaeodactylum tricornutum is a model organism for pennate diatoms with a sequenced genome size of 27.4 Mb (Bowler et al., 2008). To improve the utility of model organisms for understanding gene function and biological processes it is necessary to develop molecular tools for knockdown or overexpression of genes. Methods for genetic transformation of *Phaeodactylum tricornutum* have been developed which provide a basis for gene overexpression studies (Kroth, 2007). However, because of the lack of sexual cycle and machinery for homologous recombination, there remains a need to develop new approaches for targeted gene knockdowns in *Phaeodactylum tricornutum.* RNA interference based gene silencing in transgenic *P. tricornutum* has been achieved using antisense and inverted repeat based approaches (Allen et al., 2011; De Riso et al., 2009).

It has been demonstrated that while the *P.tricornutum* genome contains protein-coding genes necessary for siRNA mediated gene silencing, the *P. tricornutum* genome may harbour an RNA-induced silencing complex (RISC) pathway that is distinct from other eukaryotes (De Riso et al., 2009). Indeed, evidence to date suggests that there are few miRNAs in the *P. tricornutum* genome (13 currently in miRBase) and the few miRNAs that have been detected have no identifiable homologs in other organisms (Huang et al., 2011). This raises some questions as to the functionality and extent of miRNA based regulation in *P. tricornutum.*

Endogenous miRNA precursors can be redesigned to generate synthetic artificial miRNAs. The miRNA-miRNA* duplex molecule generated from miRNA precursors can be altered in sequence without changing the structural features of the precursor miRNA to generate mature artificial miRNAs that are targetted towards specific tracts of RNA sequence (Ossowski et al., 2008). Artificial miRNAs can hence be designed to target and down-regulate any target gene expressing an RNA in the genome (Schwab et al., 2006). The first use of amiRNAs for gene knockdown was in human cell lines (Zeng

et al., 2002) followed by use of amiRNAs in the model plant *Arabidopsis thaliana* (Schwab et al., 2006).

Gene knockdown strategies based on RNA interference methods (namely antisense or inverted repeat (IR)) can suffer from inherent problems due to their additional effects on transcriptional silencing. The small interfering RNA (siRNA) produced by inverted repeats can mediate post-transcriptional and transcriptional silencing of both endogenes and exogenously introduced genes (Dunoyer et al., 2010). In the green microalga *Chlamydomonas reinhardtii* the inverted repeat transgene constructs which transcribe long dsRNAs have been shown to be prone to auto-silencing at the transcriptional level (Rohr et al., 2004; Yamasaki et al., 2008). In addition, production of many distinct siRNAs from Dicer mediated cleavage of double stranded RNA (dsRNA) increases the probability of off-target silencing effects which reduce the specificity of siRNA mediated gene silencing (Xu et al., 2006). Such disadvantages can been overcome by use of artificial miRNAs (amiRNAs) which are less prone to silencing for targeted gene knockdowns in both plants (Schwab et al., 2006) and the green microalga *Chlamydomonas reinhardtii* (Molnar et al., 2009).

Given the low number of miRNAs and the distinct protein machinery for RISC based silencing in *P. tricornutum*; it is not known whether artificial miRNA techniques can be successfully deployed for targeted gene knockdowns in *P. tricornutum*. To address this question we have made an artifical miRNA transgene construct that can express a double stranded precursor artificial miRNA molecule under the control of the diatom specific promoter *FcpA* (*Fucoxanthin Chlorophyll a/c-binding Protein A*). We demonstrate that the precursor amiRNA is successfully processed into a mature artificial miRNA that downregulates the targeted *PHYTOENE SYNTHASE (PSY)* gene in *P. tricornutum.* The *PSY* gene is involved in the early steps of the carotenoids biosynthetic pathway (Steinbrenner and Linden, 2001) which is depicted in the Figure 41. Our study demonstrates that artificial miRNAs can be successfully used for gene knockdown experiments in *P. tricornutum*.

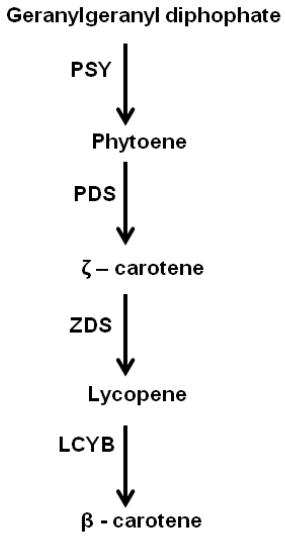

Figure 41. The carotenoid biosynthetic pathway in microalage. The enymes catalysing biosynthetic reactions are Phytoene synthase (PSY), Phytoene desaturase (PDS), ζ- carotene desaturase (ZDS), and lycopene cyclise (LCYB) (Steinbrenner and Linden, 2001).

5.2 MATERIALS and METHODS

5.2.1 Diatom strain and culturing

The marine diatom *Phaeodactylum tricornutum* CCAP 1055/A was grown in 50% natural seawater media (F2-Si), at 17 °C under 12:12 light/dark photoperiod (40 µmol photons m^{-2} s^{-1}) until the culture appears brownish.

5.2.2 Vector construction for artificial microRNA

The artificial microRNA for the target *PSY* gene Phaeo 41878 (Bowler et al., 2008) was designed using the 'Design' tool of WMD2 (Web MicroRNA Designer) platform at http://wmd3.weigelworld.org (Ossowski et al., 2008). The selected amiRNA showed high complimentarity with the target *P.tricornutum PSY* gene and has a 50% GC content (Figure 42). The artificial microRNA designer WMD identified four oligonucleotide sequences (I to IV), namely:

(I) miR-s_2 5' gaTTATTGCCACAAACGCGCCAAtctctcttttgtattcc 3'

(II) miR-a_2 5' gaTTGGCGCGTTTGTGGCAATAAtcaaagagaatcaatga 3'

(III) miR*s_2 5' gaTTAGCGCGTTTGTCGCAATATtcacaggtcgtgatatg 3'

(IV) miR*a_2 5' gaATATTGCGACAAACGCGCTAAtctacatatatattcct 3'

The four oligonucleotide sequences (I to IV) were used to engineer the amiRNA into the endogenous mir319a precursor. The overlapping PCRs were performed using the four oligonucleotide sequences (I-IV) with pBluescript template plasmid RS300 (mir319a pBSK) containing a miRNA precursor (mir319a) from *Arabidopsis thaliana* as template (Ossowski et al., 2008). The amiRNA foldbacks generated in the template mir319a pBSK plasmid was cloned into pGEM-T-easy vector after A-tailing

of PCR products and sequencing was performed out with oligonucleotide primers FA 5' CTG CAA GGC GAT TAA GTT GGG TAA C 3' and RB 5' GCG GAT AAC AAT TTC ACA CAG GAA ACA G 3' to confirm the sequence integrity and identity of the amiRNA transgene cassette. The amiRNA foldback cassette was subsequently cloned into the diatom expression vector pPhaT1-GFP (Figure 43), under the control of *FcpA* promoter to obtain the final amiRNA vector pPhaT1-GFP-AMIRNA-Psy (Figure 44). The vector pPhaT1-GFP was kindly provided by Dr Yusuke Matsuda (Kwansei Gakuin University, Japan). The expression vector pPhaT1-GFP-AMIRNA-PSY was verified by restriction digestion and DNA sequencing with insert and vector specific primers prior to diatom transformation. The sequencing results indicated the presence of a 423 nucleotide long fragment containing the stem-loop precursor sequence. The secondary structure of the artificial amiRNA precursor in vector pPhaT1-GFP-AMIRNA-PSY was predicted by RNA-fold (Vienna package) and drawn in VARNA (Darty et al., 2009).

```
Target gene (PSY) 5´ - 3´/205-225  TTGGAGCGTTTGTGGCAATAC
                                   |||| ||||||||||||||||
amiRNA (reverse complement)        TTGGCGCGTTTGTGGCAATAA
                                   * **** ****************
```

Figure 42. DNA sequence alignment showing high complimentarity of amiRNA to the intended target gene *PSY*.

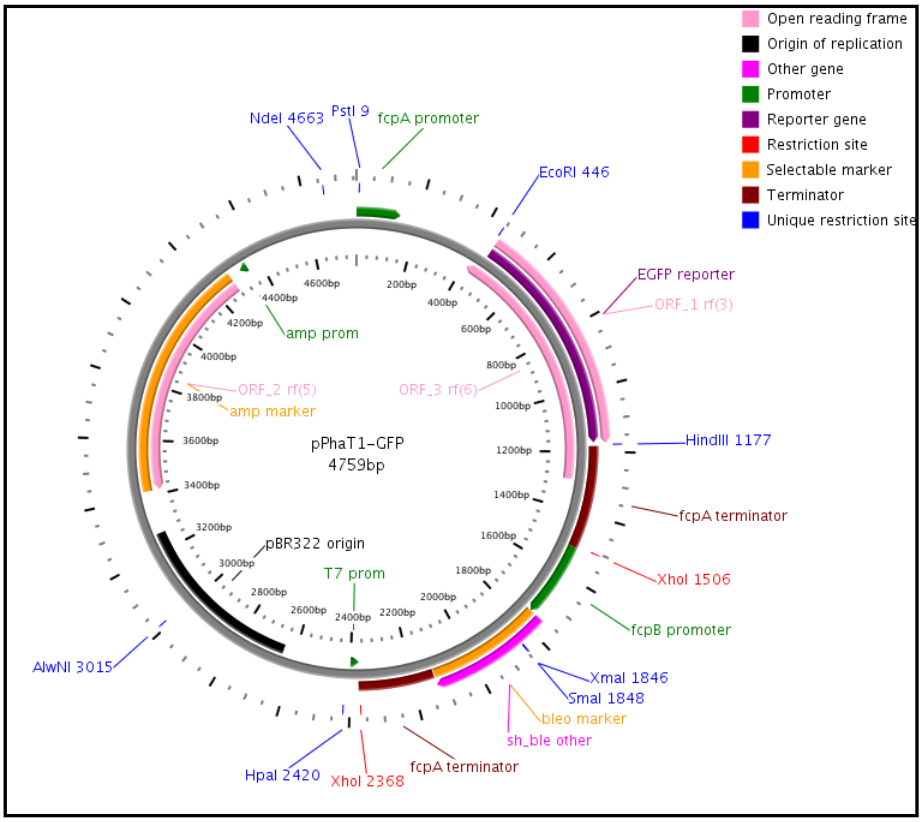

Figure 43. Map of *Phaeodactylum tricornutum* expression vector pPhaT1-GFP. (Provided by Prof. Yusuke Matsuda, Japan).

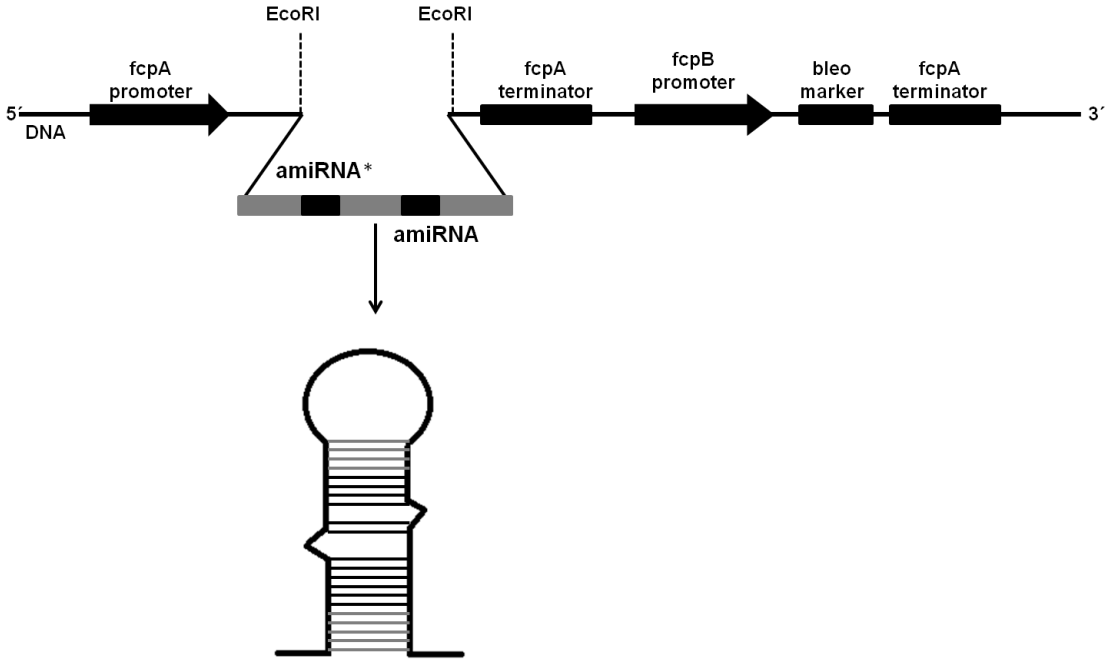

Figure 44. Diagram illustrating amiRNA cloning cassette of the construct pPhaT1-GFP-AMIRNA-Psy. fcpA- Fucoxanthin Chlorophyll a/c-binding Protein A, fcpB Fucoxanthin Chlorophyll a/c-binding Protein B; bleo, selectable marker for zeocin resistance.

5.2.3 Extraction of genomic DNA and copy number qPCR

Genomic DNA was extracted from the wild-type and amiRNA transformants by CTAB DNA extraction method. Cells were pelleted by centrifugation at 4000 rpm for 5 min and frozen at -80˚C. The frozen cell pellet was ground in liquid N_2 and powdered cells were incubated with 2X CTAB buffer (2% w/v CTAB, 1.4 M NaCl, 100 mM Tris HCl pH 8.0, 20 mM EDTA) at 65 ˚C for an hour. Upon cooling, equal volume of chloroform was added and vortexed thoroughly, layers were separated by centrifugation at 10, 000 rpm for 10 minutes. The upper layer was transferred to new eppendorf tube and DNA was precipitated with chilled isopropanol and pelleted at 10, 000 rpm for 10 minutes. The pellet was washed twice with 70 % (v/v) ethanol and pellet was air dried followed by redissolution in sterile water. The integrity of DNA was checked on 0.8% agarose gel in TBE buffer. The absorbance at A260 and A280 nm were checked with Nanophotometer (ImPlen).

For calculating the copy number of transgene in the amiRNA transformant lines, oligonucleotide primers were designed using Primer3web software version 4.0.0 for sequences specific to internal control *PSY* (Forward AGTCGCAGCCTACTTGCGTT , Reverse CCAGGGAAGGAGCGTTGTCA) and amiRNA transgene (Forward GTGGATCAAGCATGTTTTTGTGCAG, Reverse CCACAAACGCGCCAATCTCTC). Standard curves on six serial 2-fold dilutions were constructed for both sets of primer pairs to test for linearity and to ensure maximum specificity and efficiency for quantitative PCR. The quantitative PCR was performed using SensiMix SYBR No-ROX Kit (Bioline, UK) and the amplification reaction with standard thermal conditions (initial step, 95 ˚C for 10 min, 40 cycles PCR, 95 ˚C, 15 sec for melting, 60 ˚C for annealing and extension) was run in a CFX96 machine (Bio-RAd, USA). In addition, melting-curve analysis was performed at the end of PCR amplification to check PCR product specificity and primer dimer formation. The data for standard curves was analysed in CFX96 system software for calculation of efficiency, correlation coefficient and slope (Table 8). Copy number of the transgene (X_0) was derived from equation $X_0/R_0 = 10^{[(Ct,X-IX)/SX]- [(Ct,R-IR)/SR]}$ where I_X and I_R are the intercepts of standard curves of transgene and internal control genes and S_X and S_R are the slopes of standard curves of transgene and internal control genes respectively, $Ct,_X$ and $Ct,_R$ are the threshold cycles of amplification of the transgene and internal control to a tested sample, R_0 is copy number of internal control gene (Chen, 2010).

Gene	Range of Ct mean values	Amplification efficiency	Slope	Correlation coefficient (R^2)	Intercept
amiRNA	15.12-19.68	1.13	-3.035	0.996	21.6
PSY	16.72-21.60	1.10	-3.097	0.994	23.5

Table 8. Values derived from standard primer efficiency curves. Ct- threshold cycle.

5.2.4 Measurements of carotenoids content

The carotenoid content in wild-type and amiRNA transformants was measured according to (Ryckebosch et al., 2011). In brief, 10 days old diatom cultures were harvested and fresh weight was recorded. Carotenoids were extracted with methanol and absorbance (A) was measured at 470, 665, and 652 nm using a Nanophotometer (ImPlen). The following equation was used to calculate the amount of carotenoids:

$C_a = (15.65A_{665}) – (7.34A_{652})$

$$X_{carotenoids} = \frac{(1000A_{470}) – (2.86C_a)}{221} \times DF \times V$$

where; $X_{carotenoids}$ is the amount of carotenoids in µg, C_a is Chlorophyll a content, DF is the dilution factor, V is the volume of culture in ml.

5.2.5 Extraction of total RNA and Quantitative Reverse transcription polymerase chain reaction (qRT-PCR) analysis of Phytoene synthase (PSY) gene

Total RNA isolation with TRI-Reagent (Sigma-Aldrich) method (Molnar et al., 2007) was used to extract the RNA from harvested diatom cells. Briefly, 50 mL cultures of *Phaeodactylum tricornutum* growing in F2 seawater medium were harvested using a 50 mL tube by centrifugation at 4000 rpm for 5 min and flash frozen in liquid N_2. The pellet was powdered in a pestle and mortar using liquid N_2 and suspended in 6 mL of TRI-Reagent and vortexed. The pellet was centrifuged for 15 min at 400 rpm at 4˚C and upper phase was transferred into new 15 mL tube. After incubating for 5 min at room temperature, 1.2 mL chloroform was added and vortexed vigorously for 15 sec and incubated at room temperature for 5 min. The mixture was centrifuged for 15 min at 4000 rpm at 4 ˚C and upper phase containing RNA was transferred to fresh 15 mL tube on ice. The RNA was precipitated by adding equal volume of isopropanol and centrifuged at 4000 rpm, 4 ˚C for 15 min. the pellet was washed with 80% ethanol twice and dried at room temperature. The pellet was resuspended in nuclease free water.

5.2.6 TaqMan small RNA assay for mature amiRNA expression

The cDNA for mature amiRNA was prepared using TaqMan MicroRNA reverse transcription kit. In brief, 10 nanograms of RNA sample was reverse transcribed in a reaction mixture containing 1mM dNTPs, 50U of MultiScribe Reverse Transcriptase, 1X reverse transcription buffer, 20U of RNase inhibitor, 1X reverse transcriptase stem-loop primer and nuclease free water to make total reaction volume of 15 µL. The reaction tube was loaded into a thermal cycler with thermal cycling conditions of 30 min at 16 ˚C, 30 minutes at 42 ˚C and 5 min hold at 85 ˚C. The quantitative PCR amplification was performed with TaqMan Universal PCR master mix II using TaqMan Small RNA assay designed specifically for amiRNA and endogenous control as 5S rRNA. The thermal cycling conditions for TaqMan qPCR are given in Table 9.

Step	Time (minutes)	Temperature (˚C)
Hold	30	16
Hold	30	42
Hold	5	85
hold	∞	4

Table 9. Thermal cycling conditions for TaqMan qPCR.

5.2.7 Statistics

The data analysis was performed on Minitab statistical software package v. 16.2.4 (Minitab Inc.). The mean values were compared by one-way ANOVA (Tukey, $P < 0.05$).

5.3 RESULTS

5.3.1 Genetic transformation of *P. tricornutum* with amiRNA vector

amir-pPhaT1 was transformed into the *P. tricornutum* cells via biolistic or gene gun transformation. Transformed cells were plated on antibiotic (zeocin) containing agar plates and incubated for 3-4 weeks until colonies were obtained. The zeocin resistant colonies (Figure 45) were transferred and grown in liquid selection medium.

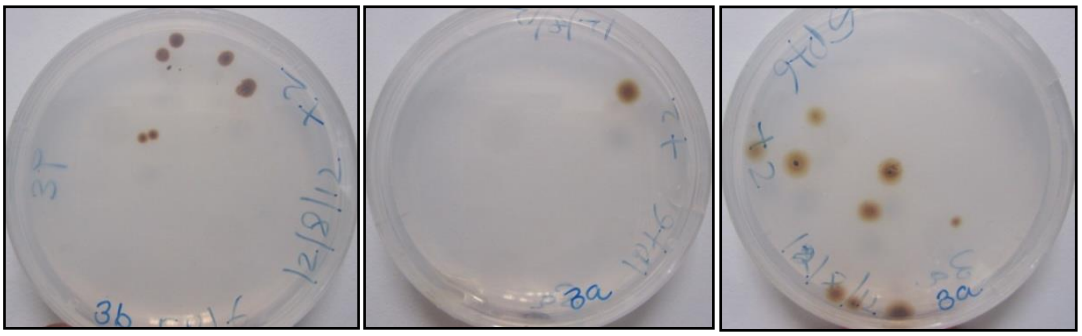

Figure 45. Photographs showing growth of zeocin resistant colonies of *P. tricornutum* transformed with amir-pPhaT1 construct.

5.3.2 Intracellular processing of artificial microRNA precursor into mature microRNA lead to silencing of endogenous gene in *P. tricornutum*

While there is now extensive genomic information regarding the model diatom *P. tricornutum,* there is a lack of experimental techniques for targetted gene knockdowns in *P. tricornutum.* To determine whether artificial miRNAs can be employed for targeted knockdown of mRNA levels of specific genes in the marine diatom *P. tricornutum*, we developed an amiRNA transgene cassette to target the mRNA of the endogenous *PHYTOENE SYNTHASE* gene in *P. tricornutum. PHYTOENE SYNTHASE* (*PSY*) catalyses the first step in the carotenoid biosynthesis pathway in both plants and microalgae. Disruption of the *PSY* gene function has previously been shown to lead to the generation of white mutants in the green alga *Chlamydomonas reinhardtii* (McCarthy et al., 2004).

To generate the amiRNA transgene cassette for targetting *PSY*, the mir319a pBSK vector containing the mir319 stemloop precursor (Schwab et al., 2006) was used. The amiRNA oligonucleotides targetting *PSY* were cloned into the mir319a pBSK vector, via exchange of endogenous miRNA and miRNA* of miR319a with amiRNA and amiRNA*. The PSY amiRNA foldback cassette was subsequently cloned into the diatom expression vector pPhaT1-GFP, to generate the vector pPhaT1-GFP-AMIRNA-PSY. The secondary structure of the artificial amiRNA precursor in vector pPhaT1-GFP-AMIRNA-PSY was predicted by RNA-fold (Figure 46). Independent zeocin resistant *P.tricornutum* transformants obtained upon transformation with the vector pPhaT1-GFP-AMIRNA-PSY indicated the presence of a 175 bp insert sequence amplified using primers specific to the stem region (Figure 47). The positive transformant colonies (amiR-PtT lines) were transferred to liquid medium and grown under antibiotic (zeocin) selection prior to analysis of carotenoid levels and PSY mRNA levels.

Figure 46. Diagram showing secondary structure of amiRNA precursor as predicted by RNA-fold (Vienna RNA webserver). The region highlighted in red box is showing mature amiRNA and amiRNA* complimentary region.

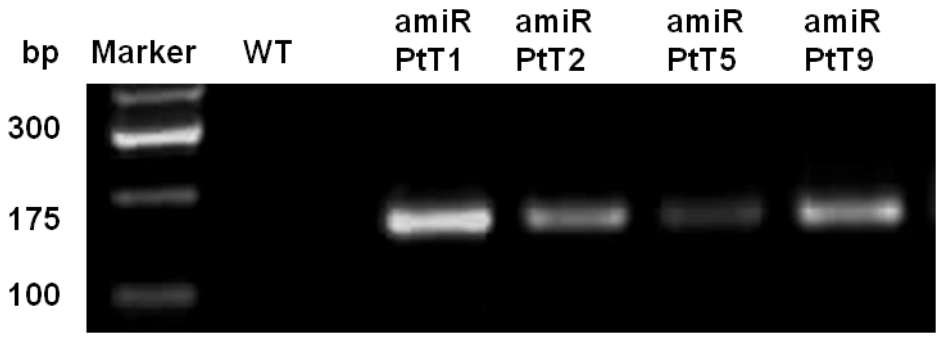

Figure 47. Gel photograph showing PCR verification of insert in transformed lines

The WT and amiR-PtT lines were analysed by qRT-PCR to determine the mRNA levels of *PSY*. Statistically significant reductions in the mRNA levels of *PSY* were observed in all four of the independent transformants compared to the *PSY* expression level in the wild-type WT line (Figure 48a). The decrease in *PSY* mRNA levels in three of the four lines (i.e. amiR-PtT1, amiR-PtT2, amiR-PtT9) was inversely but not linearily associated with the expression of mature amiRNA levels when analysed by Taqman qRT-PCR (Figure 48b). The analysis of carotenoid levels in a number of the amiR-PtT lines demonstrated a decrease in levels of carotenoids compare to wild type (WT, untransformed) levels (Figure 49). These four lines (amiR-PtT1, amiR-PtT2, amiR-PtT5, amiR-PtT9) were considered as candidate lines where reduction in the levels of carotenoids could be due to reduced PSY mRNA levels arising from expression of the amiRNA targetted against *PSY*.

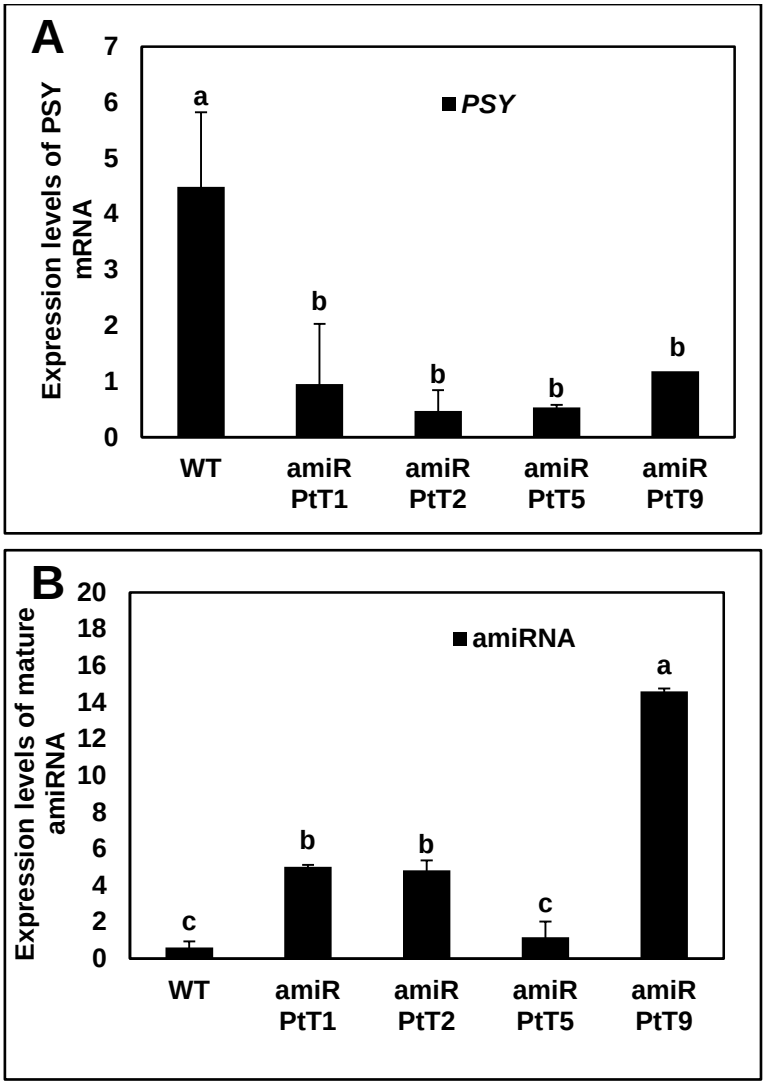

Figure 48. Knockdown of PSY mRNA levels using amiRNA targetted against *PSY* mRNA sequence in transformed lines of *P. tricornutum*. a) Expression analysis (qRT-PCR) of *PSY* mRNA levels, calculated using standard $2^{-\Delta\Delta CT}$ method with *TBP* and *RPS* as internal controls. Statistical significance tested by ONE-WAY ANOVA using Minitab v 16. b) Expression of mature amiRNA (targetted against *PSY* sequence) calculated using standard $2^{-\Delta\Delta CT}$ method with 5S rRNA as endogenous control and quantification performed by Taqman qRT-PCR.

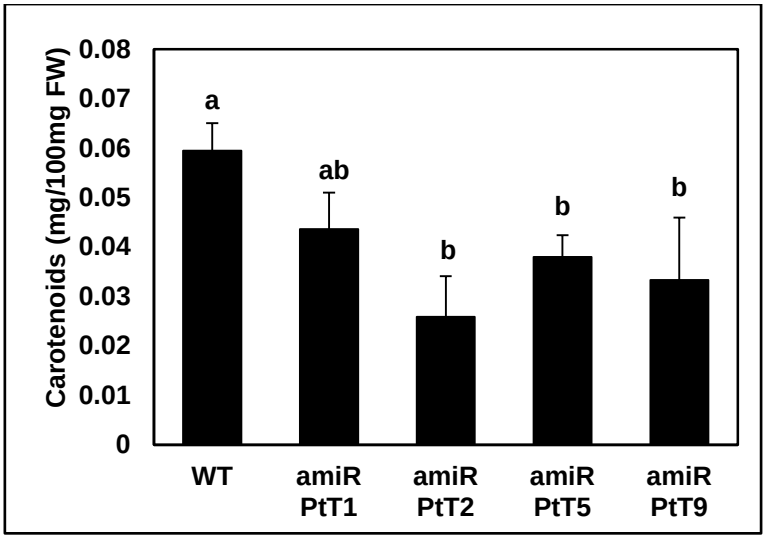

Figure 49. Total carotenoids content in wild-type and transformed lines of *P. tricornutum*. Data is mean of 3 biological replicates and coefficient of variance was tested by performing Tukey post hoc test by one-way ANOVA. Mean values that are indicated with different letters are significantly different (P = 0.000).

Amongst the four transformants there were significant differences in the expression levels of the mature amiRNAs between the wild type (WT) and three of the transformant lines (Fig 48b). The differences in transgene copy number obtained for the individual transformant lines may have contributed to these expression differences (Table 10). The copy number was positively associated with the expression level of the amiRNA in each of the four transformant lines (Table 10 and Figure 48b). For instance, the transformant amiR-PtT9 had the highest copy number (Table 10) and exhibited the highest levels of amiRNA expression but less inhibition of mRNA (Figure 48).

Transformant lines	Ct (amiRNA)	Ct (*PSY*)	Estimated copy number
amirPtT1	14.31	16.13	2
amirPtT2	14.50	16.08	2
amirPtT5	14.12	16.34	1
amirPtT9	15.56	16.64	3

Table 10. Values derived from standard primer efficiency curves. Ct- threshold cycle and estimated copy number of transgene in amiRNA transformant lines. Ct- threshold cycle.

5.4 DISCUSSIONS

Silencing RNAs are extensively used to knockdown genes of interest in both aminals and plants. Both unicellular and multicellular eukaryotes possess a repertoire of single-stranded small RNA molecules, ranging in size from 20-30 nucleotide bases. They mediate RNA-RNA and RNA-

DNA interactions and participate in transcriptional silencing of heterochromatin and mRNA stability (Ossowski et al., 2008). These small intracellular molecules are referred as silencing RNAs (sRNAs) which are broadly classified into short interfering RNAs (siRNAs) and microRNAs (miRNAs).

siRNAs are generated from long double stranded RNAs (dsRNAs) with nearly perfect complimentarity. These dsRNAs arise from diverse origins such as hairpin transcripts of long inverted repeats (IRs), convergent transcripts, RNA-dependent RNA polymerase activity, viral and transposon RNAs or exogenously introduced dsRNAs molecules (Cerutti et al., 2011). On other hand, miRNAs are 21-24 nucleotide RNA duplex molecules which are processed from a precursor (pre-miRNA) that has a characteristic hairpin secondary structure (Mathelier and Carbone, 2010).

sRNAs are processed from hairpin and long dsRNAs by RNAaseIII-like endogenuclease called Dicer which are further incorporated into multisubunit effector complexes known as RNA induced silencing complex (RISC). The immediate products of Dicer are short, 5' -phosphorylated dsRNAs with two nucleotide 3' overhangs (Bernstein et al., 2001). The 5' end of one of the strands of these dsRNAs has a lower thermodynamic stability (guide strand) which is retained by the second protein molecule called ARGONAUTE (AGO) protein (Khvorova et al., 2003). The second strand of dsRNA is called passenger strand or miRNA* which does not take part in further processing is rapidly degraded (Molnar et al., 2007). Once the guide strand is bound to ARGONAUTE, the RISC complex start scanning the cell to locate the mRNA which it aims to destruct.

The key components of RNAi are Dicer, Argonaute-Piwi and RNA-dependent RNA polymerase (RdRP). Dicer typically contain an amino-terminal DEADc/HELICASEc domain followed by domain DUF283, a PAZ domain, two RNase III domains and a double-stranded RNA-binding domain (dsRBD); however the presence of two RNase III domain is a universal feature of Dicer family (De Riso et al., 2009). AGO protein family of eukaryotes possess sRNA-binding PAZ and PIWI domains which have catalytic activity that allow sRNA-mRNA cleavage within the RISC complex (Voinnet, 2009).

In silico analysis in the diatom *P. tricornutum* show the presence of key components involved in RISC: gene model encoding dsRBD followed by two RNase III domains, putative proteins containg the cobserved PIWI domain of AGO and gene encoding putative RdRP (De Riso et al., 2009). Anti-sense and inverted repeats or hairpin (hpRNAi) mediated transcriptional and post-transcriptional gene silencing is also known to occur in *P.tricornutum* (De Riso et al., 2009). Although long hairpins generate a diverse set of effective siRNAs, they also have increase potential to produce siRNAs with off-target effects (Ossowski et al., 2008). The exchange of natural miRNA and miRNA* sequences with those of amiRNA and amiRNA* by overlapping PCRs allows highly specific knockdown of

endogenous genes in plants (Schwab et al., 2006). Like diverse multicellular organisms, the unicellular alga *Chlamydomonas reinhardtii* also contains miRNAs which resemble miRNAs of land plants and direct site-specific cleavage of target mRNA (Molnar et al., 2009).

Hitherto, artificial miRNA system based specific high-throughput gene silencing has only been achieved in plants (Schwab et al., 2006) and microalga *Chlamydomonas reinhardtii* (Molnar et al., 2009) with no reports in diatoms. This study demonstrates the application of artificial miRNAs in regulating gene expression in *P. tricornutum*, a marine diatom of importance for production of nutraceutical and biodiesel (Alonso et al., 1996; Lebeau and Robert, 2003). The detection of the mature amiRNA in the transformed *P. tricornutum* cells indicates that *P. tricornutum* possesses the RNA silencing machinery to process the stem loop precursors of amiRNA (or any miRNAs) resulting into single stranded mature amiRNAs (Figure 41b). The most common methods for detecting and quantitating miRNAs are northern blots, microarrays, and ribonuclease protection assays which are based on hybridizing labelled probesdirectly to purified RNA that require huge amounts of RNA. In this study, TaqMan miRNA assay was used for first time in microalgae to detect mature miRNAs. TaqMan real time PCR is a cost effective two-step RT-PCR assay for detection of miRNA expression (Mohammadi-Yeganeh et al., 2013). Our data indicates that *P. tricornutum* harbours a functional miRNA processing pathway which can be harnessed to generate amiRNAs for functional gene knockdown experiments in this model diatom.

5.4 CONCLUSIONS

The marine diatom *Phaeodactylum tricornutum* is amenable to reverse genetic analysis and has a completely sequenced genome. However role of artificial microRNA is hitherto not known in this model diatom. This study demonstrate that artificial miRNAs can be successfully developed and deployed for gene knockdown experiments in *P. tricornutum* which is a necessary experimental approach for understanding gene function and biology in this model diatom. To test the *in vivo* effect of artificial microRNAs, *Arabidopsis MIR319a* was used as backbone for construction of *aMIRNA* hairpins. *MIR319a*- based *aMIRNAs* were generated by replacing the miR319a/miR319a* duplex region with artificially engineered target specific sequences harboured into expression vector under the control of *P.tricornutum* specific promoter. The artificial miRNA transformants of *P. tricornutum* were altered in their mRNA expression for the target *PHYTOENE SYNTHASE* (*PSY*) gene which was associated with a decrease in their carotenoid levels. Our results open a new route for metabolic engineering of *P. tricornutum* and add amiRNA transformation in the tool kit of the current methods available for genetic manipulation of *P. tricornutum.* This is the first report on artificial miRNA mediated gene regulation in the diatom *Phaeodactylum tricornutum*.

6. CHAPTER SIX

Summary and future directions

6. Summary and Future Directions

Phaeodactylum tricornutum is a model organism for marine pennate diatoms and is a promising microalga for biodiesel and nutraceutical applications. Commercial production of microalgae biomass is economical and pro-environmental when the strain is marine, fast growing, captures high CO_2, and accumulates large amount of lipids. Integrating microalgal cultivation with industrial CO_2 emissions from power plants and cinker factories is a potential strategy for large scale biomass production which represents an opportunity for CO_2-biomitigation. In this study, we show growth rate of *P. tricornutum* is markedly improved by aeration with elevated levels of 4% CO_2. Tolerance of *P. tricornutum* to extremely high level of 10% CO_2 as found in typical industrial flue gas emissions is attained by lowering the aeration flow rate. The diatom *P. tricornutum* can produce significant quantities of extractable oil which is amenable to chemical process of transesterification for conversion to biodiesel and offers its usefulness as feedstock for large-scale fuel production. However, to make diatom biofuels and bioproducts a commercial reality require biotechnological challenges.

Unlike higher plants like oilseeds, which tend to accumulate only triacylglycerols (TAGs), microalgae synthesize vast variety of other lipid molecules such as phospholipids, glycolipids and sulpholipids; however, triglycerols are of primary interest for biodiesel (McGinn et al., 2011). Consequently, this research study focus on the development of new strains of *P. tricornutum* which can accumulate high amounts of TAGs and other favourable fatty acids for use in varied biotechnological applications. The genetic breeding and selection of new strains was based on chemical mutagenesis. *P.tricornutum* was treated with mutagen ethylmethane sulfonate (EMS) to induce random mutagenesis which was then followed by two different isolation techniques - 1) antibiotic selection and 2) flow cytometric cell sorting using lipophilic dye BODIPY.

To enhance the lipid content of *P. tricornutum* EMS- treated mutants were screened based on their resistance to antibiotic cerulenin which is specific inhibitor of the enzyme involved in fatty acid biosynthesis initiation II pathway. The mutants thus obtained showed enhanced (2- 2.5 fold) lipid accumulation and two mutants namely *Ptcer12* and *Ptcer14* produced higher TAG molecules. The fatty acids profiles of wild type and mutants also show variations. Two oleic acid rich mutants *Ptcer 12* and *Ptcer13* generated in this study can be used as potential source of skin care products. The genetic characterization by whole genome sequencing of *Ptcer14* show mutations in important genes encoding enzymes FABB, delta 5 fatty acid desaturase, delta 6 fatty acid desaturase and ACC which are involved in fatty acid biosynthesis.

The traditional method of mutant isolation using antibiotic selection is tedious and time consuming. Alternatively, random mutagenesis coupled with FACS is a viable high-throughput and

rapid method for enhancing lipid content of wild type *P. tricornutum*. In this study, we were able to select EMS mutants through single cell sorting which displayed higher lipids and altered fatty acid profiles. The three promising high lipid mutant strains *EmPt1F11, EmPt1F10* and *EmPt2F6* of *P. tricornutum* isolated using FACS show high 50%, 44.5% and 44.25% dry weight lipids respectively. The increase in lipid content was attained without any nutrient limitations. The screenings based on gas chromatographic analysis of fatty acid methyl esters (FAME) show that mutant *EmPt2A6* accumulated highest levels of linoleic and linolenic acids. The EPA overproducer mutant strain *EmPt1F11* accumulated highest lipid and lack the linolenic acid which makes it as ideal candidate for biodiesel feedstock. The EMS mutagenesis caused single nucleotide polymorphism in various genes such as FABB and FBAFb involed in fatty acid biosynthesis initiation II pathway. The mutations were also caused in delta 6 fatty acid desaturase, ACC, long chain acyl-coa synthase coding genes of genetically characterized strain *EmPt2A6*.

The new strains of *P. tricornutum* generated in this research study exhibit variations in lipid levels and fatty acid profiles. These strains can be further used for the transcriptomic analysis under nutrient stress conditions such as nitrogen and phosphorous limitations to understand the lipid biosynthesis pathways under adverse conditions. The future work for this study is the identification of EMS-induced causal mutations in mutant strains of *P. tricornutum* by whole genome sequencing which is responsible for lipid overaccumulation.

With the completion of whole genome sequences of *P.tricornutum*, research into diatom biology has entered the post-genomics era. The exploitation of the genomic resources therefore requires the development of molecular tools that can analyse and modulate the functional machinery of the diatom. Hitherto, the gene expression regulator such as artificial-microRNA has only been exploited in green microalgae *Chlamydomonas reinhardtii* and not studied in diatoms. This study is the first report on proof of concept of artificial microRNAs mediated gene regulation and use of TaqMan probe for quantification of mature microRNAs expression. In contrast to RNA blotting, the use of TaqMan probes is an easy, high-throughput method of quantifying the levels of mature microRNAs which are only 21 nucleotide long using very small amount of RNA. Besides artificial microRNAs mediated gene regulation, there are other powerful next generation tools for gene customization that can be explored in *P. tricornutum*. These are custom DNA-binding proteins such as zinc finger or TALE (transcription activator-like effector) proteins and the CRISPR (clustered regularly interspaced short palindromic repeats) systems which can provide potential platform for targeted gene regulation (Qi et al., 2013).

7. REFERENCES

Acién Fernández FG, González-López CV, Fernández Sevilla JM, Molina Grima E. Conversion of CO_2 into biomass by microalgae: how realistic a contribution may it be to significant CO_2 removal? Applied Microbiology and Biotechnology. 2012;96:577-86.

Adarme-Vega TC, Lim DK, Timmins M, Vernen F, Li Y, Schenk PM. Microalgal biofactories: a promising approach towards sustainable omega-3 fatty acid production. Microb Cell Fact. 2012;11:1475-2859.

Adarme-Vega TC, Thomas-Hall SR, Schenk PM. Towards sustainable sources for omega-3 fatty acids production. Current Opinion in Biotechnology. 2014;26:14-8.

Allen AE, Dupont CL, Obornik M, Horak A, Nunes-Nesi A, McCrow JP, et al. Evolution and metabolic significance of the urea cycle in photosynthetic diatoms. Nature. 2011;473:203-7.

Alonso DL, Segura del Castillo CI, Grima EM, Cohen Z. First insights into improvement of eicosapentaenoic acid content in *Phaeodactylum tricornutum* (Bacillariophyceae) by induced mutagenesis. Journal of Phycology. 1996;32:339-45.

Alvarez JP, Pekker I, Goldshmidt A, Blum E, Amsellem Z, Eshed Y. Endogenous and Synthetic MicroRNAs Stimulate Simultaneous, Efficient, and Localized Regulation of Multiple Targets in Diverse Species. The Plant Cell Online. 2006;18:1134-51.

Ametistova L, Twidell J, Briden J. The sequestration switch: removing industrial CO_2 by direct ocean absorption. Science of The Total Environment. 2002;289:213-23.

Armbrust EV. The life of diatoms in the world's oceans. Nature. 2009;459:185-92.

Armbrust EV, Berges JA, Bowler C, Green BR, Martinez D, Putnam NH, et al. The Genome of the Diatom *Thalassiosira Pseudonana:* Ecology, Evolution, and Metabolism. Science. 2004;306:79-86.

Benemann J. Hydrogen production by microalgae. Journal of Applied Phycology. 2000;12:291-300.

Bernstein E, Caudy AA, Hammond SM, Hannon GJ. Role for a bidentate ribonuclease in the initiation step of RNA interference. Nature. 2001;409:363-6.

References

Bougaran G, Rouxel C, Dubois N, Kaas R, Grouas S, Lukomska E, et al. Enhancement of neutral lipid productivity in the microalga *Isochrysis affinis Galbana* (T-Iso) by a mutation-selection procedure. Biotechnol Bioeng. 2012;109:2737-45.

Bowler C, Allen AE, Badger JH, Grimwood J, Jabbari K, Kuo A, et al. The *Phaeodactylum* genome reveals the evolutionary history of diatom genomes. Nature. 2008;456:239-44.

Carvalho AP, Meireles LA, Malcata FX. Microalgal reactors: a review of enclosed system designs and performances. Biotechnol Prog. 2006;22:1490-506.

Cerutti H, Ma X, Msanne J, Repas T. RNA-mediated silencing in Algae: biological roles and tools for analysis of gene function. Eukaryot Cell. 2011;10:1164-72.

Chaturvedi R, Fujita Y. Isolation of enhanced eicosapentaenoic acid producing mutants of *Nannochloropsis oculat*a ST-6 using ethyl methane sulfonate induced mutagenesis techniques and their characterization at mRNA transcript level. Phycological Research. 2006;54:208-19.

Chaturvedi R, Uppalapati S, Alamsjah M, Fujita Y. Isolation of quizalofop-resistant mutants of *Nannochloropsis oculata* (Eustigmatophyceae) with high eicosapentaenoic acid following N-methyl-N-nitrosourea-induced random mutagenesis. Journal of Applied Phycology. 2004;16:135-44.

Chen CY, Yeh KL, Su HM, Lo YC, Chen WM, Chang JS. Strategies to enhance cell growth and achieve high-level oil production of a *Chlorella vulgaris* isolate. Biotechnol Prog. 2010;26:679-86.

Chen GaL, J. Use of quantitative polymerase chain reaction for determining copy numbers of transgenes in *Lesquerella fendleri*. AmJAgri Biol Sci. 2010;5:415-21.

Cheng R-B, Lin X-Z, Wang Z-K, Yang S-J, Rong H, Ma Y. Establishment of a transgene expression system for the marine microalga *Schizochytrium* by 18S rDNA-targeted homologous recombination. World Journal of Microbiology and Biotechnology. 2011;27:737-41.

Chisti Y. Biodiesel from microalgae. Biotechnol Adv. 2007;25:294-306.

Chiu SY, Kao CY, Tsai MT, Ong SC, Chen CH, Lin CS. Lipid accumulation and CO_2 utilization of Nannochloropsis oculata in response to CO_2 aeration. Bioresour Technol. 2009;100:833-8.

References

Cicci A, Stoller M, Bravi M. Microalgal biomass production by using ultra- and nanofiltration membrane fractions of olive mill wastewater. Water Research. 2013;47:4710-8.

Cohen Z, Khozin-Goldberg I, Adlerstein D, Bigogno C. The role of triacylglycerol as a reservoir of polyunsaturated fatty acids for the rapid production of chloroplastic lipids in certain microalgae. Biochem Soc Trans. 2000;28:740-3.

Cook C, Barnett J, Coupland K, Sargent J. Effects of feeding *Lunaria* oil rich in nervonic and erucic acids on the fatty acid compositions of sphingomyelins from erythrocytes, liver, and brain of the quaking mouse mutant. Lipids. 1998;33:993-1000.

Cooper MS, Hardin WR, Petersen TW, Cattolico RA. Visualizing "green oil" in live algal cells. J Biosci Bioeng. 2010;109:198-201.

Darty K, Denise A, Ponty Y. VARNA: Interactive drawing and editing of the RNA secondary structure. Bioinformatics. 2009;25:1974-5.

de Morais MG, Costa JAV. Biofixation of carbon dioxide by *Spirulina* sp. and *Scenedesmus obliquus* cultivated in a three-stage serial tubular photobioreactor. Journal of Biotechnology. 2007;129:439-45.

De Riso V, Raniello R, Maumus F, Rogato A, Bowler C, Falciatore A. Gene silencing in the marine diatom *Phaeodactylum tricornutum*. Nucleic acids research. 2009;37:e96.

Desbois AP, Mearns-Spragg A, Smith VJ. A fatty acid from the diatom *Phaeodactylum tricornutum* is antibacterial against diverse bacteria including multi-resistant *Staphylococcus aureus* (MRSA). Mar Biotechnol. 2009;11:45-52.

Doan TTY, Obbard JP. Enhanced intracellular lipid in *Nannochloropsis* sp. via random mutagenesis and flow cytometric cell sorting. Algal Research. 2012;1:17-21.

Domergue F, Lerchl J, Zahringer U, Heinz E. Cloning and functional characterization of Phaeodactylum tricornutum front-end desaturases involved in eicosapentaenoic acid biosynthesis. Eur J Biochem. 2002;269:4105-13.

Dunoyer P, Brosnan CA, Schott G, Wang Y, Jay F, Alioua A, et al. An endogenous, systemic RNAi pathway in plants. Embo J. 2010;29:1699-712.

References

Fabris M, Matthijs M, Rombauts S, Vyverman W, Goossens A, Baart GJ. The metabolic blueprint of Phaeodactylum tricornutum reveals a eukaryotic Entner-Doudoroff glycolytic pathway. Plant J. 2012;70:1004-14.

Figueroa JD, Fout T, Plasynski S, McIlvried H, Srivastava RD. Advances in CO_2 capture technology—The U.S. Department of Energy's Carbon Sequestration Program. International Journal of Greenhouse Gas Control. 2008;2:9-20.

Flibotte S, Edgley ML, Chaudhry I, Taylor J, Neil SE, Rogula A, et al. Whole-genome profiling of mutagenesis in *Caenorhabditis elegans*. Genetics. 2010;185:431-41.

Flynn T, Ghirardi ML, Seibert M. Accumulation of O_2-tolerant phenotypes in H_2-producing strains of *Chlamydomonas reinhardtii* by sequential applications of chemical mutagenesis and selection. International Journal of Hydrogen Energy. 2002;27:1421-30.

Foley JA, Ramankutty N, Brauman KA, Cassidy ES, Gerber JS, Johnston M, et al. Solutions for a cultivated planet. Nature. 2011;478:337-42.

Franchino M, Comino E, Bona F, Riggio VA. Growth of three microalgae strains and nutrient removal from an agro-zootechnical digestate. Chemosphere. 2013;92:738-44.

Francisco ÉC, Neves DB, Jacob-Lopes E, Franco TT. Microalgae as feedstock for biodiesel production: Carbon dioxide sequestration, lipid production and biofuel quality. Journal of Chemical Technology & Biotechnology. 2010;85:395-403.

Gatenby C, Orcutt D, Kreeger D, Parker B, Jones V, Neves R. Biochemical composition of three algal species proposed as food for captive freshwater mussels. Journal of Applied Phycology. 2003;15:1-11.

Giavalisco P, Li Y, Matthes A, Eckhardt A, Hubberten HM, Hesse H, et al. Elemental formula annotation of polar and lipophilic metabolites using ^{13}C, ^{15}N and ^{34}S isotope labelling, in combination with high-resolution mass spectrometry. Plant J. 2011;68:364-76.

Gordillo FJL, Jiménez C, Figueroa FL, Niell FX. Influence of elevated CO_2 and nitrogen supply on the carbon assimilation performance and cell composition of the unicellular alga *Dunaliella viridis*. Physiologia Plantarum. 2003;119:513-8.

References

Griffin KL, Anderson OR, Gastrich MD, Lewis JD, Lin G, Schuster W, et al. Plant growth in elevated CO2 alters mitochondrial number and chloroplast fine structure. Proceedings of the National Academy of Sciences. 2001;98:2473-8.

Guillard R. Culture of phytoplankton for feeding marine invertebrates. Culture of Marine Invertebrates Animals. 1975. p. 29-60.

Harter T, Bossier P, Verreth J, Bodé S, Ha D, Debeer A-E, et al. Carbon and nitrogen mass balance during flue gas treatment with *Dunaliella salina* cultures. Journal of Applied Phycology. 2013;25:359-68.

Hartnett ME, Newcomb JR, Hodson RC. Mutations in *Chlamydomonas reinhardtii c*onferring resistance to the herbicide sulfometuron methyl. Plant Physiol. 1987;85:898-901.

Harvey OR, Qafoku NP, Cantrell KJ, Lee G, Amonette JE, Brown CF. Geochemical implications of gas leakage associated with geologic CO_2 storage—A Qualitative Review. Environmental Science & Technology. 2012;47:23-36.

Ho S-H, Chen C-Y, Lee D-J, Chang J-S. Perspectives on microalgal CO_2-emission mitigation systems — A review. Biotechnology Advances. 2011;29:189-98.

Huang A, He L, Wang G. Identification and characterization of microRNAs from *Phaeodactylum tricornutum* by high-throughput sequencing and bioinformatics analysis. BMC Genomics. 2011;12:1471-2164.

Huesemann MH, Hausmann TS, Bartha R, Aksoy M, Weissman JC, Benemann JR. Biomass productivities in wild type and pigment mutant of *Cyclotella* sp. (Diatom). Appl Biochem Biotechnol. 2009;157:507-26.

Hyka P, Lickova S, Přibyl P, Melzoch K, Kovar K. Flow cytometry for the development of biotechnological processes with microalgae. Biotechnology Advances. 2013;31:2-16.

Ibáñez González MJ, Robles Medina A, Grima EM, Giménez AG, Carstens M, Cerdán LE. Optimization of fatty acid extraction from *Phaeodactylum tricornutum* UTEX 640 biomass. Journal of the American Oil Chemists' Society. 1998;75:1735-40.

References

Keeling CD, Piper SC, Bacastow RB, Wahlen M, Whorf TP, Heimann M, et al. Exchanges of atmospheric CO_2 and $^{13}CO_2$ with the terrestrial biosphere and oceans from 1978 to 2000. I. Global Aspects UC San Diego: Scripps Institution of Oceanography. 2001.

Keeling PJ, Burger G, Durnford DG, Lang BF, Lee RW, Pearlman RE, et al. The tree of eukaryotes. Trends in Ecology & Evolution. 2005;20:670-6.

Khraiwesh B, Ossowski S, Weigel D, Reski R, Frank W. Specific Gene Silencing by Artificial MicroRNAs in *Physcomitrella patens*: An Alternative to Targeted Gene Knockouts. Plant Physiology. 2008;148:684-93.

Khvorova A, Reynolds A, Jayasena SD. Functional siRNAs and miRNAs exhibit strand bias. Cell. 2003;115:209-16.

Kilian O, Benemann CSE, Niyogi KK, Vick B. High-efficiency homologous recombination in the oil-producing alga *Nannochloropsis* sp. Proceedings of the National Academy of Sciences. 2011;108:21265-9.

Kroth PG. Genetic transformation: a tool to study protein targeting in diatoms. Methods Mol Biol. 2007;390:257-67.

Kruse O, Hankamer B. Microalgal hydrogen production. Current Opinion in Biotechnology. 2010;21:238-43.

Kuhnt K, Degen C, Jaudszus A, Jahreis G. Searching for health beneficial n-3 and n-6 fatty acids in plant seeds. European Journal of Lipid Science and Technology. 2012;114:153-60.

Kumar A, Ergas S, Yuan X, Sahu A, Zhang Q, Dewulf J, et al. Enhanced CO_2 fixation and biofuel production via microalgae: recent developments and future directions. Trends Biotechnol. 2010;28:371-80.

Kumar A, Ergas S, Yuan X, Sahu A, Zhang Q, Dewulf J, et al. Enhanced CO2 fixation and biofuel production via microalgae: recent developments and future directions. Trends in biotechnology. 2010;28:371-80.

Kumar K, Dasgupta CN, Nayak B, Lindblad P, Das D. Development of suitable photobioreactors for CO_2 sequestration addressing global warming using green algae and cyanobacteria. Bioresource Technology. 2011;102:4945-53.

References

Lackner KS. A Guide to CO_2 Sequestration. Science. 2003;300:1677-8.

Larkum AWD, Ross IL, Kruse O, Hankamer B. Selection, breeding and engineering of microalgae for bioenergy and biofuel production. Trends in Biotechnology. 2012;30:198-205.

Lebeau T, Robert JM. Diatom cultivation and biotechnologically relevant products. Part I: cultivation at various scales. Appl Microbiol Biotechnol. 2003;60:612-23.

Lee JS, Kim DK, Lee JP, Park SC, Koh JH, Cho HS, et al. Effects of SO_2 and NO on growth of *Chlorella* sp. KR-1. Bioresour Technol. 2002;82:1-4.

Lehmann J. Biological carbon sequestration must and can be a win-win approach. Climatic Change. 2009;97:459-63.

Lemahieu C, Bruneel C, Termote-Verhalle R, Muylaert K, Buyse J, Foubert I. Omega-3 long-chain polyunsaturated fatty acid enriched eggs by microalgal supplementation. Lipid Technology. 2013;25:204-6.

León-Bañares R, González-Ballester D, Galván A, Fernández E. Transgenic microalgae as green cell-factories. Trends in Biotechnology. 2004;22:45-52.

Li H-Y, Lu Y, Zheng J-W, Yang W-D, Liu J-S. Biochemical and genetic engineering of diatoms for polyunsaturated fatty acid biosynthesis. Marine Drugs. 2014;12:153-66.

Li H, Durbin R. Fast and accurate short read alignment with Burrows-Wheeler transform. Bioinformatics. 2009;25:1754-60.

Li H, Handsaker B, Wysoker A, Fennell T, Ruan J, Homer N, et al. The Sequence Alignment/Map format and SAMtools. Bioinformatics. 2009;25:2078-9.

MacDougall KM, McNichol J, McGinn PJ, O'Leary SJ, Melanson JE. Triacylglycerol profiling of microalgae strains for biofuel feedstock by liquid chromatography-high-resolution mass spectrometry. Anal Bioanal Chem. 2011;401:2609-16.

Manandhar-Shrestha K, Hildebrand M. Development of flow cytometric procedures for the efficient isolation of improved lipid accumulation mutants in a *Chlorella* sp. microalga. Journal of Applied Phycology. 2013;25:1643-51.

References

Mansour M, Frampton DF, Nichols P, Volkman J, Blackburn S. Lipid and fatty acid yield of nine stationary-phase microalgae: Applications and unusual C24–C28 polyunsaturated fatty acids. Journal of Applied Phycology. 2005;17:287-300.

Maple J, Moller SG. Mutagenesis in Arabidopsis. Methods Mol Biol. 2007;362:197-206.

Martino AD, Meichenin A, Shi J, Pan K, Bowler C. Genetic and phenotypic characterization of *Phaeodactylum tricornutum* (Bacillariophyceae) accessions1. Journal of Phycology. 2007;43:992-1009.

Mathelier A, Carbone A. MIReNA: finding microRNAs with high accuracy and no learning at genome scale and from deep sequencing data. Bioinformatics. 2010;26:2226-34.

McCarthy SS, Kobayashi MC, Niyogi KK. White mutants of *Chlamydomonas reinhardtii* are defective in phytoene synthase. Genetics. 2004;168:1249-57.

McGinn PJ, Dickinson KE, Bhatti S, Frigon JC, Guiot SR, O'Leary SJ. Integration of microalgae cultivation with industrial waste remediation for biofuel and bioenergy production: opportunities and limitations. Photosynth Res. 2011;109:231-47.

Medina AR, Grima EM, Giménez AG, González MJI. Downstream processing of algal polyunsaturated fatty acids. Biotechnology Advances. 1998;16:517-80.

Meiser A, Schmid-Staiger U, Trösch W. Optimization of eicosapentaenoic acid production by *Phaeodactylum tricornutum* in the flat panel airlift (FPA) reactor. Journal of Applied Phycology. 2004;16:215-25.

Moche M, Schneider G, Edwards P, Dehesh K, Lindqvist Y. Structure of the complex between the antibiotic cerulenin and its target, beta-ketoacyl-acyl carrier protein synthase. J Biol Chem. 1999;274:6031-4.

Mohammadi-Yeganeh S, Paryan M, Mirab Samiee S, Soleimani M, Arefian E, Azadmanesh K, et al. Development of a robust, low cost stem-loop real-time quantification PCR technique for miRNA expression analysis. Mol Biol Rep. 2013;40:3665-74.

Molnar A, Bassett A, Thuenemann E, Schwach F, Karkare S, Ossowski S, et al. Highly specific gene silencing by artificial microRNAs in the unicellular alga *Chlamydomonas reinhardtii*. Plant J. 2009;58:165-74.

References

Molnar A, Schwach F, Studholme DJ, Thuenemann EC, Baulcombe DC. miRNAs control gene expression in the single-cell alga *Chlamydomonas reinhardtii*. Nature. 2007;447:1126-9.

Morais M, Costa J. Carbon dioxide fixation by *Chlorella kessleri*, *C. vulgaris*, *Scenedesmus obliquus* and *Spirulina* sp. cultivated in flasks and vertical tubular photobioreactors. Biotechnology Letters. 2007;29:1349-52.

Nepstad DC, Boyd W, Stickler CM, Bezerra T, Azevedo AA. Responding to climate change and the global land crisis: REDD+, market transformation and low-emissions rural development. Philosophical Transactions of the Royal Society B: Biological Sciences. 2013;368.

Ochiai T, Colman B, Matsuda Y. Acclimation of wild-type cells and CO_2-insensitive mutants of the green alga *Chlorella ellipsoidea* to elevated CO_2. Plant Cell Environ. 2007;30:944-51.

Ossowski S, Schwab R, Weigel D. Gene silencing in plants using artificial microRNAs and other small RNAs. Plant J. 2008;53:674-90.

Ota M, Kato Y, Watanabe H, Watanabe M, Sato Y, Smith RL, Jr., et al. Fatty acid production from a highly CO_2 tolerant alga, *Chlorocuccum littorale*, in the presence of inorganic carbon and nitrate. Bioresour Technol. 2009;100:5237-42.

Packer M. Algal capture of carbon dioxide; biomass generation as a tool for greenhouse gas mitigation with reference to New Zealand energy strategy and policy. Energy Policy. 2009;37:3428-37.

Page DR, Grossniklaus U. The art and design of genetic screens: *Arabidopsis thaliana*. Nat Rev Genet. 2002;3:124-36.

Pereira H, Barreira L, Custódio L, Alrokayan S, Mouffouk F, Varela J, et al. Isolation and Fatty Acid Profile of Selected Microalgae Strains from the Red Sea for Biofuel Production. Energies. 2013;6:2773-83.

Pérez-López P, González-García S, Allewaert C, Verween A, Murray P, Feijoo G, et al. Environmental evaluation of eicosapentaenoic acid production by *Phaeodactylum tricornutum*. Science of The Total Environment. 2014;466–467:991-1002.

Pires JC, Alvim-Ferraz MC, Martins FG, Simoes M. Wastewater treatment to enhance the economic viability of microalgae culture. Environ Sci Pollut Res Int. 2013;20:5096-105.

References

Posadas E, García-Encina P-A, Soltau A, Domínguez A, Díaz I, Muñoz R. Carbon and nutrient removal from centrates and domestic wastewater using algal–bacterial biofilm bioreactors. Bioresource Technology. 2013;139:50-8.

Price AC, Choi K-H, Heath RJ, Li Z, White SW, Rock CO. Inhibition of β-Ketoacyl-Acyl Carrier Protein Synthases by Thiolactomycin and Cerulenin: STRUCTURE AND MECHANISM. Journal of Biological Chemistry. 2001;276:6551-9.

Prihoda J, Tanaka A, de Paula WB, Allen JF, Tirichine L, Bowler C. Chloroplast-mitochondria cross-talk in diatoms. J Exp Bot. 2012;63:1543-57.

Qi Lei S, Larson Matthew H, Gilbert Luke A, Doudna Jennifer A, Weissman Jonathan S, Arkin Adam P, et al. Repurposing CRISPR as an RNA-Guided Platform for Sequence-Specific Control of Gene Expression. Cell. 2013;152:1173-83.

Quinlan AR, Hall IM. BEDTools: a flexible suite of utilities for comparing genomic features. Bioinformatics. 2010;26:841-2.

Radakovits R, Eduafo PM, Posewitz MC. Genetic engineering of fatty acid chain length in *Phaeodactylum tricornutum*. Metab Eng. 2011;13:89-95.

Radakovits R, Jinkerson RE, Darzins A, Posewitz MC. Genetic engineering of algae for enhanced biofuel production. Eukaryotic Cell. 2010;9:486-501.

Raven JA, Cockell CS, De La Rocha CL. The evolution of inorganic carbon concentrating mechanisms in photosynthesis. Philosophical Transactions of the Royal Society B: Biological Sciences. 2008;363:2641-50.

Reinhart BJ, Weinstein EG, Rhoades MW, Bartel B, Bartel DP. MicroRNAs in plants. Genes Dev. 2002;16:1616-26.

Rezanka T, Lukavsky J, Nedbalova L, Kolouchova I, Sigler K. Effect of starvation on the distribution of positional isomers and enantiomers of triacylglycerol in the diatom *Phaeodactylum tricornutum*. Phytochemistry. 2012;80:17-27.

Rodolfi L, Chini Zittelli G, Bassi N, Padovani G, Biondi N, Bonini G, et al. Microalgae for oil: strain selection, induction of lipid synthesis and outdoor mass cultivation in a low-cost photobioreactor. Biotechnol Bioeng. 2009;102:100-12.

References

Rohr J, Sarkar N, Balenger S, Jeong BR, Cerutti H. Tandem inverted repeat system for selection of effective transgenic RNAi strains in Chlamydomonas. Plant J. 2004;40:611-21.

Ryckebosch E, Bruneel C, Muylaert K, Foubert I. Microalgae as an alternative source of omega-3 long chain polyunsaturated fatty acids. Lipid Technology. 2012;24:128-30.

Ryckebosch E, Muylaert K, Eeckhout M, Ruyssen T, Foubert I. Influence of drying and storage on lipid and carotenoid stability of the microalga *Phaeodactylum tricornutum*. J Agric Food Chem. 2011;59:11063-9.

Ryckebosch E, Muylaert K, Foubert I. Optimization of an analytical procedure for extraction of lipids from microalgae. Journal of the American Oil Chemists' Society. 2012;89:189-98.

Sakaguchi T, Nakajima K, Matsuda Y. Identification of the UMP synthase gene by establishment of uracil auxotrophic mutants and the phenotypic complementation system in the marine diatom *Phaeodactylum tricornutum*. Plant Physiology. 2011;156:78-89.

Sandesh Kamath B, Vidhyavathi R, Sarada R, Ravishankar GA. Enhancement of carotenoids by mutation and stress induced carotenogenic genes in *Haematococcus pluvialis* mutants. Bioresour Technol. 2008;99:8667-73.

Schneider JC, Livne A, Sukenik A, Roessler PG. A mutant of *Nannochloropsis* deficient in eicosapentaenoic acid production. Phytochemistry. 1995;40:807-14.

Schrag DP. Preparing to capture carbon. Science. 2007;315:812-3.

Schwab R, Ossowski S, Riester M, Warthmann N, Weigel D. Highly specific gene silencing by artificial aicroRNAs in *Arabidopsis*. The Plant Cell Online. 2006;18:1121-33.

Siaut M, Cuine S, Cagnon C, Fessler B, Nguyen M, Carrier P, et al. Oil accumulation in the model green alga *Chlamydomonas reinhardtii*: characterization, variability between common laboratory strains and relationship with starch reserves. BMC Biotechnol. 2011;11:1472-6750.

Sijtsma L, Swaaf ME. Biotechnological production and applications of the ω-3 polyunsaturated fatty acid docosahexaenoic acid. Applied Microbiology and Biotechnology. 2004;64:146-53.

Simopoulos AP. Omega-3 fatty acids in health and disease and in growth and development. Am J Clin Nutr. 1991;54:438-63.

References

Smetacek V. Diatoms and the ocean carbon cycle. Protist. 1999;150:25-32.

Sobczuk TM, Camacho FG, Rubio FC, Fernández FGA, Grima EM. Carbon dioxide uptake efficiency by outdoor microalgal cultures in tubular airlift photobioreactors. Biotechnology and Bioengineering. 2000;67:465-75.

Solovchenko A, Khozin-Goldberg I. High-CO_2 tolerance in microalgae: possible mechanisms and implications for biotechnology and bioremediation. Biotechnol Lett. 2013;26:26.

Steinbrenner J, Linden H. Regulation of two carotenoid biosynthesis genes coding for Phytoene Synthase and carotenoid hydroxylase during stress-induced astaxanthin formation in the green alga *Haematococcus pluvialis*. Plant Physiology. 2001;125:810-7.

Stuart BJ. Addressing the Grand Challenge of atmospheric carbon dioxide: geologic sequestration vs. biological recycling. J Biol Eng. 2011;5:1754-611.

Sydney EB, Sturm W, de Carvalho JC, Thomaz-Soccol V, Larroche C, Pandey A, et al. Potential carbon dioxide fixation by industrially important microalgae. Bioresour Technol. 2010;101:5892-6.

Talebi AF, Mohtashami SK, Tabatabaei M, Tohidfar M, Bagheri A, Zeinalabedini M, et al. Fatty acids profiling: A selective criterion for screening microalgae strains for biodiesel production. Algal Research. 2013;2:258-67.

Tang D, Han W, Li P, Miao X, Zhong J. CO_2 biofixation and fatty acid composition of *Scenedesmus obliquus* and *Chlorella pyrenoidosa* in response to different CO_2 levels. Bioresour Technol. 2011;102:3071-6.

Taylor DC, Falk KC, Palmer CD, Hammerlindl J, Babic V, Mietkiewska E, et al. *Brassica carinata* – a new molecular farming platform for delivering bio-industrial oil feedstocks: case studies of genetic modifications to improve very long-chain fatty acid and oil content in seeds. Biofuels, Bioproducts and Biorefining. 2010;4:538-61.

Tillich UM, Lehmann S, Schulze K, Dühring U, Frohme M. The optimal mutagen dosage to induce point-mutations in *Synechocystis* sp. PCC6803 and its application to promote temperature tolerance. PLoS ONE. 2012;7:e49467.

References

Toledo-Cervantes A, Morales M, Novelo E, Revah S. Carbon dioxide fixation and lipid storage by Scenedesmus obtusiusculus. Bioresour Technol. 2013;130:652-8.

Tripathi U, Venkateshwaran G, Sarada R, Ravishankar GA. Studies on *Haematococcus pluvialis* for improved production of astaxanthin by mutagenesis. World Journal of Microbiology and Biotechnology. 2001;17:143-8.

Ulf R. Effects of CO_2 enrichment on marine phytoplankton. Journal of Oceanography. 2004;60:719-29.

Valenzuela J, Carlson RP, Gerlach R, Cooksey K, Peyton BM, Bothner B, et al. Nutrient resupplementation arrests bio-oil accumulation in *Phaeodactylum tricornutum*. Appl Microbiol Biotechnol. 2013;97:7049-59.

Van Den Hende S, Vervaeren H, Boon N. Flue gas compounds and microalgae: (Bio-)chemical interactions leading to biotechnological opportunities. Biotechnol Adv. 2012;9:9.

Voinnet O. Origin, biogenesis, and activity of plant microRNAs. Cell. 2009;136:669-87.

Wang K, Brown RC, Homsy S, Martinez L, Sidhu SS. Fast pyrolysis of microalgae remnants in a fluidized bed reactor for bio-oil and biochar production. Bioresource Technology. 2013;127:494-9.

White SW, Zheng J, Zhang YM, Rock. The structural biology of type II fatty acid biosynthesis. Annu Rev Biochem. 2005;74:791-831.

Wong DM, Franz AK. A comparison of lipid storage in *Phaeodactylum tricornutum* and *Tetraselmis suecica* using laser scanning confocal microscopy. Journal of Microbiological Methods. 2013;95:122-8.

Xu H, Miao X, Wu Q. High quality biodiesel production from a microalga *Chlorella protothecoides* by heterotrophic growth in fermenters. J Biotechnol. 2006;126:499-507.

Xu P, Zhang Y, Kang L, Roossinck MJ, Mysore KS. Computational estimation and experimental verification of off-target silencing during posttranscriptional gene silencing in plants. Plant Physiology. 2006;142:429-40.

Yamasaki T, Miyasaka H, Ohama T. Unstable RNAi effects through epigenetic silencing of an inverted repeat transgene in *Chlamydomonas reinhardtii*. Genetics. 2008;180:1927-44.

References

Yen Doan T-T, Obbard JP. Enhanced lipid production in *Nannochloropsis* sp. using fluorescence-activated cell sorting. GCB Bioenergy. 2011;3:264-70.

Yu B, Yang Z, Li J, Minakhina S, Yang M, Padgett RW, et al. Methylation as a crucial step in plant microRNA biogenesis. Science. 2005;307:932-5.

Yuan C, Liu J, Fan Y, Ren X, Hu G, Li F. *Mychonastes afer* HSO-3-1 as a potential new source of biodiesel. Biotechnology for Biofuels. 2011;4:1-8.

Zendejas FJ, Benke PI, Lane PD, Simmons BA, Lane TW. Characterization of the acylglycerols and resulting biodiesel derived from vegetable oil and microalgae (*Thalassiosira pseudonana* and *Phaeodactylum tricornutum*). Biotechnol Bioeng. 2012;109:1146-54.

Zeng Y, Wagner EJ, Cullen BR. Both natural and designed micro RNAs can inhibit the expression of cognate mRNAs when expressed in human cells. Mol Cell. 2002;9:1327-33.